

**THE DETERMINATION OF LITHOLOGY FROM CORE
PHYSICAL
PROPERTIES MEASUREMENTS**

A Thesis

by

PAULA ANN CLARK

Submitted to the Office of Graduate Studies of
Texas A&M University
in partial fulfillment of the requirements for the degree of
MASTER OF SCIENCE

May 2006

Major Subject: Geophysics

**THE DETERMINATION OF LITHOLOGY FROM CORE
PHYSICAL
PROPERTIES MEASUREMENTS**

A Thesis

by

PAULA ANN CLARK

Submitted to the Office of Graduate Studies of
Texas A&M University
in partial fulfillment of the requirements for the degree of

MASTER OF SCIENCE

Approved by:

Chair of Committee,	Richard Gibson
Committee Members,	Richard Carlson
	Thomas Blasingame
Head of Department,	Richard Carlson

May 2006

Major Subject: Geophysics

ABSTRACT

The Determination of Lithology from Core Physical
Properties Measurements. (May 2006)

Paula Ann Clark, B.S., Southwestern University

Chair of Advisory Committee: Dr. Richard Gibson

I performed statistical analysis of shipboard physical properties data from the Ocean Drilling Program to investigate relationships between the physical properties data and the lithology of deep ocean cores. The use of non-invasive experiments on deep-sea core samples offers a near real-time view of sediments and requires little user interaction or interpretation. The speed, density, and accuracy of these experiments make efficient use of limited space and expensive ship time. The fact that these experiments are non-invasive also allows for further post-cruise studies.

For the study I chose Leg 162 (July-September 1995 in the North Atlantic) for the density of data, the experiments performed, the quantity and quality of post-cruise publications and the influence of different, yet dominant, environments. Combining similar lithologies across a Leg increased sample size and offered a more statistically normalized sample. Interpolation of the physical properties data matched the intervals used for the lithological determinations. Statistical methods included univariate and multivariate correlation matrices, mean and standard deviations, the significance of the correlations, and a model equation for each lithology and the Leg as a whole. By looking at the physical properties, one can estimate the lithology.

This research is important because sedimentological and geophysical approaches can be merged to offer a more accurate, more detailed view of the depositional history of oceanic cores. Through statistical analysis of geophysical data, the findings duplicate the findings of the sedimentologists without the painstaking examinations typical of this type of research. Performing experiments and analysis quickly and accurately with minimal operator error allows for immediate discussions and results.

Use of this research as a data verification tool provides the ability to distinguish data acquisition problems and misidentifications. This application has proven invaluable for allowing a non-sedimentologist quantitative insight into the lithology.

DEDICATION

To Dad

ACKNOWLEDGEMENTS

Thanks to the following for making this possible: The Joint Oceanographic Institutes (JOI) and member countries, the National Science Foundation (NSF), The Ocean Drilling Program (ODP) and all its employees, Texas A&M University Department of Geosciences, The Scientists of Leg 162 and especially Dr. Peter Blum for his technical assistance, Dr. Rakesh Mithal as Database Manager (ODP), and Dr. Bill O'Brien (Southwestern University) for sparking an interest in geophysics.

TABLE OF CONTENTS

	Page
ABSTRACT.....	iii
DEDICATION.....	v
ACKNOWLEDGEMENTS.....	vi
TABLE OF CONTENTS.....	vii
LIST OF FIGURES.....	ix
LIST OF TABLES.....	x
 CHAPTER	
I INTRODUCTION, OVERVIEW, AND PRINCIPLES.....	1
Introduction.....	1
Objective.....	2
Data.....	3
Previous Work.....	4
Overview of Method and Procedure.....	6
II EQUIPMENT/EXPERIMENT.....	7
Smear Slides (SS).....	7
Natural Gamma Radiation (NGR).....	9
Gamma Ray Attenuation (GRA).....	10
Magnetic Susceptibility (MS).....	11
Color Reflectance (RSC).....	12
III METHODS.....	18
IV RESULTS.....	20
Leg 162.....	20
V SUMMARY AND CONCLUSIONS.....	52
REFERENCES.....	54
APPENDIX A ACRONYMS.....	57

	Page
APPENDIX B LEG 162 DATA	59
VITA.....	74

LIST OF FIGURES

FIGURE	Page
1 Map view of Sites studied.....	5
2 Map view of Sites drilled during Leg 162.....	21
3 Summary of lithostratigraphy of Sites drilled during Leg 162 in the North Atlantic (A) and Nordic Seas (B)	22
4 Data for Sites 980-982 sorted by meters composite depth.....	24
5 Selected scatter plots (X vs. Y) with quadratic trend curve for Sites 980-982....	29
6 SAS generated scatter plot of Sites 980-982.....	30
7 Data for Sites 983, 984 sorted by meters composite depth.....	33
8 SAS generated scatter plot of Sites 983, 984.....	34
9 Selected scatter plots (X vs. Y) with quadratic trend curve for Sites 983, 984...	35
10 Data for Sites 985, 907 sorted by meters composite depth.....	40
11 SAS generated scatter plot of Sites 985, 907.....	41
12 Selected scatter plots (X vs. Y) with quadratic trend curve for Sites 985, 907...	42
13 Data for Sites 986, 987 sorted by meters composite depth.....	44
14 Selected scatter plot (X vs. Y) with quadratic trend curve for Sites 986, 987.....	45
15 SAS generated scatter plot of Sites 986, 987.....	47
16 Selected scatter plots (X vs. Y) with quadratic trend curve for Leg 162.....	49
17 SAS generated scatter plot for Leg 162.....	50

LIST OF TABLES

TABLE	Page
1 Susceptibilities of common minerals and rocks.....	13
2 D65 illuminate, 10 degree observer... ..	17
3 Lithologic summary for Sites analyzed for Leg 162.....	23
4 Univariate statistics and correlation matrix for Leg 162 Sites 980-982.....	28
5 Univariate statistics and correlation matrix for Leg 162 Sites 983, 984.....	36
6 Univariate statistics and correlation matrix for Leg 162 Sites 985, 907.....	39
7 Univariate statistics and correlation matrix for Leg 162 Sites 986, 987.....	46
8 Univariate statistics and correlation matrix for Leg 162	51

CHAPTER I

INTRODUCTION, OVERVIEW AND PRINCIPLES

INTRODUCTION

The Ocean Drilling Program (ODP) operates through Texas A&M University with financial support from the Joint Oceanographic Institutions (JOI) and member countries. The *JOIDES Resolution* sails the world's oceans, in two month periods called "Legs", drilling to recover core that provides "a global description of geological and geophysical structures including passive and active margins and sediment history, and studying in detail areas of major geophysical activity such as mid-ocean ridges and the associated hydrothermal circulations" (James D. Watkins, ex-President of JOI) (Wefer, et al., 1998).

Some important ODP discoveries have included finding gas hydrates, evidence of the Cretaceous-Tertiary boundary, hydrothermal vents, petrified palm trees off Alaska, and records of past volcanic eruptions, each providing a greater overall understanding of the Earth. The ship laboratories allow for on-board analysis of the core to detect biological organisms, chemical makeup, and the origin of the core. Plant and animal life are documented with examinations of microbiology and paleontology. Geochemistry and x-ray diffraction/fluorescence aid in understanding the chemical

This thesis follows the style of Geophysics.

makeup of the core and pore water. The paleomagnetic lab aids in determination of age and origin of the core as seen in its magnetic signature. Physical properties studies increase the knowledge of a formation through the density, magnetic susceptibility, radioactivity, porosity, strength, thermal conductivity and the velocity of sound through the formation.

The most common lithologies present in deep-sea cores are those containing nannofossils, diatoms, calcareous shells, or carbonates with varying amounts of clay, sand, and silt. Analysis of these lithologies can help identify water-level changes, water currents, continental drainage, and ice-sheets.

OBJECTIVE

The objective of this thesis is to analyze the relationship of the physical properties, specifically gamma ray attenuation, natural gamma radiation, magnetic susceptibility, and color reflectance, to the lithology of the core. At present, there is no quick or easy method to determine the lithology for large sections of core. Smear slides, examined by a sedimentologist to estimate the percentage of sand, silt, clay, and biogenic material that appeared on a sediment-smeared microscope slide, can be time consuming and rely on the investigator's subjective interpretation. In contrast, completion of the physical properties experiments takes only minutes on automated machines. Interpretations that utilize the accuracy, density, and speed of these physical

properties experiments can indicate a change in lithology, thereby leading to greater understanding of the core.

Near real-time analysis would also better utilize expensive ship time, equipment, and expertise of the science party. The method introduced here merges the disciplines of the sedimentologist and physical properties specialist, providing a common ground for discussion or analysis. At any one time, at least half of the 20-person science party is awake and available for consultation since the ship operates on two twelve-hour shifts.

Use of the method to verify physical properties data compares one property to another and to the determined lithology. This type of analysis can also help to eliminate edge effects, stray dropstones, magnetized drill pipe/bit shavings and faulty readings. Use of this method has already facilitated the detection of faulty equipment and data acquisition problems.

DATA

The true lithology of the core, as used in this thesis, was determined by smear slide analysis. Acquisition of the physical properties data in this study used automated multi-sensor tracks on board the *JOIDES Resolution*. The data are publicly available from ODP.

To explore the properties of the most common oceanic lithologies, I evaluated Legs based on the type of sediment. I then required these Legs to have substantial data to ensure accurate measurements, and the same types of data had to be available for each

Leg to allow future Leg-to-Leg comparison. I ignored Sites with widely varying lithologies to better study characteristics of a particular depositional history. I decided upon Leg 162, in the North Atlantic (see Figure 1), where the core consists of carbonate layers and ice rafted debris from glaciations and mixing of seas. Analysis of the available physical properties data taken on ship for this Leg indicates four dominant lithologies characterized by percentages of sand, silt, and clay and also the amount and type of the biogenic content.

PREVIOUS WORK

A common use of the physical properties is to create a composite section across Holes, thus creating a more complete geologic history for a particular horizon. Holes within meters of one another are combined into a composite for the area. To do this analysis, a shipboard participant studies changes in the physical properties and correlates this change across Holes. For example, a spike in the magnetic susceptibility of an area would be considered to occur at the same depth since the Holes are in close proximity. By adjusting the depths of each Hole to match, all data from many Holes can be studied as if from one Hole. This increases sample size and provides a more complete view of the environment than a single Hole could offer.

Physical properties of the core samples are often compared with other measurements depending on which parameters met the specific scientific objectives of the Leg. A study of sedimentation rates can recover substantial amounts of sedimentary

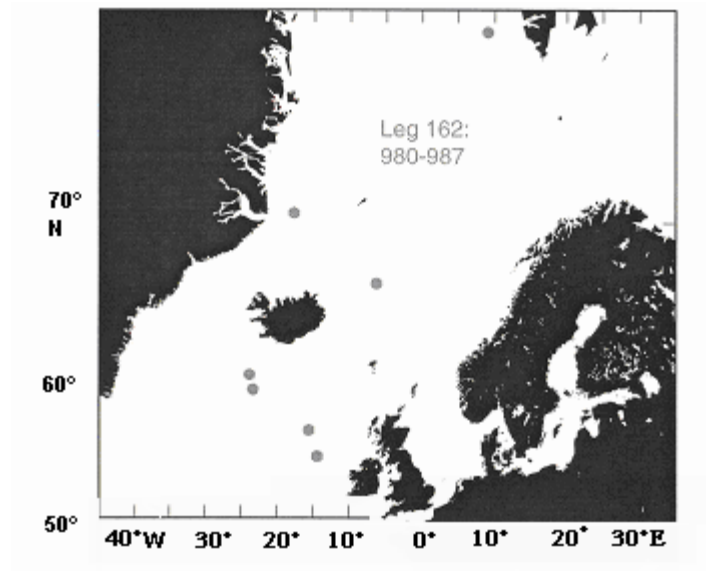


Figure 1. Map view of Sites studied.

core for analysis. If, however, the purpose of the Leg was to evaluate carbonate mounds, natural gamma radiation data would be essentially useless and color information would increase in importance. For this reason, physical properties data may not be obtained in the density required for cross-Leg studies. Likewise, logging while drilling does not provide any core to analyze. Petrologic studies often do not provide core for accurate physical properties analysis since recovery is often minimal and the pieces are broken, providing distortion of data because of the substantial water and air contained in the plastic core liner.

Ortiz and Rack (1999) compared P-wave velocity and density, providing a means of differentiating between the sediment lithologies of biogenic opal and carbonate. Ortiz and O'Connell (1999) studied the correlation between color reflectance, carbonate content, and age, showing distinct variations. Berger et al. (1998) examined magnetic

susceptibility vs. oxygen isotopes and, in a separate paper, magnetic susceptibility vs. color reflectance. These results indicate a cyclical pattern relating to monsoonal activity rather than precessional cycles. Higgins et al. (1999) examined core magnetic susceptibility vs. down-hole magnetic susceptibility to determine the accuracy of the core susceptibility experiment. Robinson (1993) also discusses magnetic susceptibility errors and the value of susceptibility as a paleomagnetic tool.

This thesis investigates the relationship between the physical properties parameters and the actual lithology rather than another property.

OVERVIEW OF METHOD AND PROCEDURE

In this thesis, I have identified a pattern of relationships through statistical analysis of the physical properties parameters. A description of the experiments performed will provide a background in which to understand the link between each experiment and general lithologic characteristics. I discuss the dominant lithologies in comparison with physical properties to demonstrate how ranges and values of the physical properties data can aid in recognizing the lithology. I also combine all the data in an attempt to develop a model equation irregardless of a particular lithology.

CHAPTER II

EQUIPMENT/EXPERIMENT

Four physical properties and one sedimentological analysis were considered for this thesis. In this chapter I will discuss the equipment utilized, the limitations, and the relevance of the experiment with the lithological parameters. I have included a list of acronyms as Appendix A. Examination of each parameter and its relationship to the other parameters further aids in identifying the lithology.

SMEAR SLIDES (SS)

Smear slide preparation involves an extremely small (“toothpick”) sample which is moistened and smeared on a microscope slide. The sample is dried, mounted, and then inspected under a microscope. The procedure can destroy fabric and grain, and larger grains tend to scatter toward the edges of the slide. Minimization of these drawbacks requires care in smear slide preparation (Mazzullo et al., 1988).

Determination of the texture and composition of the sediment, obtained from the smear slides, is by either visual estimation or the point-counting technique. In point-counting, the data resulting from measuring and counting the grains allow calculations of mean grain size and sorting. Visual estimation is more rapid and is therefore preferred for Legs with large core recovery, although this procedure is susceptible to operator

error. If time allows and scientific necessity dictates, the point-counting technique is utilized.

Shipboard analysis occurs at no particular frequency and relies on a predetermined sampling plan or sedimentologist interest. For this reason, there may be varying quantities of samples obtained for each interval. As the Leg progresses, Smear Slide sampling frequency tends to decrease in kilometers of similar core. Also, as the scientists tire, the care in Smear Slide preparation and the accuracy of the data tends to decrease.

For this research, I considered only those smear slides determined to be from dominant, rather than minor, lithologies. A thin layer of sand or ash in the midst of one “continuous” lithology would only serve to provide information on a minor lithology that would tend to skew the results of the common, or dominant, lithology. The lithologic grain size parameters were sand (> 63 micron), silt, and clay (< 4 micron). Sources of error in smear slide analysis include improper preparation of the slide regarding sediment thickness and sediment segregation, operator interpretation errors, and biased sampling. Sampling is often more frequent and results more accurate at the beginning of a Leg, Site, or Hole.

Visual changes in the core often prompt a smear slide interpretation. The smear slides facilitate interpretations of the lithostratigraphic information seen in grain size and sorting, providing hints to the sedimentation rates, the origins and the ages of the sediments, and general trends.

NATURAL GAMMA RADIATION (NGR)

Natural Gamma Radiation is an important lithological parameter since the radiation emitted from an element can indicate the origin of the sediment. The radioisotopes important in NGR analysis are potassium (^{40}K), uranium (^{238}U), and thorium (^{232}Th), all with half-lives greater than 10^9 years. Clay minerals contain most of these elements, as can certain carbonates and arkosic silt, making this experiment important in determination of the clay/shale content of a formation.

The un-split core liner containing the sediment is placed on a track that advances slowly through the sensor. The radiation spectrum is obtained at a pre-set interval, often every four centimeters. So, Natural Gamma Radiation analysis requires that the track stop every four centimeters while the experiment is performed. Depending on the scientific objectives of the Leg, the interval can be adjusted or the experiment not performed.

The data consists of the energy spectrum, divided into 256 channels or 5 non-overlapping energy windows, ranging from 200-3000 KeV, which is corrected for the number of counts per second of a particular energy less the natural background radiation. For this thesis, only the corrected sums of the counts per second were used rather than the individual spectra.

Sources of error are incorrect or infrequent calibration. Edge effects and irregular sediment composition (i.e. dropstones) are often seen as anomalies. A liner not

completely filled with sediment affects calculations, and the instrument resolution of \pm 40 cm core length or 3 - 7% accuracy (Blum, 1997) can also skew the results.

NGR focuses on the change in terrigenous particles evident through these radioactive elements. These particles are usually more evident in darker, more magnetized sediment providing a rough link between color, susceptibility, and radioactivity.

GAMMA RAY ATTENUATION (GRA)

Gamma Ray Attenuation, also known as Gamma Ray Attenuation Porosity Evaluator or GRAPE, is one method utilized by ODP to measure the density of a formation. GRA measures the scattering that results from the reflected transmission by bombarding the core with gamma rays.

Gamma Ray Attenuation is performed on the same multi-sensor track as Natural Gamma Radiation. The density is obtained at a pre-set interval, often every four centimeters. This interval usually matches that of Natural Gamma Radiation, so both analysis can be performed when the track stops. Again, depending on the scientific objectives of the Leg, the interval can be adjusted. Gamma Ray Attenuation is often considered more important than Natural Gamma, so even if Natural Gamma Radiation data is not obtained, Gamma Ray Attenuation is almost always performed .

The current calibration methods have been in use since August of 1998. In the previous method, the density was approximately 11% too high, and correction factors were required (Blum, 1997). Since I investigate data obtained during the summer of

1995, the values I used are the corrected values. Sources of error are the same as with Natural Gamma Radiation. The resolution of GRA is ± 0.5 cm of core length, or 0.5% accuracy (Blum, 1997).

The pore water (PW), the percent volume of the sediment that contains seawater, can be calculated directly from the GRA density (ρ) values. The average density of seawater (ρ_{sw}) is 1.024 g/cc (Blum, 1997). Therefore, the ratio of GRA density to seawater density provides an approximation of porosity (ϕ) where ρ_t is the total density and ρ_{sed} is the density of the sediment only.

$$PW = \rho / \rho_{sw} \quad (1)$$

$$\phi = (\rho_t - \rho_{sed}) / (\rho_t - \rho_{sw}) \quad (2)$$

Ortiz and Rack (1999) demonstrated the differentiation between percent biogenic opal, carbonate, siliceous or calcareous oozes, and terrigenous sedimentation by correlating GRA and P-wave velocity. I used GRA values to calculate the approximate percent pore water of the sample. GRA can indicate minor changes in the lithology on small scales.

MAGNETIC SUSCEPTIBILITY (MS)

Magnetic susceptibility is the degree to which a material can be magnetized in an external magnetic field. The susceptibility value depends on the mineral composition of the material. The presence of certain minerals in the sample, as determined by the

susceptibility, can indicate the lithology. Since the susceptibility of many mineral or rock types overlap (Table 1), this experiment must be used in conjunction with others to narrow the possibilities of lithologic composition. Ortiz and Rack (1999) discuss the value of MS relating grain size and sediment composition.

Magnetic Susceptibility is performed on the same multi-sensor track as Natural Gamma Radiation and Gamma Ray Attenuation. The susceptibility is obtained at a pre-set interval that usually matches the intervals of NGR and GRA, so all three analysis can be performed when the track stops. Again, depending on the scientific objectives of the Leg, the interval can be adjusted or the experiment not performed.

Sources of error are the same as with Natural Gamma Radiation. The resolution of the MS experiment is ± 15 cm of core length or 2×10^{-6} (SI) accuracy (Blum, 1997). Use of MS is often a precursor to further paleomagnetic studies (Channell and Lehman, 1999). Robinson (1993) provides a review of the application of MS using data from ODP Leg 115. Main oceanographic data obtained from MS readings are the concentration of pyrite and minor influences of other ferromagnetic and paramagnetic terrigenous particles and the often diamagnetic biogenic carbonate and silica.

COLOR REFLECTANCE (RSC)

Analysis of color reflectance occurs on the archive half of the split cores after all other non-destructive experiments are completed. The photospectrometer contacts the core through a non-interfering piece of plastic wrap. Light reflected from the material is

Table 1. Susceptibilities of common minerals and rocks (Blum, 1997). Here κ is the volume susceptibility, M is the magnetization, and H is the applied external field, $\kappa=M/H$. The mass susceptibility X is the ratio of the volume susceptibility to density, $X=\kappa/\rho$.

	$\kappa(10^{-6} \text{ SI})$	$X (10^{-8} \text{ m}^3/\text{kg})$
Iron-bearing minerals		
Biotite	1,500 to 2,900	5 to 52 to 95 to 98
Orthopyroxene, olivines, amphiboles	1,500 to 1,800	1 to 43 to 50 to 130
iron ^a	3,900,000	50,000 to 2,000,000
Iron sulfides		
Pyrite	35-5,000	11 to 30 to 100
Iron-titanium oxides		
Hematite ^a	500 to 40,000	10 to 60 to 760
Maghemite ^a	2,000,000 to 2,500,000	40,000 to 50,000
Magnetite ^a	1,000,000 to 5,700,000	20,000 to 50,000 to 110,000
Average rock values		
Sandstone, shale, limestone	0 to 25,000	0 to 1,200
Dolomite	-10 to -940	-1 to -41
Clay	170 to 250	10 to 15
Basalt, diabase	250 to 180,000	6.4 - 6,100
Gabbro	1,000 to 90,000	26 to 3,000
Granite	0 to 50,000	0 to 1,900
Rhyolite	250 to 38,000	10 to 1,500
Gneiss	0 to 25,000	0 to 900
Slate	0 to 38,000	0 to 1,400
Schist, phyllite	26 to 3,000	1 to 110
Serpentine	3,100 to 18,000	110 to 630
^a Remanence-carrying minerals		

collected in an integration sphere, normalized to the source light, and calibrated with the measurement of a pure white standard (100% reflection) and a black box (zero reflectance) over the spectrum of visible light, between 400 and 700 nm wavelength. The spectrum is then divided into 10 nanometer intervals. The light source in the

photospectrometer is a Xenon lamp since Xenon closely duplicates natural light (Blum, 1997). The reflected spectrum from the Xenon lamp is saved in a raw computer file for later analysis. This file, uploaded into the ODP database, originally had calculations based on an obsolete set of parameters describing the pure white standard (D60, 10-degree observer). I verified the correct values for the Xenon light source and re-calculated the spectrum (D65, 10-degree observer).

The Minolta photospectrometer utilized for spectral acquisition conforms to the Commission Internationale d'Eclairage (CIE) (Berger-Schunn, 1994) for spectral readings between 400 and 700 nm wavelengths. From these wavelength values, a cylindrical coordinate system can be represented. The lightness variable L^* is the axis of the cylinder and the values range from 0% to 100%. The cylinder radii are the chromaticity values where a^* is the green (positive) to red (negative) axis while b^* is the blue (positive) to yellow (negative) axis. The $L^* a^* b^*$ system is referred to as the CIELAB system and offers insight into the characteristics of the sediment. L^* values are controlled mainly by water content with a small grain size and homogenization effect indicating carbonate content; a^* and b^* are controlled by water content, oxidation of greenish materials, and grain size making these parameters sensitive to clay mineralogy (Blum, 1997). Legacy color determinations, such as Munsell values, show inherent inaccuracies in interpretation since determination of the color relies on visual matching to a color chart.

The Minolta photospectrometer, replaced on Leg 162 by an Oregon State University Spectral Reflectometer (SCAT) has identical theory and methods, but the

equipment measures reflectance in 0.628 nm-wide-bands from 250 - 900 nm. To match the 400-700 nm spectrum at 10 nm intervals of the Minolta required manipulation of the data from the Spectral Reflectometer. I manipulated the SCAT data so that I could calculate the CIELAB values which are typical of other ODP Legs. Specialized data acquisition equipment is often necessary, but standard ODP equipment should also be used to easily allow for cross-Leg comparison.

The color reflectance spectral data can help to estimate the abundance of certain compounds such as hematite, goethite, carbonates, opal, organic matter, and some combinations of clay minerals, although concentration and intensity can alter the wavelength and size of the spectral peaks. The grain size can also influence the reflectivity and band intensity.

Table 2 and equations 3-8 show the calculations necessary to obtain the L^* , a^* , and b^* parameters from the spectral data.

$$X = \sum W_x(\lambda) R(\lambda) \Delta\lambda \quad (3)$$

$$Y = \sum W_y(\lambda) R(\lambda) \Delta\lambda \quad (4)$$

$$Z = \sum W_z(\lambda) R(\lambda) \Delta\lambda \quad (5)$$

$$L^* = 116(Y/Y_n)^{1/3} - 16 \quad (6)$$

$$a^* = 500[(X/X_n)^{1/3} - (Y/Y_n)^{1/3}] \quad (7)$$

$$b^* = 200[(Y/Y_n)^{1/3} - (Z/Z_n)^{1/3}] \quad (8)$$

Each $W_i(\lambda)$ is a weighting factor based on the wavelength λ and established color matching functions in three dimensional space. X_n , Y_n and Z_n define the color of a normally white object color stimulus, also known as a White Point. $R(\lambda)$ is the measured reflectance at a particular wavelength λ (Wyszecki and Stiles, 1982).

As L^* , a^* , and b^* all rely on the same spectra and $(Y/Y_n)^{1/3}$ (eq. 2 - 7), only limited correlation between the individual RSC values can be considered. The three RSC parameters, considered across the other physical properties parameters, will offer insight as to the composition of the lithology.

Possible sources of error are incorrect calculations due to the wrong setting on the spectrophotometer (i.e. use of obsolete or incorrect parameters for the light source), infrequent or improper calibration, and the spectrophotometer not contacting the core properly. Improper core contact allows ambient light into the sensor and alters the values from core reflectance. Since RSC was not automated until Leg 180 in June of 1999, this thesis relies on a manual procedure. Another source of error is desiccation of the core. RSC is performed only minutes after splitting the core, therefore minimizing the desiccation. Balsam et al. (1997) determined that desiccation made a marked difference in brightness, first darkening, then lightening the core. Shipboard values of the spectrum were used to not introduce either desiccation or altering of the core due to oxidation, bacteria, etc.

RSC has traditionally been applied to estimate carbonate content (Ortiz, O'Connell et al., 1999 and Vidal et al., 1998). Minor depositional changes, seen in the

color or reflectance of the core, sometimes indicate sub-Milankovich time scales (Ortiz and Rack, 1999).

Table 2. D65 illuminate, 10 degree observer (AMST, 1996).

Wavelength (nm)	Wx	Wy	Wz
400	0.145	0.015	0.643
410	0.676	0.069	3.11
420	1.603	0.168	7.627
430	2.451	0.3	12.095
440	3.418	0.554	17.537
450	3.699	0.89	19.888
460	3.064	1.29	17.695
470	1.933	1.838	13
480	0.802	2.52	7.699
490	0.156	3.226	3.938
500	0.039	4.32	2.046
510	0.347	5.621	1.049
520	1.07	6.907	0.544
530	2.17	8.059	0.278
540	3.397	8.668	0.122
550	4.732	8.855	0.035
560	6.07	8.581	0.001
570	7.311	7.951	0
580	8.291	7.106	0
590	8.634	6.004	0
600	8.672	5.079	0
610	7.93	4.065	0
620	6.446	2.999	0
630	4.669	2.042	0
640	3.095	1.29	0
650	1.859	0.746	0
660	1.056	0.417	0
670	0.57	0.223	0
680	0.274	0.107	0
690	0.121	0.047	0
700	0.109	0.043	0
Check Sum	94.809	100	107.307
White Point	94.811	100	107.304
	Xn	Yn	Zn

CHAPTER III

METHODS

In this chapter, I will introduce the methodology, manipulation, and logic used to select and interpret each data set. The lithology of each Site will be described in terms of three main components: 1) Terrigenous — sand, silt, clay, or mud, 2) Biogenic — diatom, nannofossil, carbonate, and 3) Pore water which was calculated from Gamma Ray Attenuation. I considered terrigenous and biogenic percentages obtained from the smear slide analysis as the known values.

I migrated the raw data for Leg 162 from text files into the ODP Oracle database. I cleaned and verified the data prior to use as per the shipboard notes. The use of a relational database and the available web reports (www-odp.tamu.edu) supplied error-free calculations of depth, background corrected values, and other necessary calculations.

To correlate data from multiple Holes within a Site, shipboard sedimentologists derive a Site-wide depth scale called meters composite depth. Meters composite depth (mcd) provides a normalized depth scale for a particular Site by matching sedimentary units from neighboring Holes within a Site. The use of meters composite depth allows all Holes within a Site to be considered as a single Hole. I also imported and verified these depth calculations, as determined by shipboard parties, with the shipboard notes.

Sampling intervals for each experiment can be set individually; thus sampling intervals may not overlap for any two experiments. When possible, physical properties

data were interpolated inside a particular Hole to match the smear slide depths; otherwise, interpolation was performed inside a particular Site using the normalized depths (mcd) of both the physical properties experiment and smear slide interpretation. I immediately corrected or discarded obvious outliers and incorrect values, i.e. negative densities, reflectance >100%, or negative counts. The data were then separated into tables of similar lithology by overall trends (i.e. mostly clay or mostly nannofossil, etc.). These tables of raw data are included in Appendix B. A statistical program (SAS) offered another filtering opportunity for the individual compilations, allowing the discard of remaining outliers as determined by calculation of the sample interquartile range and boxplot. Since these outliers were unusually large or small, I considered these data to be errors in data acquisition or reporting and then analyzed the remaining data with SAS. I desired 100 or more data points in an effort to approach statistical normality.

I determined univariate and multivariate correlations between properties and the lithology, the descriptive level of significance or P-value of the correlations, regression analysis for selected combinations of properties, principal component analysis, and a linear model equation for the clay and silt percentages in the sediment based on all available physical properties data. Final data analysis for this thesis was based on published reports from the individual Legs and relationships were analyzed for correlations > |0.500| (50%). As a final test, I combined data from each of the four lithologies and performed the same analysis.

CHAPTER IV

RESULTS

I first introduce the geologic background of the region. I then break the section into discussions of each lithology by discussing the environmental history in more detail, the analysis of the data, and the interpretation of these analyses. I finish the discussion with a summary to demonstrate of how these values can be interpreted to understand the lithology.

LEG 162

Leg 162, as seen in Figure 2, lies in the North Atlantic and Nordic Seas. Glaciations and deep ocean currents strongly influence the lithology and paleoenvironmental history of this region. Figure 3 summarizes the lithostratigraphy of the Sites in the North Atlantic (A) and Nordic Seas (B). In each of these regions, similar lithologies exist. The summary (Table 3) describes Sites 980-982 as predominately nannofossil ooze with varying clay content. Sites 983 and 984 are predominately silty clay with nannofossils. Sites 985 and 907 are characterized by variations in clay, biogenic, and silt content. Sites 986 and 987 are siliciclastic with varying amounts of gravel. Each of these four Site groups is interpreted individually and then combined to encompass the entire Leg.

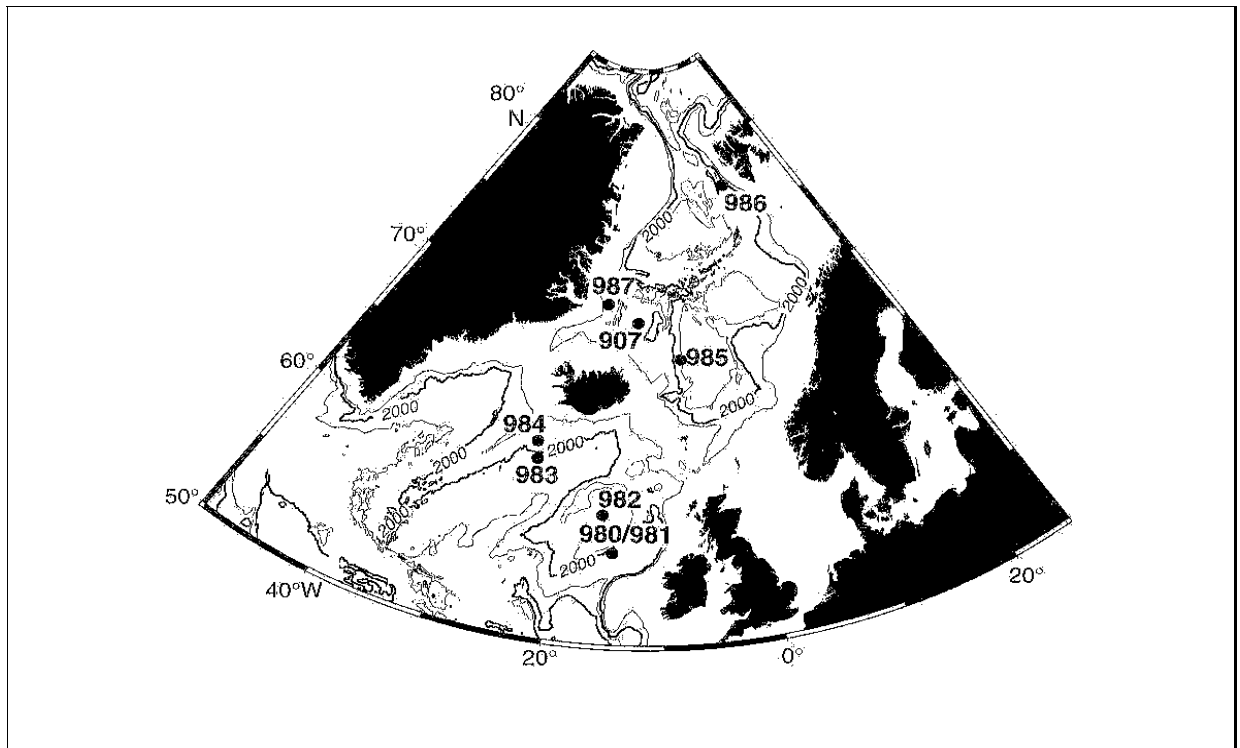


Figure 2. Map view of Sites drilled during Leg 162 (Jansen, et al., 1996).

Sites 980, 981, and 982

Sites 980 - 982 consist of rapidly accumulated nannofossil ooze with varying clay content. Variations in lithology exist on a decimeter to meter scale and sedimentation rates vary by depth (Jansen, et al., 1996). Water depths and sedimentation rates are summarized in Table 3. Sites 980 and 981, originally chosen to study Pliocene-Pleistocene climate variability, offer data for both Milankovich and millennial time scale studies. Site 982 is in considerably shallower water, and therefore is less dependent on the deep ocean currents that influence the other two Sites. Figure 4 and Appendix B

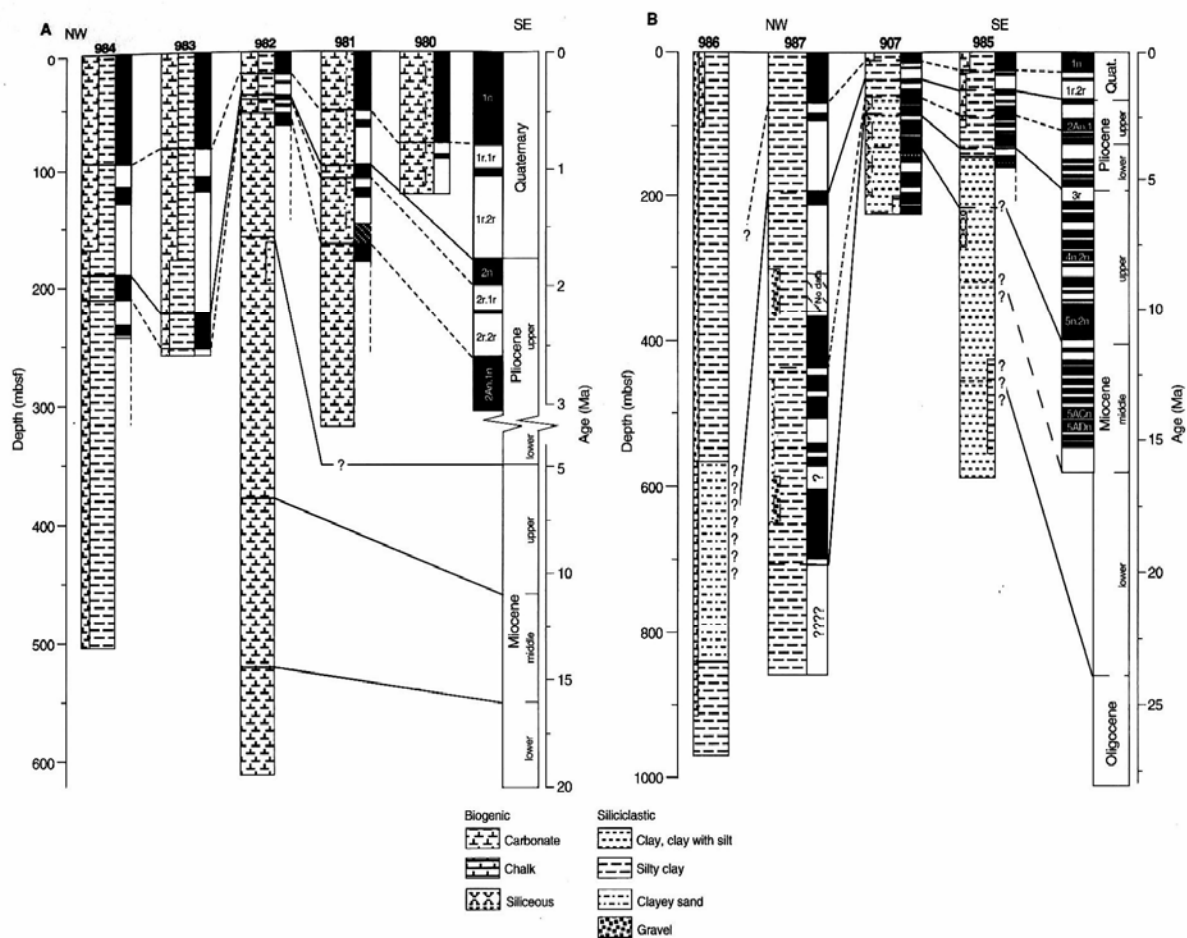


Figure 3. Summary of lithostratigraphy of Sites drilled during Leg 162 in the North Atlantic (A) and Nordic Seas (B) (Jansen, et al., 1996).

Table 3. Lithologic summary for Sites analyzed for Leg 162.

	980	981	982
Average water depth	2170 m	2170 m	1134 m
Sedimentation rates	10cm/ky	10 cm/ky	21-37 m/my
Carbonate content	54%	54%	86%
shipboard comments	rapidly accumulated nannofossil ooze with varying amounts of clays lithologic variations on decimeter to meter scale		
	983	984	
Average water depth	1980 m	1650 m	
Sedimentation rates	9-17cm/ky	10-16cm/ky	
Carbonate content	16%	8%	
shipboard comments	rapidly accumulated fine-grained terrigenous particles some ash, minor amounts of biocarbonate and biosilica		
	985	907	
Average water depth	2780 m	1800 m	
Sedimentation rates	10-25m/my	11-22m/my	
Carbonate content	0 - 50+%	0 - 50+%	
shipboard comments	silty clay, clay with silt, and clayey sediment with biogenics biogenics are highly variable with depth		
	986	987	
Average water depth	2050 m	1670 m	
Sedimentation rates	160 - 320 m/my	**	
Carbonate content	4.9%	4.9%	
shipboard comments	fine to course-grained siliciclastics with varying amounts of gravel ** 987 has many intervals barren of biogenics		

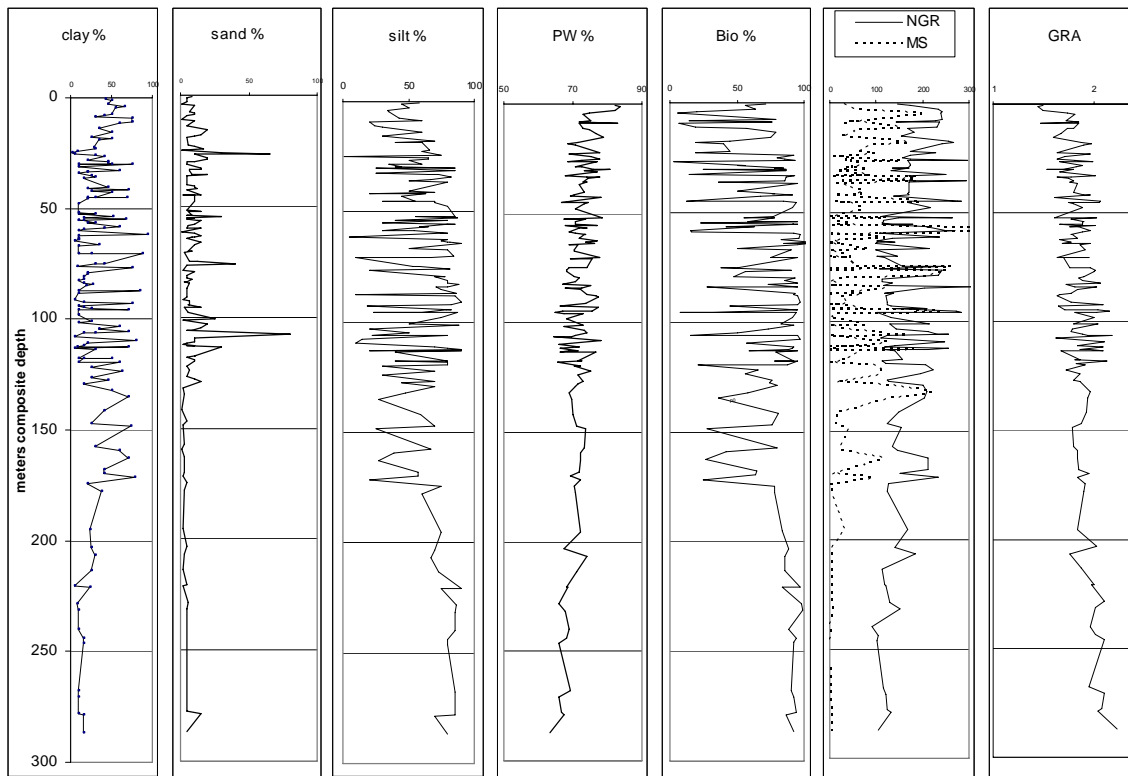


Figure 4. Data for Sites 980-982 sorted by meters composite depth.

show that the majority of the data comes from approximately the upper 125 meters of the drilled holes.

The abundance of data from near the ocean floor relates to the depth of drilling at each Site. Some Sites drilled deeper than others, but the shallowest Holes were drilled to approximately 125 meters below sea floor. Gamma Ray Attenuation (density) increases overall with depth, as we would expect with compaction. Figures 3 and 4 show that deeper than 150 meters depth, the biogenic, silt and Gamma Ray Attenuation values increase while Natural Gamma Radiation and Magnetic Susceptibility decrease. The Magnetic Susceptibility values become negative as is typical of carbonates. Magnetic

Susceptibility fluctuates more than Natural Gamma Radiation, but the pattern is similar.

A quadratic trend curve can be calculated for Magnetic Susceptibility vs. Natural

Gamma Radiation. The error can be measured using the R^2 measure, defined as

$$R^2 = 1 - \text{SSE} / \text{SST} \quad (8)$$

$$\text{SSE} = \sum (Y_i - \hat{Y}_i)^2 \quad (9)$$

$$\text{SST} = (\sum Y_i^2) - (\sum Y_i)^2 / n \quad (10)$$

Here SSE is the sum of squares as a measure of random or unexplained variability and

SST is the total sum of squares of the differences between each point $(Y_i)^2$ and its mean

$(\hat{Y}_i)^2$. R^2 is then the variance, or regression, of the data from the mean (Milton and

Arnold, 1995). The value for the fit to the quadratic equation is $R^2 = 0.7826$.

The correlation matrix of Table 4 shows that the SAS calculated correlation value of Magnetic Susceptibility vs. Natural Gamma Radiation is 0.79, thus reinforcing the R^2 value calculated from equation 8.

Differences in the graphs of Figure 4 show an increase in carbonates at approximately 180 meters depth by the sudden drop in Magnetic Susceptibility with an increase in the biogenic and silt components. Magnetic Susceptibility spikes are likely the effects of drop stones (see Figure 4) while Figure 5 shows selected scatter plots with regression analysis between two variables. However, the model equations for these Sites (eq.11-12) have R^2 values equal to 0.738 and 0.907 for clay and silt, respectively.

$$\text{Clay} = 0.8770 * \text{PW} + 0.0307 * \text{NGR} + 0.0198 * \text{MS} + 10.0718 * \text{GRA}$$

$$-0.6858 * \text{L} - 2.5820 * \text{A} - 1.1927 * \text{B} \quad (11)$$

$$\begin{aligned} \text{Silt} = & -0.7151*\text{PW} + 0.0265*\text{NGR} - 0.0219*\text{MS} + 27.5133*\text{GRA} \\ & + 0.9633*\text{L} + 2.9985*\text{A} + 0.6715*\text{B} \end{aligned} \quad (12)$$

These R^2 values show that while Magnetic Susceptibility spikes would be most noticeable in clay, the model equations are still very good.

The SAS generated scatter plot of Figure 6 provides a graphical representation of the data in Table 4. Since pore water is calculated from Gamma Ray Attenuation, there is a straight line and perfect correlation. The correlation matrix for Sites 980-982 (Table 4) shows that positive relationships exist between clay content, Natural Gamma Radiation and Magnetic Susceptibility.

To determine the significance of a relationship, I evaluated the test statistic and then determined, with SAS, the probability of the smallest level at which we could have preset our null hypothesis and still had been able to reject it in favor of the alternate, or research, hypothesis. This probability is known as the critical level, descriptive level of significance, or the P-value (Milton and Arnold, 1995). We therefore desire a P-value as close to zero as possible to reduce the possibility of discarding the null hypothesis in error.

Principal component analysis (PCA) was also performed with SAS. PCA is a way of identifying patterns and expressing the data such that these similarities and differences are highlighted (Smith, 2002). PCA is a statistical method that relies on principles of linear algebra. Smith (2002) offers an informative tutorial that outlines the steps necessary. Rather than delve into linear algebra, we must calculate the covariance

matrix, eigenvectors and eigenvalues, and then the highest eigenvalues represent the most significant experiment. In the remainder of the paper, I will only document the most significant components.

The low P-values of these correlations show that the relationships are indeed significant. According to the principal component analysis, Natural Gamma Radiation and Magnetic Susceptibility are the best components of the data set. The high Natural Gamma Radiation and Magnetic Susceptibility indicate clay and non-biogenic components that are characteristic of terrigenous sedimentation.

The biogenic content closely correlates with the silt content, thus describing the composition of the silt (in this case predominately nannofossils). High pore water percentages are an indicator of unconsolidated sediment, especially oozes. Magnetic Susceptibility has high variability (minimum = -2.0, maximum = 431.0), possibly representing variations in carbonate and silt content from the terrigenous and non-terrigenous sediments. Jansen et al. (1996, p.55) note that “A distinct boundary occurs at [174 meters and] is marked by sharp downcore decreases in magnetic susceptibility and natural gamma radiation and sharp downcore increases in calcium carbonate content and spectral reflectance.” The conclusion, therefore, is that either glaciations or continental run-off were the predominant influence or that the deep ocean currents prevailed, bringing with them the abundance of sea life.

Table 4. Univariate statistics and correlation matrix for Leg 162 Sites 980-982.

Univariate Statistics											
	N	mean	std dev	minimum	maximum						
Clay	132	31.58	23.14	1.00	94.00						
Sand	132	8.89	8.97	1.00	80.00						
Silt	132	59.39	23.82	1.00	90.00						
PW	132	71.56	3.74	63.33	82.07						
BIO	132	69.98	27.62	3.00	105.00						
NGR	132	167.52	53.78	91.33	304.82						
MS	132	59.05	75.99	-2.00	431.00						
GRA	132	1.43	0.07	1.25	1.62						
L*	132	59.26	15.30	29.23	84.94						
a*	132	2.91	1.21	0.54	6.09						
b*	132	3.17	1.31	-1.96	7.65						
Correlation Matrix											
	Clay	Sand	Silt	PW	BIO	NGR	MS	GRA	L*	a*	b*
Clay		-0.11	-0.88	0.10	0.61	0.43	0.40	-0.11	-0.48	0.29	-0.02
Sand	-0.11		-0.18	0.17	-0.01	-0.01	0.05	-0.17	-0.17	0.23	0.04
Silt	-0.88	-0.18		-0.21	0.57	-0.42	-0.40	0.22	0.54	-0.34	-0.05
PW	0.10	0.17	-0.21		0.02	-0.04	-0.09	-1.00	-0.11	0.31	0.08
BIO	0.61	-0.01	0.57	0.02		-0.69	-0.65	-0.01	0.70	-0.41	0.11
NGR	0.43	-0.01	-0.42	-0.04	-0.69		0.79	0.03	-0.82	0.55	-0.15
MS	0.40	0.05	-0.40	-0.09	-0.65	0.79		0.08	-0.76	0.51	-0.20
GRA	-0.11	-0.17	0.22	-1.00	-0.01	0.03	0.08		0.12	-0.31	-0.10
L*	-0.48	-0.17	0.54	-0.11	0.70	-0.82	-0.76	0.12		-0.68	-0.06
a*	0.29	0.23	-0.34	0.31	-0.41	0.55	0.51	-0.31	-0.68		-0.22
b*	-0.02	0.04	-0.05	0.08	0.11	-0.15	-0.20	-0.10	-0.06	-0.22	
P-Values of the Correlations											
	Clay	Sand	Silt	PW	BIO	NGR	MS	GRA	L*	a*	b*
Clay		0.20	0.00	0.24	0.00	0.00	0.00	0.21	0.00	0.00	0.78
Sand	0.20		0.03	0.06	0.91	0.90	0.60	0.06	0.54	0.01	0.62
Silt	0.00	0.03		0.02	0.00	0.00	0.00	0.01	0.00	0.00	0.59
PW	0.24	0.06	0.02		0.82	0.68	0.32	0.00	0.21	0.00	0.36
BIO	0.00	0.91	0.00	0.82		0.00	0.00	0.90	0.00	0.00	0.23
NGR	0.00	0.90	0.00	0.68	0.00		0.00	0.74	0.00	0.00	0.09
MS	0.00	0.60	0.00	0.32	0.00	0.00		0.37	0.00	0.00	0.02
GRA	0.21	0.06	0.01	0.00	0.90	0.74	0.37		0.17	0.00	0.28
L*	0.00	0.54	0.00	0.21	0.00	0.00	0.00	0.17		0.00	0.47
a*	0.00	0.01	0.00	0.00	0.00	0.00	0.00	0.00	0.00		0.01
b*	0.78	0.62	0.59	0.36	0.23	0.09	0.02	0.28	0.47	0.01	

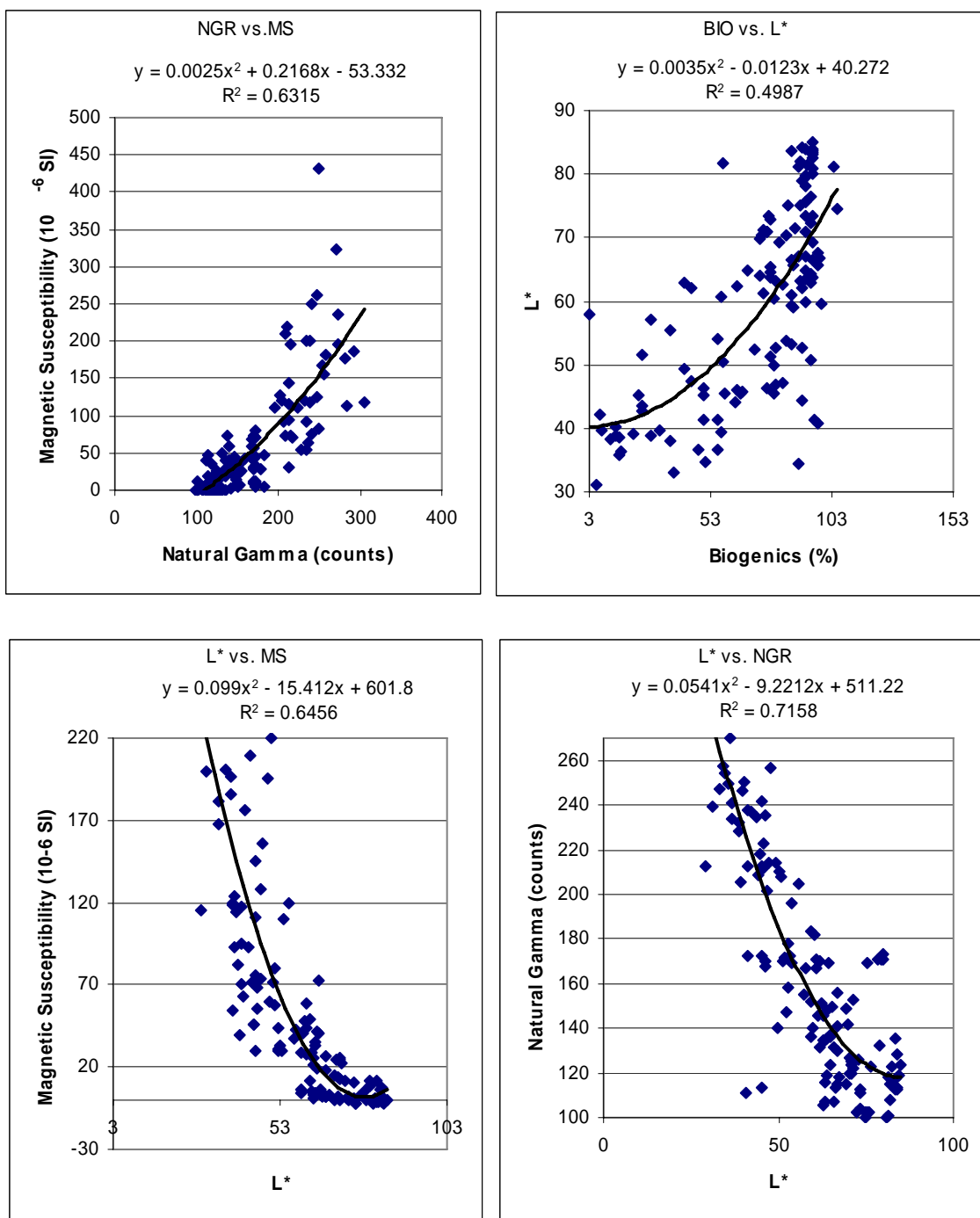


Figure 5: Selected scatter plots (X vs.Y) with quadratic trend curve for Sites 980-982.

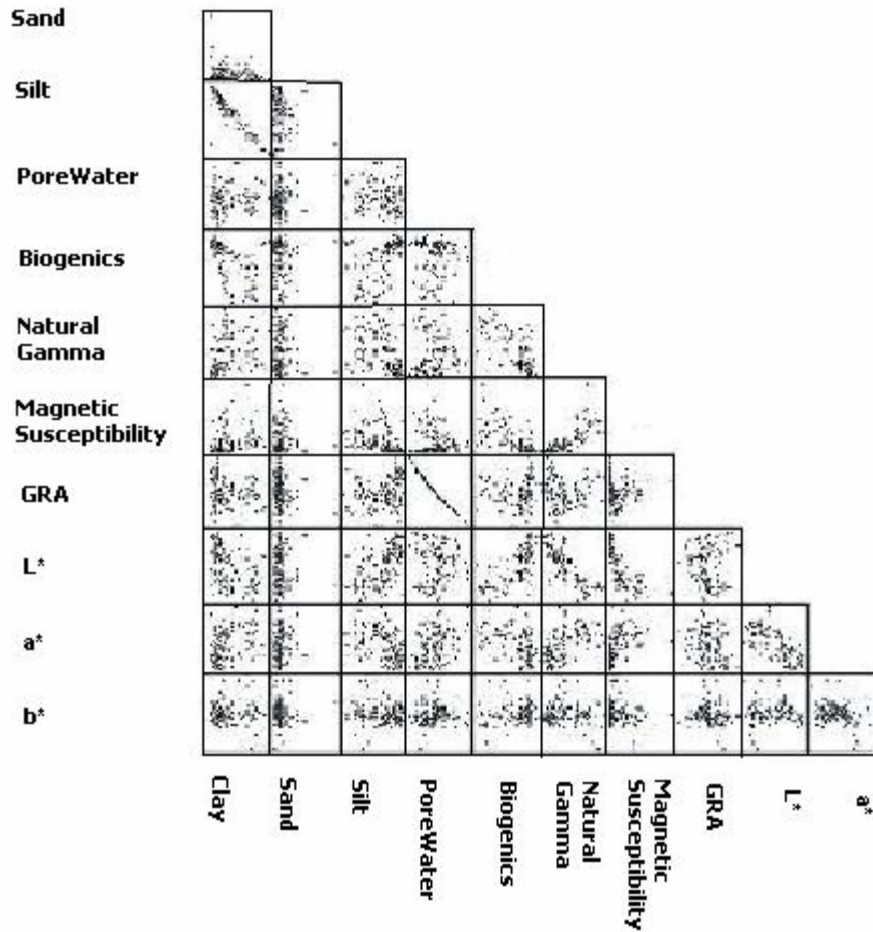


Figure 6: SAS generated scatter plot of Sites 980-982.

Sites 983 and 984

Sites 983 and 984 are in drift regions and consist of predominately rapid accumulations of fine-grain terrigenous particles with minor amounts of biocarbonate and silica (Jansen, et al., 1996). Major lithological constituents include silty clay, clay, clayey nannofossil sediment and a mixture of clay-silt-nannofossils. Sedimentation rates

for these two Sites range from 9 cm/ky. to 17 cm/ky. during the Holocene-Pliocene and carbonate values fluctuate between 0.4% and 43.3% (Jansen, et al., 1996).

Although Figure 3 shows carbonates to be approximately half of the lithology at a depth less than 170 meters below sea floor, the shipboard notes state differently. This discrepancy could relate to interpretations by different sedimentologists, biased sampling, or visualization requirements. This lack of carbonates is shown by low Gamma Ray Attenuation and high Magnetic Susceptibility values that are atypical of carbonates. The high Magnetic Susceptibility values seen in Figure 7 help to identify a terrigenous lithology. The reported biogenic content, following the same general pattern as the silt content, fluctuates erratically between 0% and 75% until, at more than 200 meters depth, the biogenic content is minimal. Natural Gamma Radiation is nearly constant, and few experiments correlate well as can be seen in the scatter plot of Figure 8.

R^2 values for the scatter plots of Figure 9 show the relationship of silt content vs. biogenic content is only slightly better than that of L^* vs. biogenic content. Even the excellent correlation of Magnetic Susceptibility vs. Natural Gamma Radiation from Sites 980-982 only have $R^2 = -0.22$ for this lithology. The P-value for this correlation is ~ 0.00 showing that although the anti-correlation is minimal, the correlation is still significant. Also, the model equations for these Sites (eq.13-14) have R^2 values equal to 0.897 and 0.841 for clay and silt, respectively.

$$\begin{aligned} \text{Clay} = & 0.6101*\text{PW} + 0.0741*\text{NGR} + 0.0010*\text{MS} + 31.6191*\text{GRA} \\ & - 1.4604*\text{L} + 1.9599*\text{A} + 0.1790*\text{B} \end{aligned} \quad (13)$$

$$\begin{aligned} \text{Silt} = & 0.0969*\text{PW} - 0.0710*\text{NGR} + 0.0033*\text{MS} - 2.1494*\text{GRA} \\ & + 1.4918*\text{L} - 2.1082*\text{A} - 0.1918*\text{B} \end{aligned} \quad (14)$$

The primary components for these Sites are pore water and L*. These equations and the primary component analysis then show that Natural Gamma Radiation and Magnetic Susceptibility are not the only experiments required for lithological parameter estimation.

Inspections of the correlation matrix for Sites 983 and 984 (Table 5) shows clay content vs. L* is anti-correlated. The low Gamma Ray Attenuation values indicate unconsolidated sediment with little biogenic influence. The Natural Gamma Radiation vs. L* relationship is positive which implies non-terrigenous sediments; a lighter sediment with higher Natural Gamma Radiation. The L* vs. Magnetic Susceptibility anti-correlation indicate terrigenous sedimentation; darker sediment with high Magnetic Susceptibility and therefore low carbonate. These conflicting results indicate that the sediment had more than one source; fluctuating between terrigenous and non-terrigenous sedimentation. Color variations relate to relative changes in biogenic carbonate, detrital clay, and silt (Jansen, et al., 1996) as seen in Table 5.

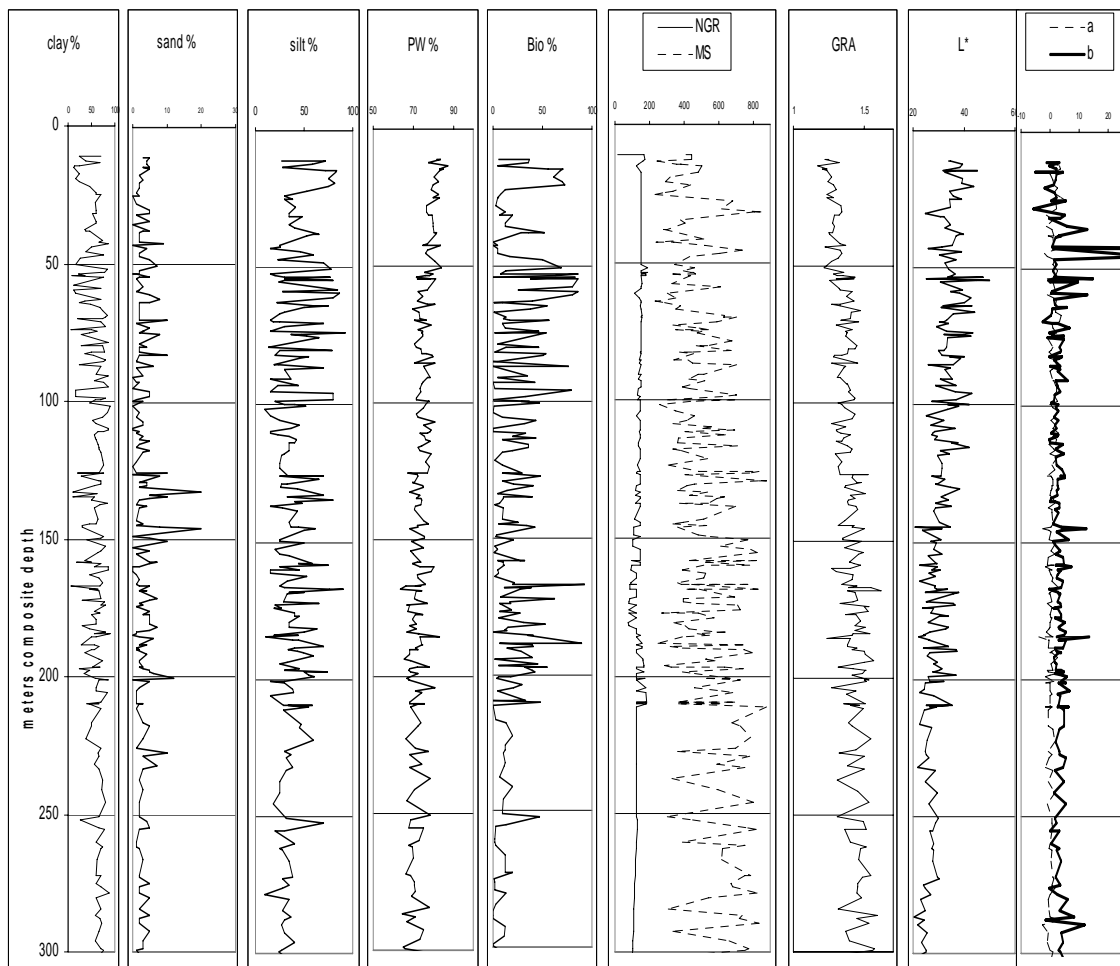


Figure 7. Data for Sites 983, 984 sorted by meters composite depth.

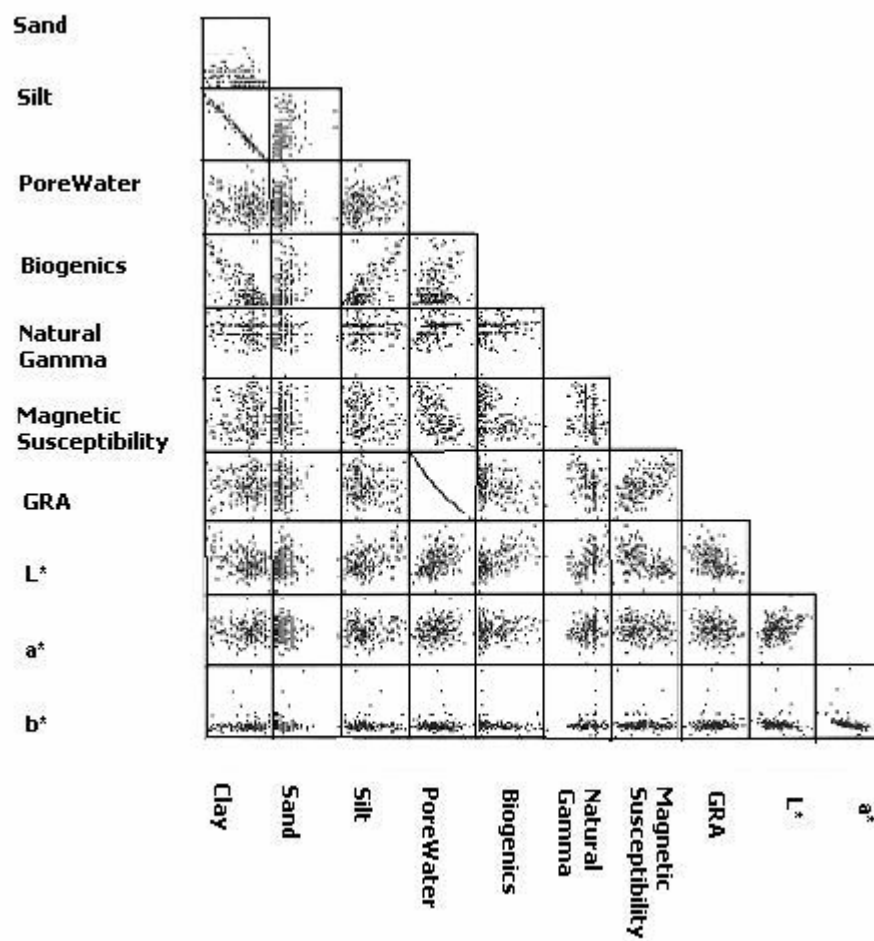


Figure 8. SAS generated scatter plot of Sites 983, 984.

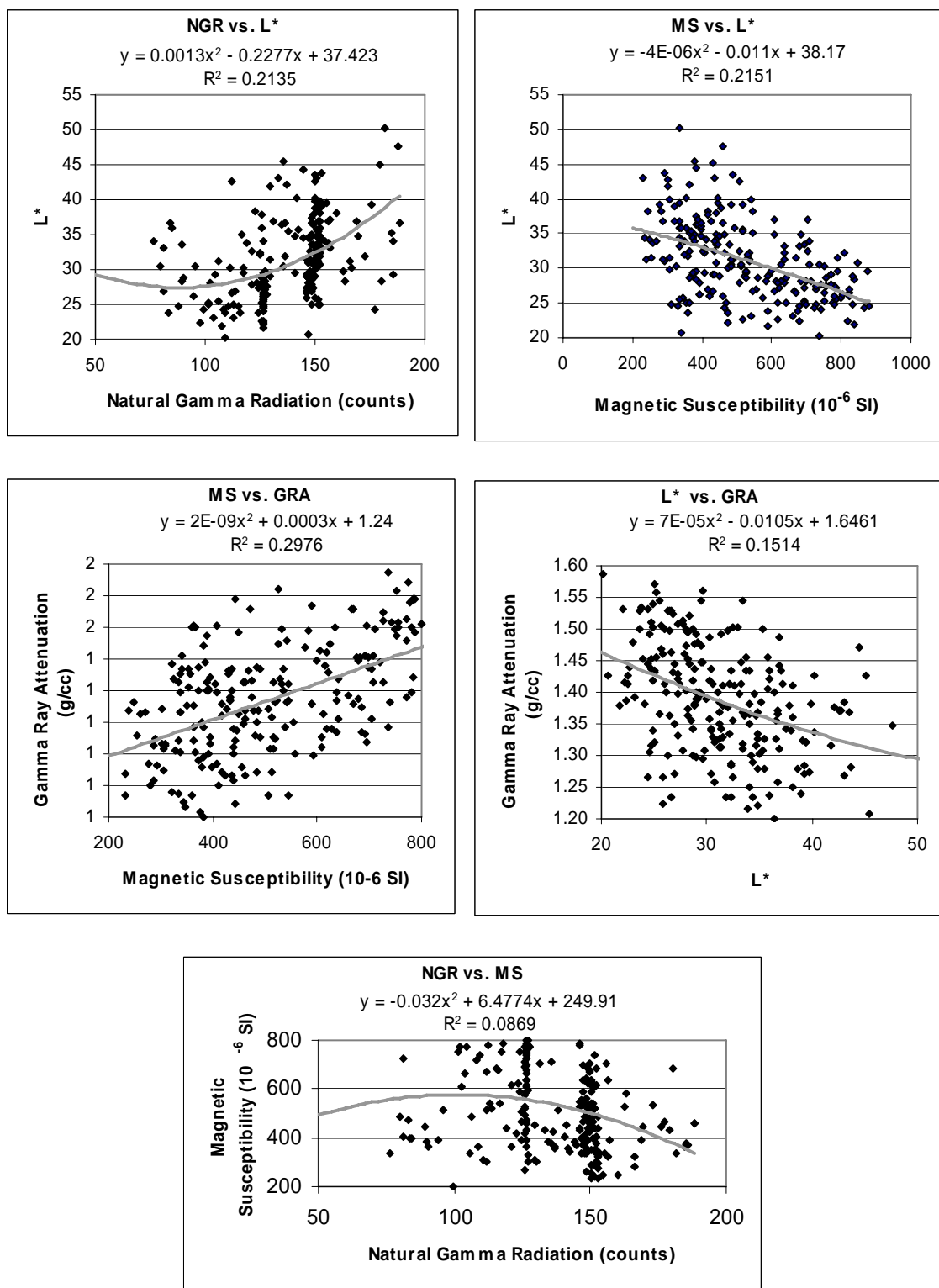


Figure 9: Selected scatter plots (X vs.Y) with quadratic trend curve for Sites 983, 984.

Table 5. Univariate statistics and correlation matrix for Leg 162 Sites 983, 984.

Univariate Statistics											
	N	mean	std dev	minimum	maximum						
Clay	225	56.56	20.78	5.00	90.00						
Sand	225	3.15	2.81	0.00	20.00						
Silt	225	40.22	19.44	10.00	92.00						
PW	225	74.06	4.82	63.52	89.35						
BIO	225	22.76	22.75	0.00	92.00						
NGR	225	136.32	23.44	16.79	188.46						
MS	225	520.36	170.19	199.00	878.00						
GRA	225	1.39	0.09	1.15	1.61						
L*	225	31.14	5.78	15.30	50.20						
a*	225	0.85	1.31	-3.92	5.44						
b*	225	3.43	4.80	-5.68	51.40						

Correlation Matrix											
	Clay	Sand	Silt	PW	BIO	NGR	MS	GRA	L*	a*	b*
Clay		-0.49	-0.98	-0.10	-0.69	-0.06	0.16	0.10	-0.34	-0.01	0.05
Sand	-0.49		0.39	-0.16	0.20	-0.13	-0.05	0.16	-0.02	-0.07	0.04
Silt	-0.98	0.39		0.13	0.71	0.07	-0.16	-0.13	0.37	0.01	0.05
PW	-0.10	-0.16	0.13		0.21	0.30	-0.54	-1.00	0.38	0.22	0.01
BIO	-0.69	0.20	0.71	0.21		0.17	-0.34	-0.21	0.55	0.06	0.09
NGR	-0.06	-0.13	0.07	0.30	0.17		-0.22	-0.32	0.40	0.17	0.03
MS	0.16	-0.05	-0.16	-0.54	-0.34	-0.22		0.54	-0.46	-0.13	0.04
GRA	0.10	0.16	-0.13	-1.00	-0.21	-0.32	0.54		-0.39	-0.22	0.01
L*	-0.34	-0.02	0.37	0.38	0.55	0.40	-0.46	-0.39		0.33	0.14
a*	-0.01	-0.07	0.01	0.22	0.06	0.17	-0.13	-0.22	0.33		0.44
b*	0.05	0.04	-0.05	-0.01	-0.09	0.03	-0.04	0.01	-0.14	-0.44	

P-Values of the Correlations											
	Clay	Sand	Silt	PW	BIO	NGR	MS	GRA	L*	a*	b*
Clay		0.00	0.00	0.12	0.00	0.38	0.02	0.14	0.00	0.83	0.49
Sand	0.00		0.00	0.02	0.00	0.05	0.44	0.02	0.75	0.31	0.52
Silt	0.00	0.00		0.05	0.00	0.29	0.02	0.06	0.00	0.83	0.43
PW	0.12	0.02	0.05		0.00	0.00	0.00	0.00	0.00	0.00	0.83
BIO	0.00	0.00	0.00	0.00		0.01	0.00	0.00	0.00	0.37	0.18
NGR	0.38	0.05	0.29	0.00	0.01		0.00	0.00	0.00	0.01	0.60
MS	0.02	0.44	0.02	0.00	0.00	0.00		0.00	0.00	0.06	0.57
GRA	0.14	0.02	0.06	0.00	0.00	0.00	0.00		0.00	0.00	0.88
L*	0.00	0.75	0.00	0.00	0.00	0.00	0.00	0.00		0.00	0.03
a*	0.83	0.31	0.83	0.00	0.37	0.01	0.06	0.00	0.00		0.00
b*	0.49	0.52	0.43	0.83	0.18	0.60	0.57	0.88	0.03	0.00	

Sites 985 and 907

Sites 985 and 907, revisited from Leg 151, are on the Iceland Plateau. These two Sites investigate the mixing of the Atlantic Ocean and the Norwegian Sea. The purpose of drilling these Sites was to provide an open-ocean record of ice-rafted debris.

Dropstones were frequent and biogenic content scarce. The lithology is silty clay, clay with silt, and clayey mixed sediment with varying amounts of biogenic material.

Lithologies, and therefore data values, vary with depth.

In Figure 3, sites 985 and 907 show silty clay overlying clay or clay with silt. Drilling for Site 907 began at the seafloor, and continued to depth of 225 meters. The data for Site 985 begins at 36 meters and continues through 331 meters depth, thereby the data does not encompass the entire drilled sequence shown in Figure 3.

Figure 10 shows that pore water percentages and clay content are nearly identical in value. Deeper than approximately 230 meters depth, the data changes to a less erratic, more consistent pattern. This pattern coincides with the transition from silty clay to clay or clay with silt. The erratic nature and lack of correlation of the data in Sites 983 and 984 was also produced by the abundance of silty clay. The carbonate lithology of Sites 980-982 was much more predictable, but when this lithology also included silty clay, the data became erratic. The data for Sites 907 and 985 is erratic because of the silty clay, and only calms after the silty clay disappears and clay or clay with silt is the predominant lithological characteristic. For completeness, Figure 11 shows the SAS generated scatter plot for Sites 907 and 985.

The frequency of dropstones would have a substantial effect on the Gamma Ray Attenuation, Magnetic Susceptibility, and Natural Gamma Radiation values. The scatter plot of Natural Gamma Radiation vs. Gamma Ray Attenuation in Figure 12 shows the best correlation (from Table 5) of 0.42 and $R^2=0.682$. The higher Natural Gamma Radiation with a higher density indicates drop stones or compacted terrigenous sediments. Natural Gamma Radiation vs. Magnetic Susceptibility has a correlation value of $R^2=0.26$ that indicates terrigenous and non-terrigenous sediments. Magnetic Susceptibility vs. Gamma Ray Attenuation has a value only slightly worse at $R^2=0.23$. However, the model equations for these Sites (eq.15-16) have R^2 values equal to 0.9615 and 0.7338 for clay and silt, respectively.

$$\begin{aligned} \text{Clay} = & 0.6170*\text{PW} - 0.0322*\text{NGR} - 0.0459*\text{MS} + 26.5662*\text{GRA} \\ & + 0.2117*\text{L} - 1.7366*\text{A} - 0.3891*\text{B} \end{aligned} \quad (15)$$

$$\begin{aligned} \text{Silt} = & -0.446*\text{PW} + 0.0317*\text{NGR} + 0.0265*\text{MS} + 11.7246*\text{GRA} \\ & - 0.0864*\text{L} + 1.3779*\text{A} + 0.4073*\text{B} \end{aligned} \quad (16)$$

Relationships can only be determined by viewing the correlation matrix (Table 6). Sites 985 and 907 show minimal correlation, but very low P-Values indicate that these are significant results even with the frequent dropstones, biogenic content, ash and the abundance of silty clay. Principal component analysis for these Sites indicate the importance of Gamma Ray Attenuation and Natural Gamma Radiation.

Table 6. Univariate statistics and correlation matrix for Leg 162 Sites 985, 907.

Univariate Statistics											
	N	mean	std dev	minimum	maximum						
Clay	177	75.20	16.10	0.00	98.00						
Sand	177	2.62	3.27	0.00	30.00						
Silt	177	22.15	14.47	2.00	98.00						
PW	177	79.71	7.99	56.48	102.09						
BIO	177	5.97	12.59	0.00	94.00						
NGR	177	193.26	49.99	76.56	317.97						
MS	177	79.55	55.64	-30.61	531.00						
GRA	177	1.30	0.14	1.00	1.81						
L*	177	35.04	6.01	11.79	63.64						
a*	177	2.35	2.86	-3.99	13.31						
b*	177	5.01	4.29	-5.70	34.24						
Correlation Matrix											
	Clay	Sand	Silt	PW	BIO	NGR	MS	GRA	L*	a*	b*
Clay		-0.62	-0.98	0.11	-0.63	0.22	-0.18	-0.12	-0.01	-0.25	0.13
Sand	-0.62		0.47	0.08	0.27	0.14	0.32	-0.08	-0.10	0.35	-0.16
Silt	-0.98	0.47		-0.16	0.64	0.23	0.14	0.17	0.03	0.22	-0.12
PW	0.11	0.08	-0.16		0.26	-0.43	-0.26	-0.99	-0.26	0.03	0.33
BIO	-0.63	0.27	0.64	0.26		-0.17	-0.20	-0.26	0.17	0.18	-0.02
NGR	0.22	0.14	0.23	-0.43	-0.17		0.26	0.42	0.01	0.23	-0.27
MS	-0.18	0.32	0.14	-0.26	-0.20	0.26		0.23	0.12	-0.02	-0.12
GRA	-0.12	-0.08	0.17	-0.99	-0.26	0.42	0.23		0.23	0.01	-0.32
L*	-0.01	-0.10	0.03	-0.26	0.17	0.01	0.12	0.23		0.23	-0.38
a*	-0.25	0.35	0.22	0.03	0.18	0.23	-0.02	0.01	0.23		-0.61
b*	0.13	-0.16	-0.12	0.33	-0.02	-0.27	-0.12	-0.32	-0.38	-0.61	
P-Values of the Correlations											
	Clay	Sand	Silt	PW	BIO	NGR	MS	GRA	L*	a*	b*
Clay		0.00	0.00	0.15	0.00	0.00	0.02	0.11	0.92	0.00	0.09
Sand	0.00		0.00	0.28	0.00	0.07	0.00	0.27	0.19	0.00	0.04
Silt	0.00	0.00		0.04	0.00	0.00	0.07	0.02	0.66	0.00	0.12
PW	0.15	0.28	0.04		0.00	0.00	0.00	0.00	0.00	0.61	0.00
BIO	0.00	0.00	0.00	0.00		0.02	0.01	0.00	0.02	0.02	0.77
NGR	0.00	0.07	0.00	0.00	0.02		0.00	0.00	0.92	0.00	0.00
MS	0.02	0.00	0.07	0.00	0.01	0.00		0.00	0.10	0.77	0.12
GRA	0.11	0.27	0.02	0.00	0.00	0.00	0.00		0.00	0.85	0.00
L*	0.92	0.19	0.66	0.00	0.02	0.92	0.10	0.00		0.00	0.00
a*	0.00	0.00	0.00	0.61	0.02	0.00	0.77	0.85	0.00		0.00
b*	0.09	0.04	0.12	0.00	0.77	0.00	0.12	0.00	0.00	0.00	

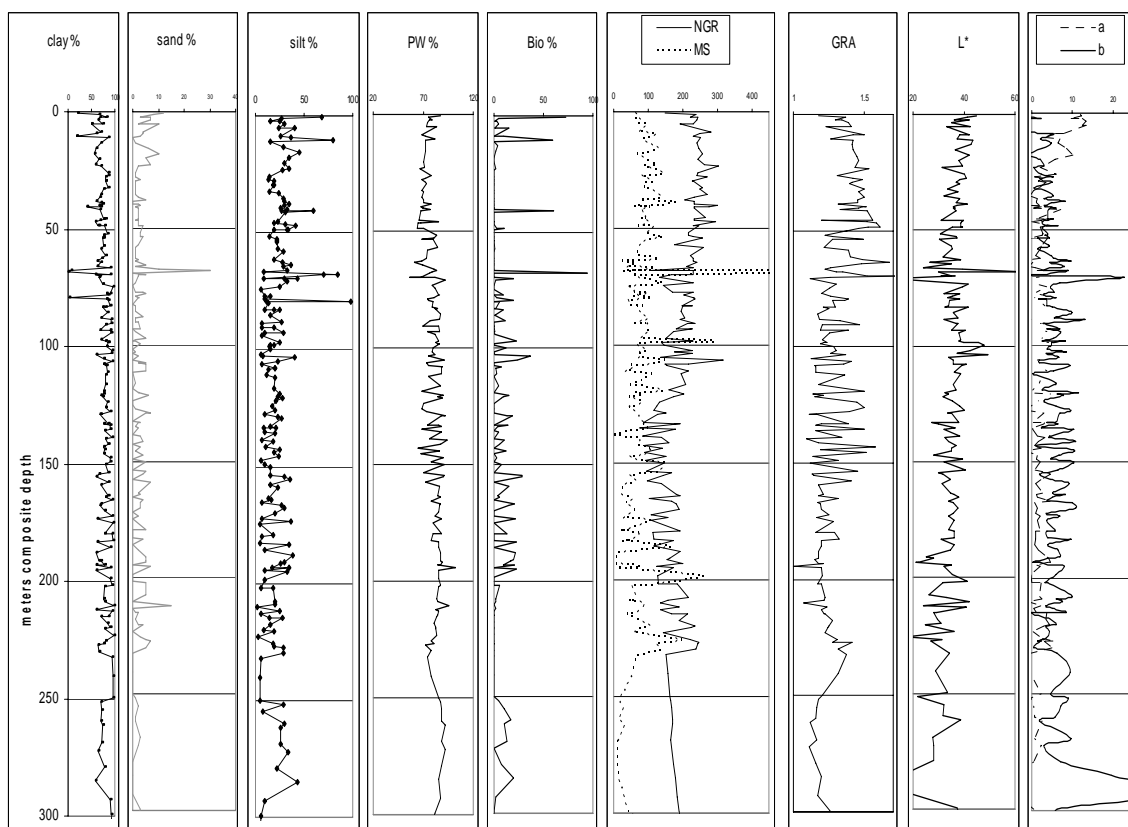


Figure 10. Data for Sites 985, 907 sorted by meters composite depth.

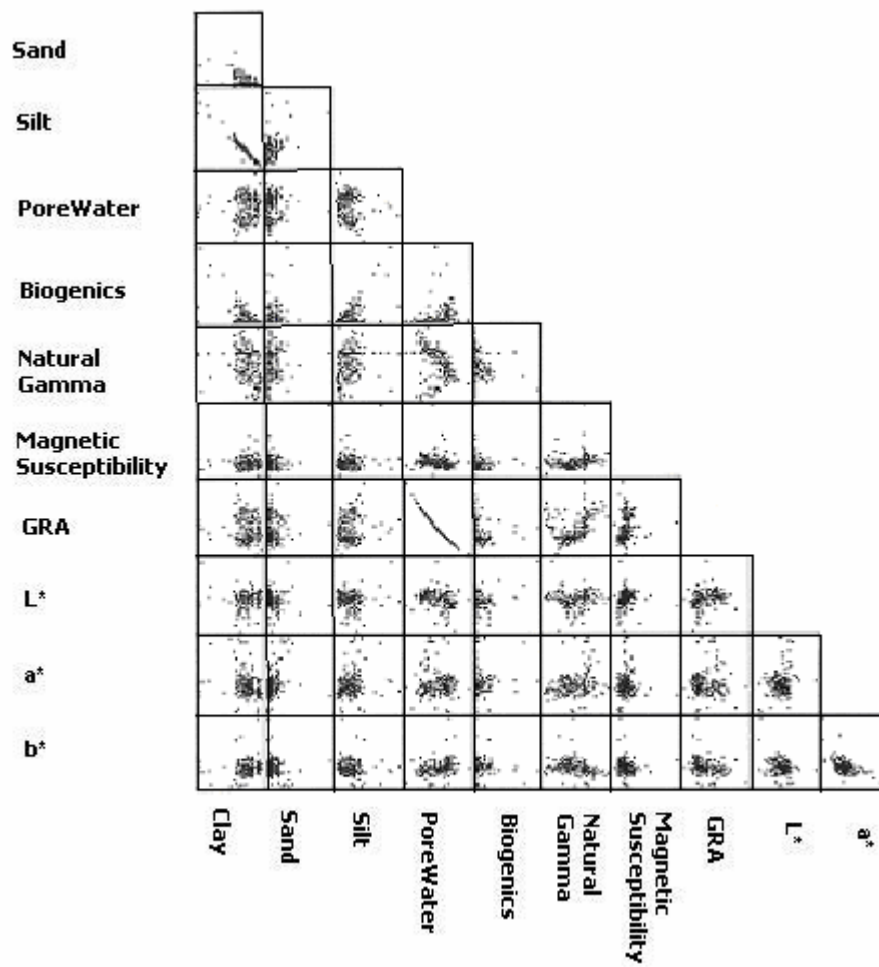


Figure 11. SAS generated scatter plot of Sites 985, 907.

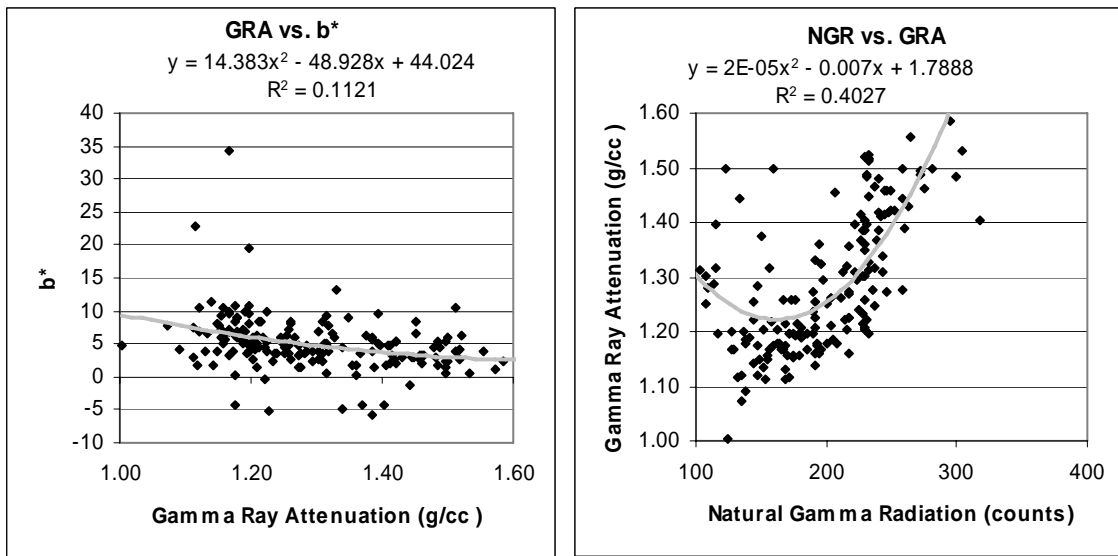


Figure 12: Selected scatter plots (X vs. Y) with quadratic trend curve for Sites 985, 907

Sites 986 and 987

Sites 986 and 987 were drilled to investigate the nature of ice sheets. These two Sites consist of predominately fine-to course-grained siliciclastics with varying amounts of gravel. Dropstones are abundant, many greater than 1 cm. (Jansen, et al., 1996). Intervals barren of biogenic content is predominant, and sedimentation rates appear to be between 160 and 320 m/m.y. Five formations were defined.

Figure 3 shows that the majority of lithology for these two Sites is silty clay. In the study of the previous Sites, silty clay has been shown to provide erratic results and few relationships between experimental data. This erratic behavior is only compounded by the existence of dropstones. From Figure 13, we can see that Natural Gamma Radiation is relatively constant, biogenic content nearly non-existent, and pore water is

approximately 60%. Gamma Ray Attenuation consistently exceeds 1.6 g/cc, the value typical of carbonates. Since Magnetic Susceptibility is high, the high Gamma Ray Attenuation is the effect of either compaction or dropstones rather than the existence of carbonates. The high Magnetic Susceptibility and even higher Natural Gamma Radiation point to terrigenous deposits yet the lack of correlation with the lithology suggests that the effects are from dropstones.

The trend curve for the scatter plot of Magnetic Susceptibility vs. Gamma Ray Attenuation in Figure 14 provides an R^2 value of 0.3306. Table 7 shows Magnetic Susceptibility and Gamma Ray Attenuation to correlate at 54%. The SAS scatter plot in Figure 15 and the related P-Values demonstrates the lack of substantial relationships.

Sites 986 and 987 show minimal correlation because of the abundance of drop stones and silty clay. As seen in the correlation matrix of Table 6, the relationships and significance of the data between experiments are limited. Gamma Ray Attenuation again is the principal component, followed by Magnetic Susceptibility. However, the model equations for these Sites (eq. 17-18) have R^2 values equal to 0.9569 and 0.9148 for clay and silt, respectively.

$$\begin{aligned} \text{Clay} = & 0.3860 \cdot \text{PW} - 0.0529 \cdot \text{NGR} - 0.0249 \cdot \text{MS} + 31.4080 \cdot \text{GRA} \\ & + 0.1479 \cdot \text{L} - 0.2594 \cdot \text{A} - 0.1950 \cdot \text{B} \end{aligned} \quad (17)$$

$$\begin{aligned} \text{Silt} = & 0.1740 \cdot \text{PW} + 0.0543 \cdot \text{NGR} + 0.0060 \cdot \text{MS} + 2.2300 \cdot \text{GRA} \\ & + 0.1048 \cdot \text{L} + 0.4125 \cdot \text{A} + 0.2771 \cdot \text{B} \end{aligned} \quad (18)$$

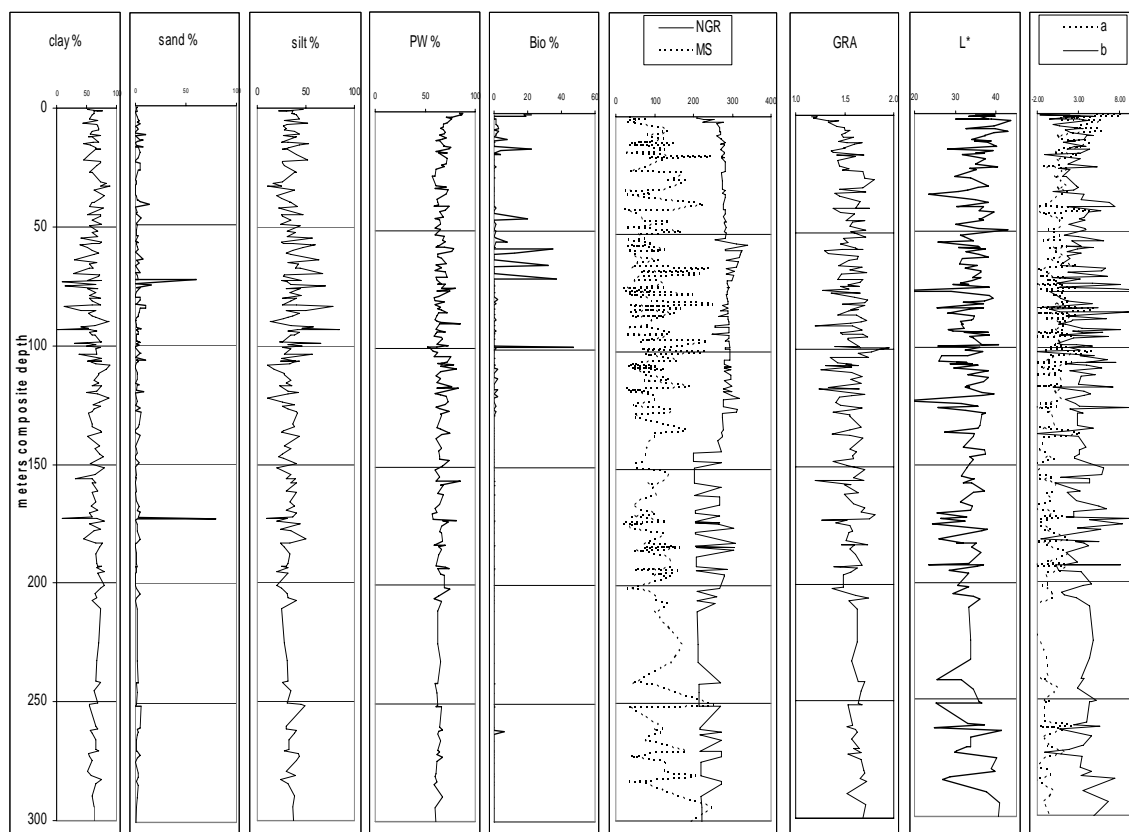


Figure 13. Data for Sites 986, 987 sorted by meters composite depth.

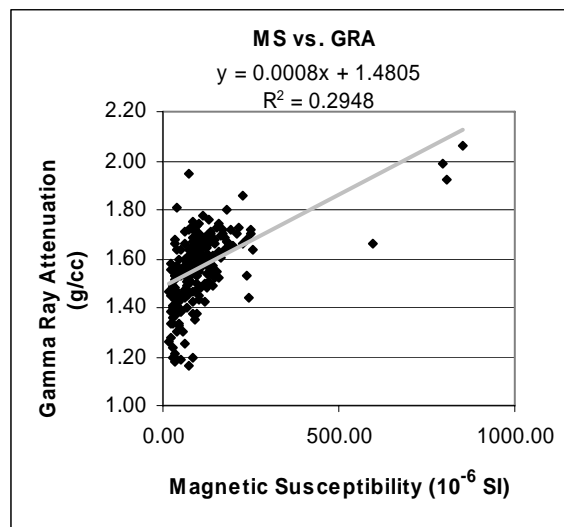


Figure 14: Selected scatter plot (X vs. Y) with quadratic trend curve for Sites 986, 987.

Table 7. Univariate statistics and correlation matrix for Leg 162 Sites 986, 987.

Univariate Statistics											
	N	mean	std dev	minimum	maximum						
Clay	221	62.13	13.50	1.00	89.00						
Sand	221	3.02	7.19	0.00	80.00						
Silt	221	34.66	10.81	10.00	85.00						
PW	221	66.20	6.55	49.71	87.90						
BIO	221	1.49	5.95	0.00	47.00						
NGR	221	267.05	32.19	200.73	340.40						
MS	221	106.06	104.52	18.00	852.00						
GRA	221	1.55	0.15	1.17	2.06						
L*	221	33.81	4.46	12.22	43.61						
a*	221	0.19	1.90	-3.95	8.25						
b*	221	3.31	2.36	-2.36	13.29						

Correlation Matrix											
	Clay	Sand	Silt	PW	BIO	NGR	MS	GRA	L*	a*	b*
Clay		-0.56	-0.82	-0.07	-0.32	-0.12	-0.08	0.05	0.05	-0.03	-0.04
Sand	-0.56		0.05	0.08	0.00	0.07	0.13	-0.05	-0.16	-0.04	0.11
Silt	-0.82	0.05		0.06	0.40	0.15	0.01	-0.06	0.03	0.08	0.00
PW	-0.07	0.08	0.06		0.32	0.03	-0.48	-0.99	-0.02	0.25	-0.19
BIO	-0.32	0.00	0.40	0.32		0.10	-0.12	-0.31	0.08	0.10	-0.03
NGR	-0.12	0.07	0.15	0.03	0.10		-0.16	-0.06	-0.16	0.12	-0.05
MS	-0.08	0.13	0.01	-0.48	-0.12	-0.16		0.54	0.05	-0.10	0.28
GRA	0.05	-0.05	-0.06	-0.99	-0.31	-0.06	0.54		0.01	-0.24	0.20
L*	0.05	-0.16	0.03	-0.02	0.08	-0.16	0.05	0.01		0.29	-0.22
a*	-0.03	-0.04	0.08	0.25	0.10	0.12	-0.10	-0.24	0.29		-0.67
b*	-0.04	0.11	0.00	-0.19	-0.03	-0.05	0.28	0.20	-0.22	-0.67	

P-Values of the Correlations											
	Clay	Sand	Silt	PW	BIO	NGR	MS	GRA	L*	a*	b*
Clay		0.00	0.00	0.31	0.00	0.07	0.23	0.42	0.44	0.67	0.59
Sand	0.00		0.49	0.27	0.98	0.31	0.05	0.45	0.02	0.57	0.10
Silt	0.00	0.49		0.39	0.00	0.02	0.88	0.39	0.71	0.26	0.96
PW	0.31	0.27	0.39		0.00	0.62	0.00	0.00	0.79	0.00	0.00
BIO	0.00	0.98	0.00	0.00		0.13	0.09	0.00	0.23	0.12	0.63
NGR	0.07	0.31	0.02	0.62	0.13		0.02	0.38	0.02	0.09	0.45
MS	0.23	0.05	0.88	0.00	0.09	0.02		0.00	0.45	0.12	0.00
GRA	0.42	0.45	0.39	0.00	0.00	0.38	0.00		0.88	0.00	0.00
L*	0.44	0.02	0.71	0.79	0.23	0.02	0.45	0.88		0.00	0.00
a*	0.67	0.57	0.26	0.00	0.12	0.09	0.12	0.00	0.00		0.00
b*	0.59	0.10	0.96	0.00	0.63	0.45	0.00	0.00	0.00	0.00	

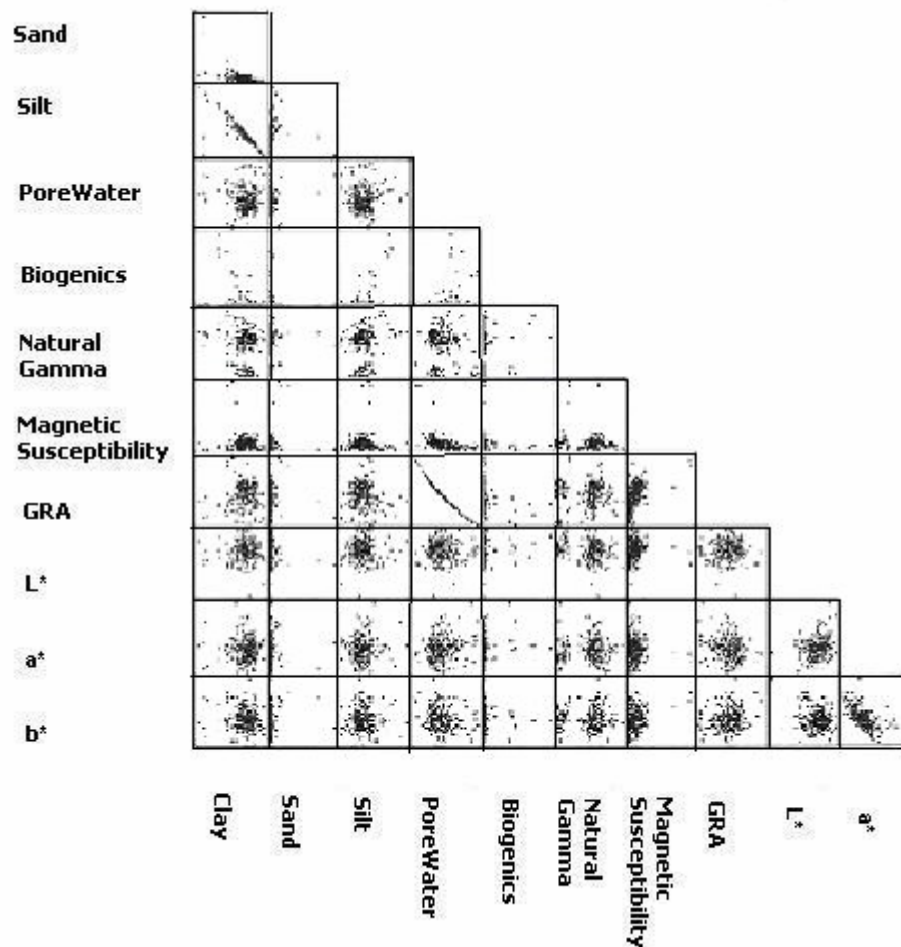


Figure 15. SAS generated scatter plot of Sites 986, 987.

Leg 162 All Sites

We have seen that the carbonate lithology of Sites 980-982 has very good correlation between Magnetic Susceptibility, Natural Gamma Radiation, biogenic content, and silt. Sites 983 and 984 are distinguished by very high Magnetic Susceptibility. Sites 907 and 985 have erratic data behavior, in part caused by the abundance of silty clay in the majority of the data accumulated. Sites 986 and 987 also

have major accumulations of silty clay, but also have rare biogenic content and the added complication of frequent dropstones.

For completeness, scatter plots for the entire Leg are included as Figures 16 and 17. Although the correlation matrix of Table 8 shows few excellent correlations, the P-values are overall low, indicating the high significance of the correlations. The principal component analysis for the entire Leg is L*. Considering that L* was not the principal component for the individual Site analysis, having L* as the principal component for the entire Leg is unexpected. The model equations for this Leg (eq.19-20) have R² values equal to 0.9083 and 0.8426 for clay and silt, respectively.

$$\begin{aligned} \text{Clay} = & 0.8528*\text{PW} - 0.0156*\text{NGR} - 0.0246*\text{MS} + 32.4970*\text{GRA} \\ & - 01.1090*\text{L} - 0.20757*\text{A} + 0.0446*\text{B} \end{aligned} \quad (19)$$

$$\begin{aligned} \text{Silt} = & -0.1579*\text{PW} + 0.0184*\text{NGR} + 0.254*\text{MS} + 1.1303*\text{GRA} \\ & + 1.0514*\text{L} - 0.3349*\text{A} - 0.1865*\text{B} \end{aligned} \quad (20)$$

Considering the varied depositional history for this Leg, the model equations are quite accurate.

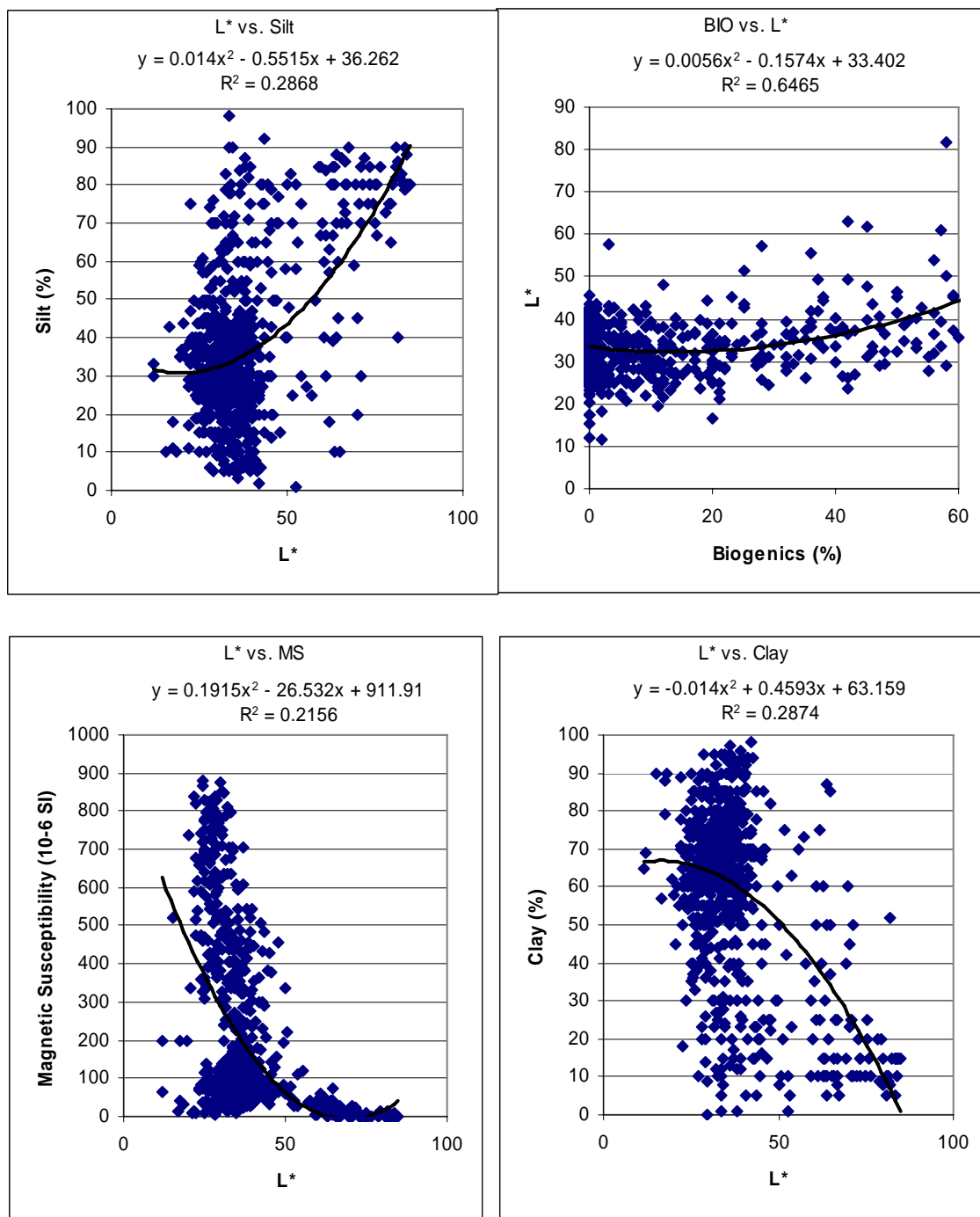


Figure 16: Selected scatter plots (X vs. Y) with quadratic trend curve for Leg 162.

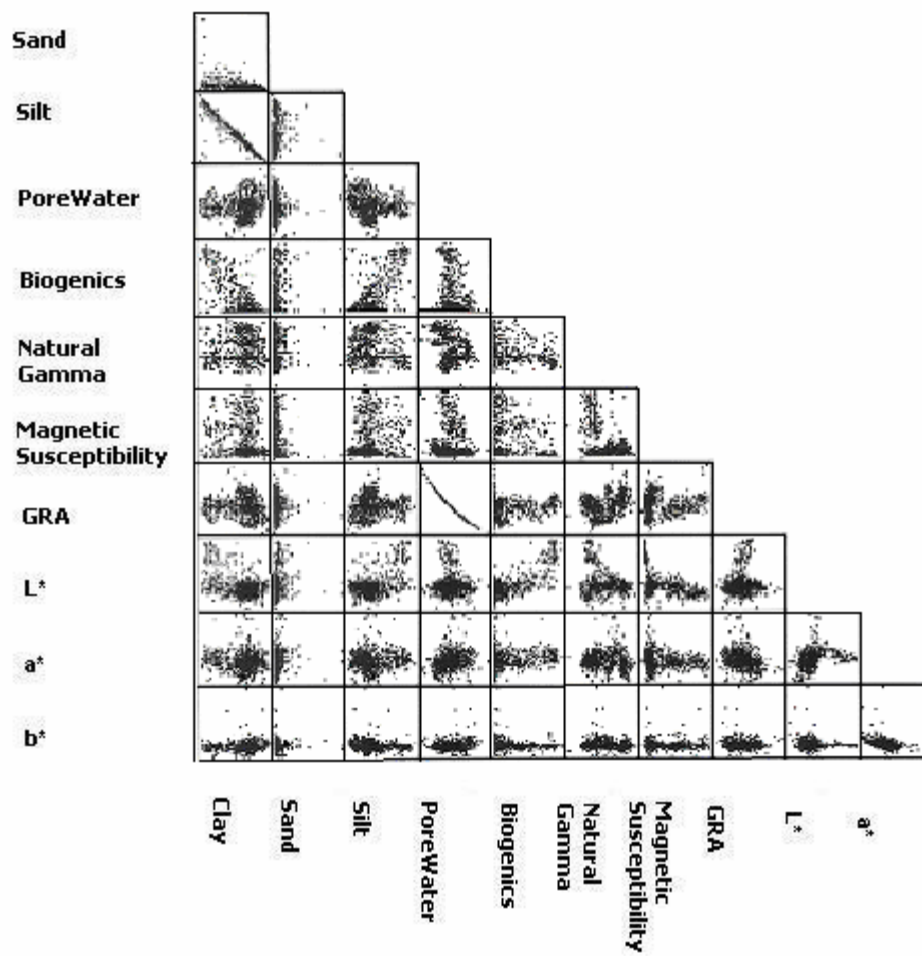


Figure 17. SAS generated scatter plot for Leg 162.

Table 8. Univariate statistics and correlation matrix for Leg 162.

Univariate Statistics											
	N	mean	std dev	minimum	maximum						
Clay	755	58.19	23.07	0.00	98.00						
Sand	755	3.99	6.25	0.00	80.00						
Silt	755	37.71	20.92	1.00	98.00						
PW	755	72.65	7.84	49.71	102.09						
BIO	755	20.85	30.32	0.00	105.00						
NGR	755	193.39	65.05	16.79	340.40						
MS	755	215.09	231.05	-30.61	878.00						
GRA	755	1.43	0.15	1.00	2.06						
L*	755	37.75	12.85	11.79	84.94						
a*	755	1.37	2.21	-3.99	13.31						
b*	755	3.72	3.69	-5.70	51.40						

Correlation Matrix											
	Clay	Sand	Silt	PW	BIO	NGR	MS	GRA	L*	a*	b*
Clay		-0.45	-0.95	0.14	-0.73	0.17	0.02	-0.11	-0.52	-0.12	0.12
Sand	-0.45		0.23	0.00	0.31	-0.06	-0.07	-0.01	0.20	0.18	-0.02
Silt	-0.95	0.23		-0.16	0.71	-0.17	0.00	0.13	0.51	0.08	-0.13
PW	0.14	0.00	-0.16		0.09	-0.37	-0.07	-0.99	-0.05	0.28	0.16
BIO	-0.73	0.31	0.71	0.09		-0.43	-0.11	-0.12	0.74	0.24	-0.09
NGR	0.17	-0.06	-0.17	-0.37	-0.43		-0.43	0.39	-0.21	-0.04	-0.07
MS	0.02	-0.07	0.00	-0.07	-0.11	-0.43		0.04	-0.42	-0.18	-0.05
GRA	-0.11	-0.01	0.13	-0.99	-0.12	0.39	0.04		0.02	-0.29	-0.14
L*	-0.52	0.20	0.51	-0.05	0.74	-0.21	-0.42	0.02		0.28	-0.13
a*	-0.12	0.18	0.08	0.28	0.24	-0.04	-0.18	-0.29	0.28		-0.39
b*	0.12	-0.02	-0.13	0.16	-0.09	-0.07	-0.05	-0.14	-0.13	-0.39	

P-Values of the Correlations											
	Clay	Sand	Silt	PW	BIO	NGR	MS	GRA	L*	a*	b*
Clay		0.00	0.00	0.00	0.00	0.00	0.51	0.00	0.00	0.00	0.00
Sand	0.00		0.00	0.94	0.00	0.13	0.07	0.74	0.00	0.00	0.63
Silt	0.00	0.00		0.00	0.00	0.00	0.90	0.00	0.00	0.02	0.00
PW	0.00	0.94	0.00		0.02	0.00	0.07	0.00	0.18	0.00	0.00
BIO	0.00	0.00	0.00	0.02		0.00	0.00	0.00	0.00	0.00	0.02
NGR	0.00	0.13	0.00	0.00	0.00		0.00	0.00	0.00	0.23	0.05
MS	0.51	0.07	0.90	0.07	0.00	0.00		0.27	0.00	0.00	0.21
GRA	0.00	0.74	0.00	0.00	0.00	0.00	0.27		0.52	0.00	0.00
L*	0.00	0.00	0.00	0.18	0.00	0.00	0.00	0.52		0.00	0.00
a*	0.00	0.00	0.02	0.00	0.00	0.23	0.00	0.00	0.00		0.00
b*	0.00	0.63	0.00	0.00	0.02	0.05	0.21	0.00	0.00	0.00	

CHAPTER V

SUMMARY AND CONCLUSIONS

The 4 variations in lithology examined for the thesis all appear to fit well with the individual Site characteristics. By observing the physical properties, one may develop an educated guess as to the lithology and the nature of the sediment.

I have shown that Magnetic Susceptibility is an indicator of clay (if Natural Gamma Radiation and Magnetic Susceptibility are high), and carbonates if Magnetic Susceptibility is negative. Natural Gamma Radiation only indicates dropstones or clay. Reflectance, coupled with Natural Gamma Radiation, indicates a combination of carbonates (if Natural Gamma Radiation and Magnetic Susceptibility are low and the core has a high L^*) or clay (if Natural Gamma Radiation is high and L^* is low). Gamma Ray Attenuation estimates the compaction of the lithology and, if Gamma Ray Attenuation is high, carbonates.

By comparing physical properties data to the lithologies studied, we arrive at conclusions regarding the paleoenvironmental history of that region. Dropstones and ice – rafted debris can provide high Natural Gamma Radiation and Magnetic Susceptibility values that tend to contradict the other physical property relationships. Conflicting relationships can indicate lithological units that were subject to different depositional histories, e.g. glacial vs. interglacial or oceanic vs. terrigenous influences.

The value in this thesis is the creation of model equations and the principal components. The correlations between physical property data and the lithology do not

rely on a single experiment. The correlations may be significant, but not easily seen. While one physical property experiment can aid in interpretation of a particular lithology, all experiments provide a piece of the puzzle and lithologic determination regarding clay and silt content would not be possible if a piece were missing.

Practical use of this thesis has been invaluable in data verification efforts. Often shipboard data is mistyped and verification can help us to correct those errors. If the physical properties values do not pair well with the lithology, often the data has been misidentified or intended as test data, so further investigation is required. This method also provides a check for data acquisition or equipment problems. Optimally, all data would be collected, collected in the same format, and at a reasonable frequency or interval, to easily allow comparison between Legs.

REFERENCES

- American Society for Testing and Materials, 1996, Standard Practice for Computing the Colors of Objects by Using the CIE System: AMST Designation E 308 – 96.
- Balsam, W.L., Deaton, R.C., and Damuth, J.E., 1997, The Effects of Water Content on Diffuse Reflectance Measurements of Deep-Sea Core Samples: An Example from ODP Leg 164 Sediments, *Marine Geology*, **149**, 177-189.
- Berger, W. H., Wefer, G., Lange, C.B., Giraudeau, J., Hermelin, O., et al., 1998, The Angola-Benguela Upwelling System: Paleoceanographic Synthesis of Shipboard Results from Leg 175 *in* Wefer, G., Berger, W.H., Richter, C., Adams, D.D., Anderson, L.D., et al., 1998, Proceedings of the Ocean Drilling Program, Initial Reports 175: Ocean Drilling Program, College Station, Texas.
- Berger-Schunn, Anni, 1994, Practical Color Measurement: A Primer for the Beginner, A Reminder for the Expert: John Wiley and Sons.
- Blum, P., 1997, Physical Properties Handbook: Ocean Drilling Program, College Station, Texas.
- Channell, J.E.T., and Lehman, B., 1999, Magnetic Stratigraphy of North Atlantic Sites 980-984 *in* Raymo, M.E., Jansen, E., Blum, P., Anderson, E.S., Austin, W.E.N., et al., 1999, Proceedings of the Ocean Drilling Program, Scientific Results 162: Ocean Drilling Program, College Station, Texas.
- Higgins, S.M., Kreitz, S., King, T., and Goldberg, D., 1999, Data Report: Magnetic Polarity and Susceptibility Measurements from the Geological High-Resolution

- Magnetometer Tool at Sites 984, 986, and 987 *in* Raymo, M.E., Jansen, E., Blum, P., Anderson, E.S., Austin, W.E.N., et al., 1999, Proceedings of the Ocean Drilling Program, Scientific Results 162: Ocean Drilling Program, College Station, Texas.
- Jansen, E., Raymo, M.E., Blum, P., Anderson, E.S., Austin, W.E.N., et al., 1996, Proceedings of the Ocean Drilling Program, Initial Reports, 162: Ocean Drilling Program, College Station, Texas.
- Mazzullo, J., Graham, A., 1988, Handbook for Shipboard Sedimentologists-Technical Note No.8: Ocean Drilling Program, College Station, Texas.
- Milton, J.S., Arnold, J.C., 1995, Introduction to Probability and Statistics: Principles and Applications for Engineering and the Computing Sciences: Irwin, McGraw-Hill.
- Ortiz, J., O'Connell, S., Mix, A., 1999, Data Report: Spectral Reflectance Observations from Recovered Sediments *in* Raymo, M.E., Jansen, E., Blum, P., Anderson, E.S., Austin, W.E.N., et al., 1999, Proceedings of the Ocean Drilling Program, Scientific Results 162: Ocean Drilling Program, College Station, Texas.
- Ortiz, J. D., and Rack, F.R., 1999, Non-invasive Sediment Monitoring Methods: Current and Future Tools for High-Resolution Climate Studies *in* Abrantes, F., and Mix, A.C., Eds., 1999, Reconstructing Ocean History: A Window into the Future: Kluwer Academic/Plenum Publishers.
- Robinson, S.G., 1993, Lithostratigraphic Applications for Magnetic Susceptibility Logging of Deep Sea Sediment Cores: Examples from ODP Leg 115, *in*

Hailwood, E.A., and Kidd, R.B., Eds., High Resolution Stratigraphy, 70:
Geological Society London.

Smith, L.I., 2002, A Tutorial on Principal Component Analysis, retrieved 12/5/05 from
http://www.cs.otago.ac.nz/cosc453/student_tutorials/principal_components.pdf

Vidal, L., Breuchert, V., Wefer, G., Berger, W.H., Richter, C., et al., 1998, Regional and
Stratigraphic Patterns in Color Reflectance of Sediments from Leg 175, *in*
Wefer, G., Berger, W.H., Richter, C., Adams, D.D., Anderson, L.D., et al., 1998,
Proceedings of the Ocean Drilling Program, Initial Reports 175: Ocean Drilling
Program, College Station, Texas.

Wefer, G., Berger, W.H., Richter, C., Adams, D.D., Anderson, L.D., et al., 1998,
Proceedings of the Ocean Drilling Program, Initial Reports 175: Ocean Drilling
Program, College Station, Texas.

Wyszecki, G., and Stiles, W.S., 1982, Color Science: Concepts and Methods,
Quantitative Data and Formulae: John Wiley and Sons.

APPENDIX A

ACRONYMS

a*	Calculated color reflectance parameter sensitive to water content, oxidation of greenish materials, and grain size making them sensitive to clay mineralogy. Core hue.
b*	Calculated color reflectance parameter sensitive to water content, oxidation of greenish materials, and grain size making them sensitive to clay mineralogy. Core chromaticity.
BIO	Biogenic content. The percentage of biogenic material in a location of the drilled sequence.
CIELAB	Numerical color values that represent a cylindrical coordinate system.
GRA	Gamma Ray Attenuation
GRAPE	Gamma Ray Attenuation Porosity Evaluator-- replaced by GRA in name only.
Hole	A Site can contain many Holes. The Holes are actual drilled areas in the vicinity of a Site.
JOI	Joint Oceanographic Institutions. They are the governing body for the Ocean Drilling Program.
L*	Calculated color reflectance parameter sensitive to water content with a small grain size and homogenization effect including carbonate content. Core lightness.
Leg	Generally a two month voyage
mbsf	Meters Below Sea Floor from which the sample was recovered.
mcd	Meters Composite Depth. For each Site, the Holes are combined such that one depth, the mcd, will describe all the Holes for a particular period in time.
MS	Magnetic Susceptibility

Munsell Values	Legacy method of estimating color of sediments by visual comparison with chips on a color chart. [Example 5GY7/1]
NGR	Natural Gamma Radiation
ODP	The Ocean Drilling Program
PCA	Principal Component Analysis—a linear algebra method to determine the most significant data component in a multivariate analysis.
PW	Pore water. The percentage of pore water in a location of the drilled sequence. I calculated this from the GRA values.
RSC	Color Reflectance experiment that flashes a Xenon arc lamp and measures the percent of light reflected back to the equipment in 10 nm increments.
SAS	Computerized statistical program created by the SAS Institute
SCAT	Oregon State University color reflectometer. Not standard ODP equipment but the data can be manipulated to correspond to RSC.
Site	A Leg can contain many Sites. A Site is a general area for drilling.
SS	Smear Slide. Sedimentologist determined percentages of the lithology by smearing a small quantity of sediment on a microscope slide and counting particles of a particular size.
SSE	Sum of squares as a measure of random or unexplained variability for regression analysis.
SST	Total sum of squares of the differences between each point $(Y_i)^2$ and its mean $(\hat{Y}_i)^2$ (for regression analysis).

LEG 162 DATA

Site	Hole	mbsf	med	clay	sand	silt	PW	Bio	NGR	MS	GRA	L	a	b
907	B	0.1	0.43	20	12	68	87.07	73	147.78	61.57	1.18	44.92	12.06	-4.42
907	B	1	1.33	65	8	27	74.80	5	237.95	68.17	1.37	41.19	12.30	-4.34
907	C	2.3	2.3	82	3	15	79.07	1	223.57	73.31	1.30	36.04	9.59	2.35
907	B	2	2.33	68	7	25	76.53	3	243.00	61.69	1.34	42.09	12.34	-4.98
907	C	3.3	3.3	63	7	30	73.88	5	240.00	78.55	1.39	34.95	13.31	-5.70
907	B	3.5	5.07	74	2	24	72.99	1	230.12	71.00	1.40	42.24	12.44	-4.40
907	C	5.3	5.3	50	10	40	83.46	15	192.05	97.03	1.23	33.18	13.26	-5.32
907	B	7.32	8.89	70	4	26	68.40	0	281.13	70.00	1.50	42.04	7.84	1.49
907	C	8.18	9.04	59	4	37	72.06	9	249.86	125.03	1.42	38.35	5.84	5.26
907	C	9.58	10.44	17	3	80	81.35	59	229.85	109.27	1.26	37.16	3.42	3.53
907	B	9.3	10.87	85	0	15	72.09	0	251.93	83.27	1.42	43.58	6.98	1.97
907	B	11.55	13.12	70	1	29	72.57	4	241.74	98.71	1.41	42.69	6.47	4.81
907	C	14.58	15.44	59	6	45	72.14	2	247.86	129.75	1.42	36.62	8.60	2.51
907	B	15.7	17.85	55	10	35	71.01	0	257.74	68.79	1.44	42.10	10.05	-1.37
907	C	17.9	20.09	65	5	30	70.14	0	244.92	93.06	1.46	37.87	5.72	2.18
907	B	20.4	22.55	58	7	35	71.61	2	262.90	124.93	1.43	39.60	2.89	3.03
907	C	20.9	23.09	70	2	28	66.81	0	304.60	88.00	1.53	31.42	2.17	0.47
907	B	23.84	25.99	85	1	14	78.17	0	243.22	146.34	1.31	40.10	5.99	2.34
907	B	25.22	27.37	86	1	13	72.11	0	240.43	79.63	1.42	40.94	0.74	5.25
907	B	25.69	27.84	80	1	19	68.91	0	271.65	85.97	1.49	38.31	2.74	1.85
907	C	27.4	29.35	79	3	18	72.42	0	226.49	114.20	1.41	36.97	1.56	3.31
907	C	27.8	29.75	80	1	19	73.40	0	231.18	89.20	1.40	38.33	3.37	5.17
907	C	30.4	32.35	85	1	14	68.39	0	258.88	85.80	1.50	33.56	1.79	0.57
907	B	31.06	33.21	75	1	24	70.23	0	248.85	107.47	1.46	37.50	0.46	3.28
907	C	33.4	35.35	70	1	29	68.45	0	271.45	130.20	1.50	32.02	-0.46	5.37
907	B	34.9	37.97	60	5	35	70.47	0	206.78	76.57	1.45	36.79	1.13	8.27
907	B	36.77	39.84	65	2	33	69.08	0	300.00	60.03	1.48	35.79	-0.11	2.90
907	C	37.2	40.38	70	3	27	70.09	0	275.82	104.50	1.46	36.62	2.38	3.24
907	C	42.28	45.46	75	2	23	65.85	0	264.67	93.00	1.56	31.17	1.11	3.99
907	B	42.7	46.77	57	2	41	64.65	0	295.14	101.20	1.58	38.72	0.09	2.49
907	C	46.3	48.8	77	4	19	70.19	0	246.70	117.86	1.46	35.48	2.05	2.51
907	C	49.3	51.8	83	3	14	83.66	0	217.01	93.42	1.22	30.48	2.74	4.00
907	B	48.7	52.77	75	3	22	80.42	0	217.64	107.74	1.27	36.73	2.45	3.22
907	C	51.24	53.74	74	4	22	80.19	0	258.40	97.66	1.28	30.11	3.91	1.38
907	B	52.4	56.97	75	2	23	84.42	1	177.45	73.00	1.21	34.93	2.24	4.46
907	C	54.2	58.22	70	1	29	73.78	0	260.03	70.07	1.39	35.35	2.10	1.33
907	C	57.42	61.44	80	1	19	73.30	0	221.76	66.19	1.40	31.82	0.86	4.87
907	C	60.3	64.32	70	1	29	69.24	0	240.48	64.84	1.48	35.02	0.12	4.38
907	B	60.78	66.05	62	5	33	81.14	0	211.57	35.50	1.26	24.22	-0.68	8.08
907	B	62.44	67.71	5	10	85	78.65	94	108.20	28.38	1.30	63.64	3.32	2.72
907	C	65.25	69.89	68	2	30	81.33	20	166.93	64.00	1.26	36.47	3.75	4.66
907	B	65.5	70.77	65	2	33	91.82	2	132.20	64.40	1.12	11.79	1.05	22.86
907	C	69.85	74.49	96	0	6	81.72	0	144.36	37.73	1.25	39.28	3.72	4.60
907	B	71.51	77.19	89	1	10	85.58	9	171.38	58.50	1.20	32.07	1.24	5.49
907	C	73.12	78.3	85	5	10	81.21	3	203.54	57.28	1.26	35.38	2.48	2.68
907	B	74.4	80.08	85	2	13	80.19	6	236.16	40.03	1.28	34.46	1.32	3.56
907	C	77.54	82.72	90	0	10	79.07	2	198.15	47.40	1.30	33.78	3.21	3.74
907	B	77.52	83.2	74	1	25	81.92	9	200.60	67.62	1.25	41.62	1.99	5.10
907	B	79.5	85.52	84	1	15	87.75	1	196.08	70.40	1.17	35.84	0.97	9.83
907	B	81.9	87.92	69	4	27	86.49	11	205.08	99.42	1.18	37.78	1.54	5.63
907	C	82.75	88.52	92	1	7	76.99	0	192.03	85.00	1.33	32.12	-0.48	13.18
907	C	84.65	90.42	92	1	7	69.95	0	236.76	54.50	1.46	36.98	0.25	3.23
907	B	84.5	90.52	79	2	19	85.08	0	215.19	94.00	1.20	37.77	2.24	2.80
907	B	86.94	92.96	68	3	29	85.98	1	182.39	102.44	1.19	34.88	1.56	7.00
907	C	88.42	94.19	92	1	7	81.41	1	173.63	97.00	1.26	37.99	3.75	7.04
907	B	90.4	97.03	70	5	25	85.19	23	151.64	76.80	1.20	38.79	2.62	5.31
907	B	91.9	98.53	85	1	14	86.27	0	138.66	68.67	1.19	45.66	4.16	4.92
907	C	93.48	99.78	82	3	15	79.72	12	147.21	66.45	1.28	47.96	4.12	4.77
907	C	96.64	102.94	91	1	8	81.27	1	175.96	68.50	1.26	37.29	3.82	8.42
907	B	98.57	105.13	75	2	23	91.31	24	134.78	70.41	1.12	34.01	3.45	6.78
907	B	101.41	107.97	79	2	20	89.11	8	149.45	50.80	1.15	41.05	3.34	7.92
907	C	101.45	108.28	82	5	13	88.66	2	154.37	59.20	1.16	39.21	1.73	9.40

Site	Hole	mbsf	mcd	clay	sand	silt	PW	Bio	NGR	MS	GRA	L	a	b
907	C	104.22	111.05	83	5	12	88.40	3	217.68	32.03	1.16	36.11	3.71	5.20
907	B	109.14	116.37	80	1	19	86.85	5	207.45	47.86	1.18	35.85	1.94	5.88
907	C	112.96	120.38	75	2	23	89.90	15	191.00	63.00	1.14	32.31	-1.08	11.52
907	B	113.6	120.83	70	2	28	84.63	9	203.96	77.35	1.21	34.05	4.50	6.30
907	B	114.4	121.63	73	6	21	88.89	8	174.40	43.16	1.15	31.70	3.04	7.72
907	B	120.7	129.09	70	7	23	92.09	13	153.09	65.32	1.11	33.62	2.71	7.36
907	C	120.95	129.15	68	5	27	87.82	19	127.20	65.33	1.17	35.12	3.09	6.91
907	C	125	133.2	76	3	21	85.76	14	176.05	93.00	1.19	27.25	3.34	3.57
907	B	125.2	133.59	90	2	9	88.28	4	193.74	84.17	1.16	29.75	2.99	6.44
907	B	127.2	135.91	78	2	20	88.50	5	179.29	47.48	1.16	31.99	0.28	10.37
907	C	130.15	139.45	79	3	18	93.77	10	138.56	78.00	1.09	32.61	3.28	4.17
907	B	132.7	141.41	85	4	11	87.19	6	158.89	67.72	1.17	34.11	1.52	10.83
907	C	134.85	144.15	78	3	19	86.20	12	141.50	104.50	1.19	34.94	2.25	7.31
907	B	137.8	147.27	90	4	6	90.26	3	152.40	45.58	1.13	28.21	1.35	6.69
907	B	140.72	150.19	80	5	15	91.43	8	146.66	149.41	1.12	32.02	2.05	10.40
907	C	144.5	154.53	65	5	30	90.62	28	168.27	70.80	1.13	29.97	4.00	3.96
907	C	145.28	155.31	60	4	36	89.70	28	144.12	46.00	1.14	31.65	4.49	1.74
907	B	148.85	159.09	70	7	23	86.82	15	138.00	28.19	1.18	31.32	0.84	9.12
907	C	152.3	163.57	85	2	13	84.77	4	180.37	21.00	1.21	34.61	2.85	5.04
907	B	153.77	164.01	79	3	16	87.15	6	193.21	33.60	1.18	36.05	1.22	8.27
907	C	155.51	166.78	69	4	27	87.30	21	168.15	36.00	1.17	33.87	4.50	3.92
907	B	155.68	167.6	67	3	30	86.01	15	180.52	34.81	1.19	35.65	0.80	9.90
907	B	158.2	170.12	77	3	20	85.60	0	190.42	61.86	1.20	37.77	1.40	10.79
907	C	161.6	173.38	61	2	37	87.82	22	156.88	28.00	1.17	33.90	2.01	6.80
907	B	166.37	179.56	77	5	18	88.28	13	191.24	19.13	1.16	33.88	2.14	5.72
907	C	169.9	183.4	61	4	35	85.49	23	174.18	24.00	1.20	30.96	0.84	9.72
907	C	174.4	187.9	60	2	38	87.00	22	192.39	11.40	1.18	34.73	1.51	6.40
907	B	176.3	191.07	65	5	30	86.85	20	162.72	9.34	1.18	24.99	3.76	6.96
907	B	176.81	191.58	69	5	26	89.07	17	154.79	6.00	1.15	28.15	4.05	3.87
907	B	178.31	193.08	78	5	17	87.00	9	200.81	11.17	1.18	22.03	4.70	0.26
907	C	178.92	193.12	60	5	35	84.78	21	190.84	9.20	1.21	21.13	3.86	1.46
907	C	180.9	195.1	60	7	33	85.60	23	172.19	12.00	1.20	32.04	1.98	8.12
907	B	187.04	202.17	77	5	18	85.55	6	184.80	51.45	1.20	31.74	2.37	3.94
907	C	192.1	207.57	75	5	20	83.59	2	217.90	64.00	1.23	26.13	1.94	9.98
907	C	193.25	208.72	77	3	20	84.07	2	158.30	43.00	1.22	33.36	2.43	6.04
907	B	195.2	211.99	60	15	25	82.78	2	189.70	83.17	1.24	24.05	2.41	3.45
907	C	198.2	214.82	85	1	14	84.31	0	167.92	44.50	1.21	29.36	1.11	8.37
907	B	198.2	214.99	70	2	28	83.80	0	213.71	38.97	1.22	28.14	3.71	-0.33
907	C	201.2	217.82	84	1	15	80.52	0	190.20	79.00	1.27	29.60	3.41	4.71
907	C	203.3	219.92	89	2	9	82.20	0	236.88	104.69	1.25	31.12	4.30	5.91
907	B	202.9	220.42	77	4	19	82.65	0	224.89	71.81	1.24	24.70	2.88	3.49
907	B	208.15	225.67	79	3	18	78.31	0	222.18	198.16	1.31	17.51	2.47	3.41
907	B	209.24	226.76	76	5	19	80.50	0	246.74	127.83	1.27	31.36	5.40	1.41
907	C	209.45	227.19	64	7	29	72.47	0	244.56	121.52	1.41	26.86	3.05	2.19
907	C	212.1	229.84	66	5	29	77.81	0	237.43	138.00	1.32	30.36	4.97	0.50
980	B	0.5	0.5	42	8	58	82.0513	71	147	31.00	1.25	52.38	6.09	1.53
980	B	2.73	2.73	45	5	50	82.071	64	235.1	55.00	1.25	46.04	4.67	3.45
980	A	0.7	4.81	55	10	35	72.779	6	239	199.50	1.41	31.15	4.47	2.90
980	B	6.44	7.65	50	7	43	75.1836	79	241.5	75.25	1.36	45.45	3.37	3.21
980	A	3.9	8.01	40	10	50	71.7841	14	228	54.67	1.43	38.75	4.47	3.41
980	A	4.92	9.03	75	5	20	71.9101	7	236.727	63.33	1.42	42.12	3.34	3.77
980	A	7.3	11.41	60	10	30	74.6356	57	167	58.33	1.37	60.80	3.97	3.86
980	B	12.44	13.65	35	5	60	76.7041	79	182	48.00	1.34	60.44	3.61	2.58
980	A	10.3	15.44	50	20	30	78.7087	75	153	24.00	1.30	71.13	3.52	2.74
980	B	15.32	17.76	25	15	70	71.3092	45	256.444	155.50	1.44	47.53	3.77	2.88
980	A	13.2	18.34	50	10	40	68.6327	19	268	172.00	1.49	38.98	4.81	-1.05
980	A	17.7	22.84	30	10	60	68.9795	19	229	96.00	1.48	44.44	3.50	1.72
980	B	22.52	24.96	1	1	1	77.8116	80	158.1	43.33	1.32	52.55	1.91	4.81
980	A	19.8	26.52	40	10	50	76.9173	3	167	42.67	1.33	57.84	4.10	2.32
980	A	23.1	29.82	50	10	40	77.6935	78	134	31.00	1.32	60.58	3.36	2.81
980	B	26.65	30.02	10	5	85	80.8527	87	136	28.33	1.27	59.13	4.10	1.81
980	A	25.9	32.62	60	15	25	67.7921	14	250	82.67	1.51	40.21	2.62	3.36
980	B	32.52	35.89	30	20	50	73.9884	36	293.3	186.00	1.38	38.08	3.75	1.20

Site	Hole	mbsf	mcd	clay	sand	silt	PW	Bio	NGR	MS	GRA	L	a	b
980	A	33.7	41.61	70	10	20	70.4022	76	168	68.00	1.45	46.18	3.90	2.63
980	B	38.33	42.78	50	5	45	78.2875	68	136.546	41.00	1.31	64.72	3.49	2.82
980	A	37	44.91	30	15	55	66.6667	12	274	196.50	1.54	38.28	3.84	1.65
980	B	40.48	44.93	68	2	30	66.8844	25	282.4	176.00	1.53	42.61	4.69	-1.96
980	A	38.5	47.73	10	10	80	70.816	91	218	71.50	1.45	44.48	3.78	3.22
980	B	46.26	52.02	10	5	85	78.4674	77	111	1.00	1.31	73.30	2.43	2.72
980	A	43.33	52.56	10	6	87	73.6956	78	149.3	6.33	1.39	65.32	2.99	4.08
980	A	46.27	55.5	10	10	80	72.3164	91	178	29.33	1.42	52.54	4.44	3.41
980	B	50.84	56.6	30	12	58	74.0419	42	214.2	195.25	1.38	49.30	3.70	2.78
980	A	47.41	56.64	20	15	65	71.9101	63	208.4	209.00	1.42	44.09	3.99	2.23
980	A	48.33	58.4	60	10	30	68.8866	15	249.8	431.00	1.49	35.70	3.19	3.04
980	B	51.9	58.68	40	6	54	70.7182	16	270	323.25	1.45	36.25	4.73	1.60
980	A	51.4	61.47	94	1	5	71.9606	96	238	117.67	1.42	41.41	3.88	3.51
980	B	55.5	62.28	10	10	80	76.952	83	135	28.67	1.33	62.68	4.29	2.34
980	B	62.3	70.27	10	6	84	77.6935	75	146	43.75	1.32	61.14	1.95	3.67
980	A	59.05	70.6	87	3	10	75.6837	95	118.5	35.00	1.35	63.65	1.98	3.06
980	B	67	74.97	30	12	58	68.9562	38	247	262.50	1.49	33.18	4.34	3.47
980	A	65.15	76.7	75	5	20	68.0173	56	241	251.00	1.51	36.69	4.64	0.06
980	A	66.77	79.08	20	2	78	70.4749	48	234.111	201.00	1.45	36.58	2.87	4.12
980	B	72.97	82.67	10	8	88	75.0183	73	135.3	19.00	1.37	63.92	2.62	2.67
980	B	74.34	84.04	26	3	71	67.6801	28	304.818	118.00	1.51	38.97	3.09	3.03
980	A	75.07	87.38	85	5	10	76.7616	92	136.9	72.50	1.33	64.80	2.90	3.48
980	A	79.55	92.74	75	7	18	77.2247	45	131.5	49.33	1.33	61.96	4.16	2.43
980	B	83.95	95.38	25	15	60	64.9334	32	272.091	235.50	1.58	39.57	4.04	2.95
980	A	82.52	95.71	70	7	23	67.5016	8	284	114.00	1.52	39.66	2.87	4.37
980	B	89.55	100.98	25	25	50	73.0646	83	214.364	74.00	1.40	47.08	4.21	2.82
980	A	89	103.23	60	20	20	73.405	73	142	24.00	1.40	69.88	2.50	2.34
980	A	91.6	105.83	70	8	22	70.9141	15	232	120.00	1.44	38.64	2.84	3.08
980	B	93.75	106.04	30	5	65	69.7548	51	254.6	167.50	1.47	34.65	3.55	1.69
980	B	95.41	107.7	5	80	15	78.0309	97	111	39.67	1.31	40.67	4.03	4.68
980	A	95.57	109.44	80	10	10	65.9369	57	246.5	124.00	1.55	39.48	3.86	2.56
980	B	99.78	112.5	8	2	90	71.3589	89	257.2	181.33	1.44	34.35	3.29	3.90
980	A	98.89	112.76	70	10	20	68.8774	59	212	145.00	1.49	45.51	5.08	3.04
980	A	99.57	113.44	30	30	40	76.5321	79	140.2	59.67	1.34	49.97	2.55	3.72
980	B	104.74	117.46	10	10	80	71.4086	92	155.6	27.00	1.43	66.91	2.18	4.49
980	A	103.67	117.54	50	10	40	72.6499	78	148	32.75	1.41	63.77	1.94	5.04
980	A	104.68	119.64	60	10	30	70.2814	21	205.6	92.50	1.46	39.17	4.78	1.35
980	A	108.73	123.69	63	7	30	71.3738	56	196	110.00	1.43	53.95	3.85	4.29
980	A	112.6	127.56	45	10	45	71.4086	74	127	14.33	1.43	70.23	2.19	3.15
980	B	117	128.97	15	15	70	70.6353	80	201.8	128.00	1.45	46.97	4.92	1.83
981	A	83.38	94.31	10	7	83	75.5999	94	207.909	72.00	1.35	50.80	4.32	2.46
981	A	84.88	95.81	10	3	87	72.779	94	102	12.00	1.41	72.22	1.75	2.74
981	A	93.02	104.58	35	15	50	73.8923	50	212.889	94.50	1.39	41.29	3.83	3.97
981	A	99.44	111	20	10	70	72.0113	92	140.191	40.00	1.42	59.76	2.60	2.78
981	A	107.3	119.4	10	10	80	72.3164	88	122.3	22.00	1.42	71.54	1.35	4.05
981	A	109.9	122	25	5	70	75.0733	66	222.9	110.50	1.36	45.71	5.13	2.91
981	A	113.25	126.61	25	5	70	73.1429	76	125	26.00	1.40	70.87	1.04	3.53
981	A	118.6	131.96	50	2	48	68.9562	58	210	220.00	1.49	50.32	3.05	3.78
981	A	120.81	134.83	70	3	27	69.4708	36	204.556	120.00	1.47	55.56	1.73	2.95
981	A	127.61	141.63	40	1	59	70.041	81	148.8	15.00	1.46	69.22	1.06	2.62
981	A	132.26	147.02	25	5	70	71.1605	76	123.333	12.25	1.44	70.80	1.18	2.67
981	A	133.68	148.44	73	2	25	73.5368	28	155.4	37.67	1.39	57.08	1.96	3.68
981	A	142.22	157.28	30	3	67	73.1951	80	134.6	21.75	1.40	63.20	1.77	4.14
981	A	144.18	159.24	60	1	39	72.2399	42	146	26.00	1.42	62.94	0.54	6.68
981	A	147.75	162.81	70	3	27	72.1635	27	212.6	115.00	1.42	29.23	3.12	7.39
981	A	152.93	167.89	40	3	57	71.9101	65	212.2	30.33	1.42	45.37	2.66	4.43
981	A	154.64	169.6	40	3	57	69.4237	64	150.8	5.00	1.48	62.24	1.74	3.51
981	A	156.62	171.58	78	2	20	72.1635	25	234.6	92.67	1.42	43.67	1.93	3.35
981	A	158.71	174.49	20	5	75	70.3297	78	126.3	1.00	1.46	72.82	0.89	3.53
981	A	161.9	177.68	37	3	60	70.6694	78	124	3.75	1.45	64.61	2.43	2.85
981	A	177.88	195.27	23	2	75	72.2653	84	169.2	29.67	1.42	53.78	3.94	3.25
981	A	185.9	203.29	25	5	70	67.5462	89	141	2.00	1.52	66.92	1.70	5.18
981	A	188.95	206.68	30	3	67	74.2567	86	183.5	4.00	1.38	59.40	3.63	4.19

Site	Hole	mbsf	mcd	clay	sand	silt	PW	Bio	NGR	MS	GRA	L	a	b
981	A	195.62	213.35	25	2	73	71.21	86	113.2	2.00	1.44	66.56	2.72	2.86
981	A	201.4	220.59	5	5	90	68.1758	97	118	3.00	1.50	67.53	2.93	3.33
981	A	201.7	220.89	23	2	75	68.6327	84	120	2.00	1.49	70.28	2.41	3.87
981	A	208.3	228.47	8	6	86	65.8521	98	130.091	2.00	1.56	66.75	1.09	4.38
981	A	211.28	231.45	10	5	85	67.8146	99	152.2	6.00	1.51	59.54	2.08	3.69
981	A	219.73	239.9	10	5	85	69.0492	89	91.3333	-2.00	1.48	81.05	1.59	2.83
981	A	223.63	243.8	15	5	80	67.9947	94	105.636	3.00	1.51	62.77	1.64	3.72
981	A	225.94	246.11	15	5	80	66.0219	92	102	-2.00	1.55	75.74	0.98	3.71
981	A	247.67	267.84	10	5	85	69.3626	90	115.636	1.27	1.48	63.15	2.33	4.42
981	A	250.69	270.86	10	5	85	65.8521	92	119.909	-0.41	1.56	70.91	1.45	3.66
981	A	257.66	277.83	10	5	85	66.4935	94	123.2	2.20	1.54	76.47	1.02	3.53
981	A	258.57	278.74	15	15	70	67.2445	87	131.8	2.30	1.52	65.61	3.67	3.06
981	A	266.7	286.87	15	5	80	63.3271	92	103.9	1.64	1.62	73.54	1.23	2.98
982	D	22.21	24.14	8	17	75	75.3274	92	172.812	8.48	1.36	79.71	1.51	3.54
982	D	23.73	25.66	5	30	65	72.6241	86	172.543	33.00	1.41	53.12	5.44	3.11
982	D	26.43	28.36	20	20	60	70.7182	56	172.065	70.00	1.45	41.29	4.49	5.58
982	C	25.1	28.62	45	20	35	72.4187	50	172.019	45.65	1.41	45.17	2.18	7.60
982	A	27.58	30.08	75	5	25	73.258	25	171.76	79.88	1.40	51.58	5.81	3.95
982	B	30.1	33.18	20	15	65	73.919	92	171.212	12.06	1.39	79.59	1.33	3.06
982	A	30.8	33.3	20	7	73	77.6346	92	171.19	5.00	1.32	78.19	1.83	1.24
982	B	32.36	35.44	25	8	67	73.0489	86	170.812	28.03	1.40	60.87	3.85	3.73
982	B	33.44	36.52	15	5	80	72.0113	95	170.62	8.50	1.42	80.10	2.95	2.66
982	B	36.34	40.42	45	5	50	73.1951	50	169.93	72.87	1.40	46.28	4.61	4.87
982	A	37.14	41.07	20	10	70	71.8596	78	169.815	57.48	1.43	51.34	3.73	4.95
982	C	38.6	41.86	25	12	63	69.0958	91	169.675	12.00	1.48	62.01	2.56	7.65
982	B	41.02	45.1	20	10	70	74.2836	85	169.102	10.52	1.38	75.13	1.93	3.26
982	A	41.67	45.6	20	10	70	73.1899	94	169.013	41.33	1.40	64.17	3.25	3.75
982	C	49.36	53.94	52	8	40	70.6256	58	115.139	12.00	1.45	81.75	1.88	2.63
982	B	48.62	54.13	15	5	80	70.8651	95	114.87	18.00	1.45	66.62	2.54	4.60
982	A	48.4	54.93	67	30	30	70.8651	23	113.738	46.00	1.45	45.27	3.02	2.15
982	B	50.12	55.63	15	5	80	67.7697	95	112.747	6.20	1.51	83.22	1.13	1.62
982	A	53.15	59.68	15	5	80	73.7115	92	107.013	4.40	1.39	63.56	3.46	3.50
982	B	53.95	59.72	10	15	75	73.4313	97	106.956	3.19	1.39	65.75	2.71	3.70
982	B	57.45	63.22	10	15	75	73.7221	105	102.001	0.40	1.39	74.65	2.50	4.14
982	B	58.2	63.97	10	8	82	69.0492	104	100.939	1.00	1.48	81.22	2.27	2.55
982	A	56.4	64.37	5	5	90	71.3589	95	100.373	0.16	1.44	80.92	2.01	2.19
982	A	59.2	67.17	10	10	80	70.3635	90	99.672	0.58	1.46	74.97	2.74	3.16
982	C	64.6	70.39	25	8	67	69.2828	92	102.661	-2.00	1.48	75.57	2.42	2.02
982	A	67.34	76.12	8	40	82	67.9902	90	107.979	-1.00	1.51	82.07	2.03	2.08
982	C	75.12	80.94	15	5	80	70.7671	86	112.453	7.80	1.45	83.69	1.61	1.90
982	B	74.18	82.12	15	5	80	66.8669	95	113.548	1.00	1.53	83.92	1.32	2.91
982	B	75.95	83.89	15	5	80	72.6757	95	115.191	0.00	1.41	69.32	1.87	3.87
982	A	77.2	87.03	9	5	86	73.935	93	118.105	-0.45	1.39	81.37	2.00	2.14
982	C	85.08	92.27	15	2	83	66.1926	95	122.968	-1.10	1.55	82.41	1.76	2.88
982	B	85.2	94.41	15	6	79	67.1475	95	135.429	0.51	1.53	83.33	1.93	1.90
982	A	86.6	98.03	9	6	75	68.2439	91	131.884	-0.55	1.50	78.96	2.67	2.61
982	C	93.1	101.27	10	2	88	67.2799	92	128.711	0.10	1.52	83.79	1.27	1.55
982	B	96.11	106.18	15	5	80	64.3216	95	123.903	0.00	1.59	84.94	2.07	1.92
982	C	102.6	111.65	15	5	80	66.1499	91	118.546	-1.89	1.55	84.30	1.20	2.85
982	B	102.6	113.09	5	5	90	66.2354	95	117.136	-1.00	1.55	83.52	1.70	2.19
982	B	107.45	117.94	15	5	80	65.4522	95	112.386	0.00	1.56	73.39	2.18	3.13
983	A	46.12	52.08	83	2	15	75.54	13	188.46	460.50	1.36	36.66	1.92	2.11
983	C	45.60	53.5	22	1	77	75.96	63	188.23	458.00	1.35	47.63	2.75	1.57
983	B	50.00	54.4	8	2	80	78.65	83	181.51	337.00	1.30	50.20	2.54	0.18
983	A	48.74	54.7	68	2	30	71.86	38	179.27	430.81	1.43	45.06	2.59	0.62
983	B	52.96	57.94	12	3	85	77.46	80	155.06	333.00	1.32	39.44	2.10	0.85
983	B	55.96	60.94	15	5	80	74.64	80	111.90	301.20	1.37	42.67	2.29	1.25
983	A	55.45	62.75	70	8	22	71.86	40	141.78	355.00	1.43	40.24	2.10	1.65
983	A	58.64	65.94	68	2	30	69.57	38	144.48	381.39	1.47	44.40	1.93	0.78
983	A	61.76	69.06	83	2	15	73.31	13	156.69	635.74	1.40	33.14	3.41	-2.55
983	B	63.90	70.03	20	10	70	70.33	57	155.83	706.84	1.46	33.80	0.76	2.55
983	A	65.10	72.97	80	5	15	72.47	12	153.25	334.23	1.41	33.21	2.37	-0.33
983	B	68.30	74.43	61	2	37	74.47	2	151.97	351.00	1.38	31.96	0.61	4.76

Site	Hole	mbsf	med	clay	sand	silt	PW	Bio	NGR	MS	GRA	L	a	b
983	B	75.40	82.58	35	10	55	79.38	53	144.81	373.50	1.29	34.44	0.14	3.14
983	A	76.40	85.25	80	1	19	70.43	5	142.46	341.45	1.45	35.75	2.22	3.56
983	B	79.54	86.72	24	6	70	75.07	76	141.17	449.53	1.36	34.70	0.76	3.60
983	B	82.40	90.46	60	3	37	78.29	35	137.88	517.00	1.31	35.38	0.95	6.27
983	B	84.50	92.56	55	1	44	74.64	42	136.04	425.80	1.37	36.70	2.01	2.55
983	A	86.60	95.94	15	5	80	73.95	79	133.07	433.80	1.38	43.08	1.48	1.75
983	A	88.65	97.99	15	5	80	71.46	33	131.27	703.93	1.43	37.02	2.75	1.38
983	B	90.80	99.53	70	0	30	77.81	37	129.92	301.41	1.32	41.85	0.17	2.58
983	B	96.78	105.51	74	1	25	72.42	9	124.66	463.00	1.41	32.19	0.50	3.13
983	B	101.50	111.27	64	1	35	73.22	33	140.86	406.00	1.40	29.41	1.38	2.80
983	A	104.66	115.48	63	2	35	74.36	36	136.96	362.19	1.38	42.06	1.29	2.04
983	B	106.79	116.56	66	1	35	72.52	36	135.97	708.83	1.41	30.60	1.57	2.69
983	B	112.70	123.19	75	0	25	78.01	9	129.84	307.65	1.31	31.39	1.65	4.24
983	A	114.20	125.81	20	10	70	67.28	16	127.41	837.00	1.52	28.39	0.50	3.47
983	B	115.70	126.19	75	0	25	72.05	9	127.06	782.67	1.42	27.21	0.60	5.32
983	B	119.12	130.78	55	2	43	75.24	41	122.82	417.00	1.36	38.22	0.23	2.42
983	A	121.15	132.76	10	20	70	68.16	14	120.99	363.00	1.50	32.55	-0.09	2.79
983	A	122.30	134.61	10	10	80	71.36	40	119.28	436.16	1.44	33.79	1.58	0.09
983	B	125.39	137.05	84	1	15	73.98	7	117.02	544.00	1.38	35.09	-0.60	3.27
983	B	130.50	142.95	64	1	35	75.41	9	111.57	514.00	1.36	30.27	0.92	1.14
983	A	133.10	145.91	30	20	50	68.31	42	108.83	361.00	1.50	23.70	0.25	2.36
983	B	136.45	148.9	75	0	25	75.88	4	106.06	485.00	1.35	31.17	-0.35	6.38
983	A	137.70	150.51	40	10	50	69.24	21	104.57	771.77	1.48	29.23	1.65	1.80
983	B	138.59	152.64	80	0	20	75.13	2	102.61	611.00	1.36	28.17	0.46	3.72
983	A	144.35	158.25	18	7	75	71.76	5	97.42	818.00	1.43	22.47	0.52	4.68
983	B	146.04	160.09	85	0	15	80.57	11	95.72	514.33	1.27	30.48	-0.26	3.87
983	B	147.22	161.56	85	0	15	78.79	5	94.36	392.24	1.30	26.30	0.33	2.63
983	B	151.76	166.1	74	1	25	76.30	22	90.16	364.00	1.34	28.72	3.11	3.87
983	C	150.30	166.81	68	2	30	70.91	20	89.50	383.60	1.44	28.30	1.17	0.73
983	A	152.20	166.92	5	5	90	66.24	92	89.40	443.06	1.55	33.47	1.91	-0.14
983	C	151.75	168.26	63	2	35	63.52	11	88.16	831.00	1.61	24.85	0.11	3.09
983	A	157.45	172.17	30	5	65	72.12	62	84.55	395.42	1.42	35.95	-0.79	3.50
983	B	157.44	173.06	78	2	20	77.17	17	83.72	396.00	1.33	36.61	0.42	4.03
983	C	157.10	173.85	70	3	27	66.98	18	82.99	472.72	1.53	23.70	0.91	1.43
983	B	160.45	176.07	55	5	40	67.15	19	80.94	727.50	1.53	26.85	-0.10	3.96
983	A	161.50	177.18	50	5	45	71.23	27	79.91	485.00	1.44	30.38	0.83	1.79
983	C	164.10	180.85	60	5	35	71.41	31	76.52	339.00	1.43	34.06	0.09	2.83
983	A	165.90	181.58	30	7	63	68.18	53	81.15	407.00	1.50	32.98	-0.38	3.22
983	B	167.08	183.75	80	1	19	66.71	11	124.17	590.00	1.54	23.87	0.15	4.81
983	C	167.40	185.42	60	2	38	82.98	41	146.10	545.00	1.23	26.65	-0.50	2.92
983	B	171.62	188.29	28	2	70	74.10	90	154.82	247.94	1.38	34.05	-0.47	4.54
983	A	172.63	189.28	65	1	34	70.96	40	156.23	322.00	1.44	36.89	0.76	2.29
983	C	171.90	189.92	55	2	43	72.42	41	157.14	389.00	1.41	37.14	-0.10	3.90
983	A	177.13	193.78	65	2	33	65.64	40	162.64	525.13	1.56	29.70	0.94	1.53
983	C	175.58	194.41	73	2	25	68.47	2	163.54	582.13	1.50	28.22	0.50	2.40
983	C	177.50	196.33	52	3	45	78.02	45	166.28	285.19	1.31	31.28	1.11	1.99
983	A	179.10	196.53	68	2	30	72.16	6	166.56	325.00	1.42	30.20	-0.89	3.89
983	B	180.91	198.25	40	5	55	68.86	40	169.02	388.71	1.49	36.95	-0.04	4.28
983	A	183.60	201.03	85	0	15	68.40	6	172.98	533.00	1.50	31.95	-1.41	5.53
983	B	186.00	203.95	60	2	38	80.82	29	177.14	462.80	1.27	24.37	-0.04	6.70
983	C	186.60	206.05	84	1	15	74.47	5	180.14	685.06	1.38	28.23	-0.06	3.77
983	A	191.58	209.37	70	1	29	68.22	33	184.87	366.42	1.50	35.25	0.14	2.92
983	C	190.20	209.65	65	1	34	75.79	30	185.27	380.00	1.35	34.01	0.46	2.74
983	B	191.98	209.93	43	2	55	73.09	48	185.67	370.93	1.40	29.31	0.67	3.70
984	C	8.67	10.9	70	3	27	81.85	6	16.79	412.00	1.25	34.05	2.27	-1.25
984	B	9.50	11.24	23	5	72	83.87	37	169.58	442.45	1.22	34.79	0.38	3.36
984	A	10.30	12.43	37	4	59	77.52	36	176.07	444.00	1.32	39.36	3.41	-0.39
984	C	11.01	13.24	68	4	28	87.60	5	160.12	246.00	1.17	38.21	3.61	2.23
984	A	12.30	14.43	23	5	72	83.06	56	136.69	358.00	1.23	31.82	1.80	1.88
984	C	12.25	14.48	16	4	79	84.77	59	135.70	377.00	1.21	45.39	2.37	-5.04
984	B	12.80	14.54	13	3	84	85.25	71	134.52	382.17	1.20	36.41	-1.16	4.65
984	B	13.30	15.04	12	5	83	83.06	68	124.67	506.87	1.23	32.38	0.11	2.34
984	A	15.30	17.53	23	2	75	80.57	61	152.95	483.48	1.27	39.27	0.98	1.88

Site	Hole	mbsf	mcd	clay	sand	silt	PW	Bio	NGR	MS	GRA	L	a	b
984	A	17.00	19.23	15	3	82	82.57	70	152.86	321.48	1.24	39.00	1.19	1.19
984	C	17.15	20.5	23	2	75	79.94	73	152.80	292.29	1.28	43.72	2.78	-1.77
984	B	19.00	22.07	45	2	53	78.83	12	152.73	438.00	1.30	34.22	1.33	1.82
984	A	21.80	24.03	59	1	30	82.78	8	152.63	333.50	1.24	35.90	3.83	2.42
984	C	21.70	25.05	60	2	38	79.78	5	152.58	276.59	1.28	39.27	5.44	0.43
984	B	22.05	25.12	70	0	30	82.99	5	152.58	233.07	1.23	34.43	2.15	5.44
984	C	24.62	27.97	58	1	41	76.70	3	152.44	685.83	1.34	34.81	2.34	-5.68
984	A	27.84	30.38	60	5	35	76.47	12	152.32	617.00	1.34	24.95	-1.29	5.31
984	A	28.97	31.51	60	5	35	77.46	7	152.27	847.38	1.32	30.73	0.39	3.49
984	B	28.00	31.6	51	1	48	79.63	20	152.26	809.31	1.29	32.27	1.77	-0.12
984	A	31.90	34.44	60	5	35	80.13	12	152.12	379.00	1.28	34.86	-1.18	5.84
984	C	31.06	35.53	60	0	40	79.69	12	152.07	407.74	1.29	32.34	0.77	13.07
984	C	33.35	37.82	35	5	65	80.44	52	151.96	305.60	1.27	39.81	1.25	2.82
984	B	34.32	37.92	37	3	60	81.92	36	151.95	280.56	1.25	38.18	-0.70	3.81
984	A	34.40	38.15	45	2	53	81.37	28	151.94	287.48	1.26	36.81	1.17	2.05
984	B	37.25	41.64	73	2	25	77.22	0	151.77	517.55	1.33	35.52	1.20	0.56
984	C	37.60	42.47	65	9	26	74.81	5	151.73	239.83	1.37	31.24	1.21	51.40
984	A	38.92	42.67	85	0	15	83.66	0	151.72	342.65	1.22	25.78	2.92	1.02
984	C	39.10	43.97	50	4	46	77.33	5	151.66	518.50	1.32	39.09	-1.81	21.63
984	C	40.60	45.47	38	2	60	76.36	5	151.59	736.61	1.34	30.45	-0.86	33.02
984	B	42.39	46.78	75	2	23	78.11	17	151.52	609.00	1.31	36.93	1.68	1.36
984	A	43.70	48.04	25	5	70	80.92	50	151.46	436.10	1.27	32.52	0.96	2.28
984	A	46.20	50.54	15	7	78	84.28	69	151.34	347.00	1.22	33.92	2.50	0.95
984	B	48.50	53.06	78	2	20	79.99	8	151.22	397.00	1.28	35.54	3.31	1.25
984	C	47.10	53.37	70	0	30	78.19	86	151.20	439.60	1.31	33.46	-0.86	14.88
984	A	49.90	54.24	35	5	30	71.52	0	151.16	468.00	1.43	25.09	2.09	-0.50
984	C	48.60	54.87	75	1	24	81.41	86	151.13	439.83	1.26	30.67	0.94	9.84
984	B	54.25	58.81	70	2	28	77.17	25	150.94	610.00	1.33	34.79	2.66	0.48
984	C	53.10	59.37	12	1	87	72.62	86	150.91	544.00	1.41	38.23	-0.85	13.03
984	A	57.80	63.87	35	5	60	77.11	1	150.69	254.00	1.33	31.57	2.19	2.55
984	C	56.60	63.88	23	2	75	80.69	9	150.69	232.00	1.27	43.07	0.90	5.97
984	B	59.70	64.68	48	2	50	77.28	55	150.65	290.00	1.33	30.96	1.89	0.60
984	A	60.80	66.87	73	2	25	72.88	1	150.55	352.97	1.41	35.80	4.01	0.51
984	B	64.56	69.54	80	2	18	76.82	10	150.42	636.00	1.33	32.20	2.08	0.85
984	A	63.02	69.82	73	2	25	76.52	17	150.40	629.00	1.34	30.44	1.92	1.30
984	C	64.10	71.38	69	1	30	78.86	9	150.33	591.43	1.30	29.02	0.96	6.96
984	C	65.90	73.94	5	3	92	74.85	46	150.20	485.83	1.37	43.59	1.14	1.36
984	A	67.35	74.15	50	3	47	74.07	45	150.19	543.00	1.38	39.82	1.92	0.61
984	B	69.43	74.91	45	2	53	74.64	54	150.16	505.31	1.37	42.61	2.68	-0.85
984	C	67.40	75.44	27	8	65	74.86	46	150.13	477.35	1.37	33.41	-0.71	5.04
984	B	73.25	78.73	85	2	13	70.72	5	149.97	679.00	1.45	33.27	1.03	3.22
984	C	71.90	79.94	27	4	79	71.41	46	149.91	534.94	1.43	32.28	0.50	3.96
984	A	72.50	80.05	73	2	25	73.73	13	149.91	474.00	1.39	30.01	-0.11	3.53
984	C	73.55	81.89	78	2	20	74.26	2	149.82	670.67	1.38	31.54	1.31	-0.32
984	B	75.84	82.26	50	5	45	76.53	53	149.80	446.47	1.34	40.24	0.17	4.40
984	A	75.52	83.07	53	2	45	80.07	51	149.76	456.00	1.28	38.70	1.85	1.44
984	B	78.93	85.35	75	1	24	80.81	0	149.65	422.50	1.27	25.88	2.21	-0.08
984	C	78.84	87.18	69	1	30	75.63	0	149.56	703.00	1.35	32.45	-0.04	2.63
984	A	82.70	90.81	85	0	15	77.11	5	149.38	482.00	1.33	30.66	1.23	1.97
984	B	85.50	92.92	75	2	23	74.10	0	149.28	520.00	1.38	28.87	2.30	2.51
984	A	86.83	94.94	85	0	15	73.20	2	149.18	388.00	1.40	36.36	2.31	3.59
984	C	89.20	98.93	79	1	20	71.71	0	148.99	621.00	1.43	27.27	1.45	0.25
984	C	89.90	99.63	57	3	40	77.60	28	148.95	695.00	1.32	33.47	0.47	2.94
984	B	92.90	100.32	45	2	52	76.38	47	148.92	438.23	1.34	37.96	1.05	1.96
984	A	91.47	101.59	90	0	10	75.13	1	148.86	260.52	1.36	33.63	2.62	2.96
984	B	95.95	103.81	83	2	15	71.44	0	148.75	354.41	1.43	25.12	1.73	1.42
984	B	99.20	107.06	52	3	45	80.63	43	148.59	415.50	1.27	26.95	2.10	1.56
984	C	97.40	108.24	60	3	37	75.02	32	148.53	336.55	1.37	36.69	0.89	2.46
984	A	99.55	109.67	85	0	15	78.84	0	148.47	558.00	1.30	28.61	2.88	0.47
984	A	100.41	110.3	85	0	15	78.35	0	148.43	508.80	1.31	27.82	1.71	3.00
984	C	100.05	110.89	75	2	23	76.88	0	148.41	692.00	1.33	27.21	1.02	1.24
984	C	102.05	112.42	55	3	42	75.63	20	148.33	641.00	1.35	28.52	2.22	-0.28
984	A	103.58	113.47	58	2	40	76.28	43	148.28	382.13	1.34	37.50	1.98	0.07

Site	Hole	mbsf	med	clay	sand	silt	PW	Bio	NGR	MS	GRA	L	a	b
984	B	105.40	113.86	60	5	35	78.59	9	148.26	366.00	1.30	35.03	-0.27	4.74
984	C	107.25	117.62	65	5	30	73.29	20	148.08	336.00	1.40	34.45	0.00	4.97
984	B	109.90	118.36	70	3	27	79.01	9	148.04	383.00	1.30	29.68	2.70	2.06
984	A	110.32	121.42	74	1	25	76.30	2	147.89	538.19	1.34	31.35	0.58	2.42
984	A	114.70	125.8	65	1	34	77.18	29	147.68	489.50	1.33	31.19	-0.90	5.14
984	B	116.74	127.01	27	8	65	72.57	48	147.62	404.23	1.41	32.56	1.15	2.81
984	C	117.96	128.98	65	2	33	70.78	12	147.53	876.50	1.45	29.63	0.87	2.56
984	B	118.76	129.03	69	4	27	69.40	9	147.52	831.66	1.48	28.83	0.65	2.62
984	C	119.08	130.1	70	4	26	74.85	21	147.47	462.65	1.37	34.81	0.64	3.13
984	C	121.90	133.55	62	5	33	73.20	5	147.30	536.29	1.40	31.04	0.99	0.41
984	A	122.60	134.94	55	5	40	74.04	10	147.24	636.00	1.38	31.17	1.39	1.76
984	B	124.80	135.67	50	2	48	74.20	10	147.20	589.00	1.38	28.89	1.63	3.40
984	C	125.90	137.55	68	4	28	71.26	2	147.11	371.80	1.44	28.85	0.75	1.68
984	B	127.80	138.67	55	2	43	70.47	10	147.06	699.03	1.45	28.16	0.75	3.09
984	C	131.85	144.29	60	3	37	77.78	25	146.78	396.00	1.32	34.64	0.31	4.11
984	B	132.44	144.62	45	1	44	71.81	6	146.77	338.40	1.43	20.67	-2.41	12.86
984	A	132.10	145.23	30	8	62	72.65	34	146.74	533.00	1.41	31.54	-0.38	4.12
984	C	137.00	149.44	70	5	25	75.91	3	146.53	555.33	1.35	26.88	1.71	1.08
984	A	140.40	154.25	70	5	25	68.59	5	146.30	787.94	1.49	31.44	1.81	2.05
984	C	142.10	155.07	64	1	35	70.14	1	146.26	825.20	1.46	25.88	-0.55	4.70
984	B	145.00	158.03	36	5	59	73.67	27	146.11	432.00	1.39	29.04	-0.96	5.05
984	C	145.14	158.11	50	6	44	73.09	32	146.11	436.97	1.40	29.01	1.20	2.04
984	A	144.92	158.77	70	5	25	69.52	10	146.08	524.00	1.47	29.40	-1.47	7.39
984	B	146.90	159.93	55	2	45	73.25	10	146.02	779.50	1.40	27.33	0.65	2.68
984	B	149.70	162.73	46	1	53	72.16	6	126.02	527.71	1.42	28.73	1.13	2.43
984	C	150.50	164.24	65	2	33	72.42	2	126.04	517.50	1.41	22.53	0.76	4.66
984	A	152.00	166.84	20	4	76	73.73	58	126.07	772.00	1.39	29.09	2.06	0.09
984	B	154.50	168.33	46	4	50	74.31	39	126.09	416.20	1.38	37.84	-0.21	3.06
984	C	154.91	168.65	65	2	33	71.36	27	126.09	490.48	1.44	35.91	0.17	3.68
984	B	157.80	171.63	70	7	29	70.43	8	126.12	692.75	1.45	25.19	0.70	2.71
984	C	159.60	174.05	80	1	19	68.40	7	126.15	712.00	1.50	28.09	0.83	2.78
984	C	162.60	177.05	67	3	40	74.90	7	126.18	270.00	1.37	34.00	0.29	3.82
984	B	164.40	179.05	60	5	35	69.73	6	126.20	576.00	1.47	25.75	-0.02	5.09
984	B	168.12	182.77	45	5	50	71.57	15	126.25	429.00	1.43	26.76	-1.18	5.69
984	C	169.10	184.14	55	1	44	72.26	14	126.26	639.20	1.42	24.92	1.12	2.23
984	D	169.70	184.46	89	0	11	72.38	0	126.26	474.60	1.41	22.19	-3.92	13.62
984	D	170.97	185.73	50	6	44	73.20	35	126.28	391.50	1.40	26.23	-0.16	5.46
984	B	172.20	188.49	56	4	40	74.10	7	126.31	740.38	1.38	24.03	3.10	1.59
984	C	175.12	190.16	50	1	49	68.36	14	126.33	749.35	1.50	26.43	0.83	2.87
984	B	175.30	191.59	36	4	60	68.03	28	126.34	799.40	1.51	25.65	2.73	1.23
984	C	180.20	197.01	23	3	74	68.21	55	126.40	635.00	1.50	27.99	-0.44	4.84
984	B	181.69	197.52	45	5	50	67.95	32	126.41	743.50	1.51	27.70	2.59	1.71
984	C	182.10	198.91	33	6	61	72.52	42	126.42	460.00	1.41	26.05	-1.49	5.91
984	B	184.70	200.53	58	12	30	66.97	18	126.44	664.97	1.53	26.66	1.27	4.02
984	C	184.50	201.31	65	5	30	67.81	4	126.45	725.20	1.51	24.77	-0.08	2.98
984	C	188.10	205.1	60	1	39	71.16	21	126.49	615.40	1.44	22.72	0.67	2.63
984	C	192.62	209.62	40	1	59	68.15	21	126.54	695.00	1.50	24.96	0.32	2.71
984	B	191.40	209.8	47	3	50	69.94	0	126.54	606.67	1.46	26.68	-1.60	6.67
984	B	192.90	211.3	70	1	29	68.63	0	126.56	878.00	1.49	24.55	-0.73	4.97
984	C	198.85	216.73	50	3	47	73.88	3	126.62	678.00	1.39	22.44	-0.54	5.01
984	B	199.00	217.8	50	5	45	72.47	13	126.63	727.20	1.41	27.39	1.18	3.36
984	B	203.60	222.4	37	3	60	66.33	20	126.68	784.10	1.54	25.49	1.79	2.07
984	C	207.10	226.05	69	1	30	71.21	12	126.72	698.75	1.44	24.76	-0.46	3.15
984	C	208.60	227.55	63	10	37	77.55	12	126.74	363.60	1.32	25.06	0.86	3.44
984	B	208.69	228.77	65	3	32	68.26	10	126.75	781.50	1.50	26.08	-0.43	5.54
984	C	213.12	232.07	55	7	38	74.31	12	126.79	589.56	1.38	21.74	-1.69	4.57
984	B	213.25	233.33	65	3	32	68.27	11	126.80	755.97	1.50	28.72	1.03	1.56
984	C	217.54	237.38	73	2	25	78.49	7	126.85	328.50	1.30	24.62	-0.55	5.05
984	B	220.88	241.15	72	3	25	70.69	20	126.89	598.00	1.45	29.53	1.61	1.31
984	B	225.30	245.57	80	2	18	66.93	10	126.94	802.59	1.53	26.33	-0.90	5.53
984	B	229.07	250.79	66	2	32	78.29	9	126.99	305.00	1.31	29.73	0.84	1.70
984	C	230.70	252.23	26	4	70	68.59	47	129.58	450.50	1.49	28.95	0.85	2.17
984	C	233.50	255.03	65	5	30	67.72	13	127.93	772.00	1.51	27.67	0.98	0.20

Site	Hole	mbsf	mcd	clay	sand	silt	PW	Bio	NGR	MS	GRA	L	a	b
984	B	233.73	255.45	78	2	20	75.13	3	127.68	821.00	1.36	26.47	0.69	3.17
984	C	237.10	260.13	59	1	40	73.05	2	124.91	393.00	1.40	27.98	0.05	0.38
984	C	238.60	261.63	74	1	25	67.93	2	124.02	755.00	1.51	27.32	-0.43	3.42
984	B	239.77	262.36	70	2	28	69.47	3	123.59	624.79	1.47	28.10	0.68	2.19
984	B	243.81	266.4	62	3	35	70.15	12	121.20	618.00	1.46	27.84	0.29	3.90
984	C	249.25	272.28	60	2	38	66.32	12	117.72	788.52	1.54	29.53	1.16	2.06
984	B	250.04	272.54	70	2	28	68.91	20	117.56	752.00	1.49	30.33	1.42	2.33
984	C	251.88	274.91	60	5	35	70.49	1	116.16	674.40	1.45	23.91	0.80	3.76
984	B	253.70	276.2	70	2	28	70.46	2	115.40	681.80	1.45	24.67	1.82	-0.16
984	B	256.25	278.75	88	2	10	70.89	2	113.89	824.19	1.44	26.98	-0.03	2.56
984	C	256.30	280.1	60	5	35	69.19	13	113.09	541.00	1.48	23.08	-0.55	6.23
984	B	261.75	284.25	70	2	28	77.81	3	110.64	309.14	1.32	24.79	-0.31	3.42
984	C	262.73	286.53	58	5	37	64.50	0	109.29	736.97	1.59	20.21	-0.10	8.40
984	B	265.58	288.08	68	2	30	70.91	0	108.37	721.00	1.44	24.39	3.33	-1.46
984	C	265.21	289.44	71	2	27	66.84	0	107.56	836.50	1.53	21.98	-2.63	11.99
984	B	270.05	292.55	65	5	30	75.02	12	105.72	336.75	1.37	25.56	-0.64	3.99
984	C	271.95	296.18	57	3	40	73.56	11	103.58	661.00	1.39	23.20	-0.92	4.62
984	B	276.60	299.1	70	3	27	65.14	0	101.85	775.23	1.57	25.09	-0.10	2.84
984	C	274.60	299.5	75	1	24	65.77	0	101.61	753.00	1.56	25.23	1.17	3.58
984	C	277.57	302.47	62	3	35	89.35	11	99.85	199.00	1.15	19.56	0.26	4.78
984	B	281.10	303.6	75	1	24	66.84	0	99.19	865.74	1.53	24.35	1.59	0.72
984	C	283.34	308.24	90	0	10	73.93	0	113.55	522.61	1.39	15.30	0.95	6.91
984	C	284.74	309.64	90	0	10	66.52	1	112.56	778.00	1.54	24.89	-1.37	8.25
984	B	287.80	310.3	52	3	45	67.00	10	112.09	669.00	1.53	26.55	2.55	-0.21
985	A	35.2	36.57	68	2	30	70.67	0	232.78	140.00	1.45	38.50	1.39	2.94
985	B	35.86	38.54	70	0	30	77.90	0	232.61	177.81	1.31	41.25	1.18	4.94
985	B	36.75	39.43	74	0	26	67.72	0	232.53	142.00	1.51	37.28	1.85	3.74
985	A	38.92	40.6	39	1	60	77.11	60	232.43	104.00	1.33	35.88	0.49	6.03
985	A	39.75	41.43	67	2	31	67.46	0	232.36	79.00	1.52	36.84	7.24	4.24
985	B	42.36	45.77	79	2	19	85.66	0	231.99	79.59	1.20	39.94	3.72	5.19
985	A	44.65	46.33	68	1	31	67.55	0	231.94	95.44	1.52	38.94	2.33	3.84
985	B	45.22	48.63	64	2	34	63.72	3	231.75	76.42	1.61	38.69	4.90	3.65
985	A	46.18	48.65	65	2	33	67.28	10	231.74	70.00	1.52	39.38	3.59	6.41
985	A	51.05	53.52	75	3	22	68.77	0	231.33	144.81	1.49	37.30	-0.32	4.37
985	A	58.79	62.7	71	1	28	68.94	0	230.54	129.00	1.49	38.66	1.97	5.37
985	A	59.75	63.66	61	2	37	61.23	0	230.46	23.44	1.67	26.48	-3.16	9.55
985	B	61.2	66.63	90	1	9	83.73	0	230.21	120.48	1.22	39.36	0.97	5.36
985	A	64.06	67.97	0	30	70	75.96	0	230.09	531.00	1.35	29.78	-0.36	9.02
985	B	64.05	69.48	90	0	9	67.45	0	229.96	154.00	1.52	34.94	-0.37	2.79
985	A	64.94	69.65	58	5	43	56.48	0	229.95	54.97	1.81	30.84	1.81	-3.73
985	A	68.5	73.21	74	1	25	78.59	0	229.64	141.60	1.30	41.78	-0.10	6.79
985	B	72	77.26	81	4	15	85.13	0	229.30	99.33	1.20	38.27	0.14	4.53
985	B	74.08	79.34	1	1	98	73.88	20	229.12	110.00	1.39	33.72	0.65	6.03
985	A	74.8	79.72	81	2	12	75.27	0	229.09	96.00	1.36	38.27	1.52	1.70
985	A	78.25	83.17	80	1	19	84.89	0	228.79	85.00	1.21	32.41	2.57	4.19
985	A	87.44	92.98	90	0	10	73.99	0	227.95	91.63	1.38	40.64	1.72	3.74
985	A	92.42	97.96	80	1	19	82.98	0	227.53	292.00	1.23	37.87	1.10	2.42
985	B	91.2	98.31	85	0	15	84.42	0	227.50	133.26	1.21	39.67	1.77	8.38
985	A	95.5	101.84	94	0	6	78.59	0	227.20	98.42	1.30	42.54	3.26	3.86
985	A	97.1	103.44	60	0	40	74.91	37	227.06	81.50	1.37	49.50	3.15	3.53
985	A	100	106.34	93	0	7	72.88	0	317.97	150.00	1.41	35.76	1.46	1.79
985	B	100.64	107.65	75	5	20	75.57	0	217.34	93.00	1.36	35.81	2.32	1.80
985	A	105.1	112.08	80	0	20	75.24	0	194.64	111.03	1.36	38.83	2.67	0.34
985	B	110.2	118.84	75	0	25	68.36	0	160.01	143.83	1.50	37.02	0.13	2.47
985	A	116.4	123.89	83	0	17	70.85	0	134.14	84.50	1.45	35.46	1.70	2.98
985	A	118.5	125.99	80	0	20	68.31	0	123.38	43.00	1.50	38.22	-0.30	6.03
985	B	118.2	127.53	89	1	10	73.39	0	115.49	57.32	1.40	40.29	-1.23	9.57
985	A	125.08	132.92	85	0	15	73.97	0	87.88	86.26	1.38	38.07	0.30	5.65
985	B	125.8	135.13	89	1	10	68.27	0	76.56	101.35	1.50	36.60	0.17	2.22
985	A	131	138.84	93	0	7	76.44	0	84.01	-30.61	1.34	38.39	1.28	4.34
985	A	134.9	142.74	75	0	25	65.10	0	86.79	70.03	1.57	36.79	0.63	1.02
985	A	137.7	145.54	75	1	24	67.68	0	88.79	100.00	1.51	35.14	-1.54	10.47
985	A	141.26	149.1	90	0	10	77.93	0	91.32	70.00	1.31	39.48	1.21	4.89

Site	Hole	mbsf	mcd	clay	sand	silt	PW	Bio	NGR	MS	GRA	L	a	b
985	A	145.76	153.6	85	0	15	70.54	0	94.53	129.20	1.45	40.45	0.68	6.52
985	A	149.9	157.74	85	0	15	72.73	0	97.49	64.19	1.41	34.81	2.37	4.65
985	A	157.6	165.44	93	0	7	78.04	0	102.98	55.00	1.31	37.80	1.47	4.99
985	A	164.22	172.06	93	0	7	81.85	0	107.70	39.04	1.25	35.82	1.02	3.53
985	A	167.07	174.91	95	0	5	79.98	0	109.73	107.50	1.28	36.04	1.27	3.69
985	A	171.79	179.63	93	0	7	79.63	0	113.10	72.69	1.29	36.04	1.00	3.75
985	A	174.98	182.82	95	0	5	77.71	0	115.37	53.50	1.32	36.05	0.82	3.80
985	A	177.7	185.54	90	0	10	85.62	0	117.31	164.14	1.20	36.05	0.67	3.84
985	A	186.6	194.44	90	0	10	102.09	0	123.66	78.00	1.00	34.97	1.23	4.76
985	A	190.89	198.73	90	0	10	85.21	0	126.72	261.45	1.20	35.24	-0.31	5.90
985	A	193.9	201.74	94	0	6	87.67	0	128.86	105.00	1.17	41.33	0.00	3.23
985	A	202.4	210.24	98	0	2	95.35	0	134.92	89.64	1.07	42.06	-0.89	7.68
985	A	205.1	212.94	94	0	6	85.40	0	136.85	73.52	1.20	41.04	0.37	5.06
985	A	215.2	223.04	97	0	3	83.89	0	144.05	57.00	1.22	36.23	0.30	4.43
985	A	224.5	232.34	94	0	6	74.42	0	150.68	64.00	1.38	34.45	-0.34	6.12
985	A	232.65	240.49	95	0	5	77.87	0	156.50	53.19	1.32	28.76	-0.51	9.37
985	A	242.02	249.86	95	0	5	85.19	0	163.18	17.63	1.20	33.60	2.23	4.70
985	A	243.8	251.64	70	1	29	86.93	5	164.45	13.00	1.18	22.00	-0.22	9.01
985	A	247.03	254.87	72	2	8	87.82	10	166.75	27.74	1.17	31.94	0.45	7.10
985	A	251.93	259.77	69	1	30	88.64	17	170.25	14.00	1.16	31.87	0.70	5.82
985	A	253.58	261.42	73	1	26	91.67	10	171.42	31.68	1.12	38.58	2.53	1.83
985	A	260.96	268.8	71	3	26	87.82	13	165.43	11.00	1.17	27.85	0.71	9.59
985	A	264.38	272.22	64	2	34	92.00	0	168.23	10.00	1.11	27.96	2.19	3.07
985	A	271.27	279.11	78	0	22	88.66	8	173.88	10.60	1.16	28.18	0.39	7.18
985	A	277.1	284.94	57	0	43	85.55	20	178.66	13.00	1.20	16.59	-3.52	19.62
985	A	285.18	293.02	90	0	10	87.72	2	185.28	31.00	1.17	18.31	-3.99	34.24
985	A	291.84	299.68	91	3	6	81.66	0	190.74	40.31	1.25	37.38	0.46	6.32
985	A	297.88	305.72	94	1	5	77.34	0	195.69	115.50	1.32	39.63	-0.35	6.52
985	A	314.32	322.16	92	0	8	78.23	0	213.28	41.00	1.31	40.77	-3.02	8.24
985	A	320.8	328.64	95	0	5	77.60	0	215.65	40.00	1.32	31.80	-0.40	7.62
985	A	323.8	331.64	95	0	5	80.76	0	216.75	43.00	1.27	34.87	0.16	6.02
986	C	0.2	0.31	55	1	44	87.90	22	207.96	76.50	1.17	34.99	5.15	1.95
986	B	0.2	0.32	51	2	47	84.28	18	210.37	33.00	1.22	39.79	8.25	-1.62
986	A	0.92	0.92	69	1	30	86.34	19	225.37	50.00	1.19	33.38	1.49	4.82
986	C	1.2	1.31	77	1	22	85.39	0	254.06	33.00	1.20	39.63	2.48	1.22
986	B	1.2	1.32	62	1	37	86.63	0	251.71	36.81	1.18	36.15	2.53	3.29
986	A	2.21	2.21	62	2	36	76.60	0	224.61	28.00	1.34	38.17	2.43	-0.53
986	B	2.1	2.22	62	0	38	73.82	0	227.83	49.50	1.39	30.04	0.64	2.84
986	C	2.2	2.31	62	1	37	71.06	1	277.27	49.48	1.44	38.70	0.83	3.15
986	A	2.72	2.72	60	0	40	77.05	1	261.13	46.00	1.33	43.61	5.92	4.20
986	A	7.06	8.42	70	0	30	69.75	1	259.72	85.87	1.47	39.55	1.99	2.08
986	C	10.1	10.95	57	0	43	71.08	8	280.98	47.67	1.44	33.88	0.76	3.66
986	B	9.28	11.93	53	10	37	61.13	0	280.01	32.00	1.68	34.79	4.04	2.73
986	A	11	12.36	60	0	40	64.12	0	280.05	63.00	1.60	37.83	4.42	1.20
986	C	14.22	15.07	45	2	53	75.41	22	280.33	27.00	1.36	28.12	0.25	1.71
986	B	12.83	15.48	57	0	43	74.12	4	280.37	29.55	1.38	39.22	0.37	4.37
986	A	15.15	17.21	74	0	26	72.03	1	280.55	85.13	1.42	37.19	0.57	3.16
986	C	17.5	19.45	55	5	40	71.51	0	280.78	100.00	1.43	37.50	0.27	3.24
986	C	19.9	21.85	45	3	52	70.57	0	281.02	56.00	1.45	34.82	0.81	1.72
986	A	20.67	22.73	74	0	26	66.19	1	281.11	37.13	1.55	40.47	-1.26	5.29
986	A	21.24	23.3	74	0	26	69.57	0	281.17	36.00	1.47	33.42	1.86	0.68
986	C	28.77	31.57	83	1	16	70.57	0	282.01	23.83	1.45	35.69	0.43	3.03
986	C	30.3	33.1	89	0	11	72.93	0	282.17	28.00	1.40	30.75	1.77	-0.11
986	A	31.57	34.51	62	0	38	70.62	0	282.32	68.61	1.45	23.33	0.57	3.70
986	A	36.62	39.88	60	5	35	74.15	1	282.86	21.00	1.38	36.90	0.07	1.66
986	C	37.73	41.34	55	14	41	70.33	0	283.01	55.29	1.46	35.71	4.38	5.76
986	C	41.1	44.71	51	2	47	67.81	20	283.36	67.40	1.51	36.32	-0.12	3.67
986	A	43.34	47.14	59	6	35	65.85	1	283.61	23.00	1.56	30.06	0.96	1.83
986	A	45.84	49.64	54	2	44	65.58	1	283.86	55.00	1.56	42.90	-0.57	3.89
986	A	53.24	52.64	60	1	39	69.14	1	256.55	31.00	1.48	32.16	-0.04	3.07
986	C	49.3	54.33	68	1	31	66.99	8	311.95	97.00	1.53	34.56	-1.32	6.07
986	A	55.23	54.63	40	3	57	70.21	1	340.40	28.19	1.46	25.76	0.84	2.18
986	C	52.3	57.33	44	1	55	69.28	0	324.61	30.00	1.48	30.86	-0.51	4.37

Site	Hole	mbsf	mcd	clay	sand	silt	PW	Bio	NGR	MS	GRA	L	a	b
986	A	58.22	57.62	39	1	60	78.85	35	323.98	59.00	1.30	37.50	0.57	2.94
986	A	59.54	58.94	51	2	47	76.59	12	321.12	42.63	1.34	32.58	-0.11	1.67
986	C	54.8	59.83	60	3	37	62.44	0	319.19	53.80	1.64	35.92	0.21	3.37
986	A	62.4	61.8	63	2	35	66.19	0	314.92	56.00	1.55	31.72	-0.69	2.04
986	A	64.73	64.13	30	7	63	71.06	32	309.88	39.69	1.44	30.93	0.95	0.95
986	C	60.8	65.83	54	4	42	66.12	0	306.19	62.42	1.55	32.37	-2.33	6.36
986	A	68.15	67.55	55	1	44	69.69	0	302.47	60.97	1.47	36.28	-0.39	1.81
986	C	64.4	69.79	28	5	67	71.81	37	297.62	44.60	1.43	34.28	-1.76	6.58
986	A	73.25	72.65	52	3	45	66.71	0	291.42	57.00	1.54	31.27	0.84	0.35
986	C	67.47	72.86	9	60	31	70.07	0	290.97	19.60	1.46	29.51	-3.25	8.18
986	C	69.35	74.74	14	16	70	80.38	0	286.89	24.00	1.27	29.32	-2.87	7.33
986	A	76.5	75.9	51	5	44	74.93	0	284.38	32.50	1.37	28.99	1.45	-0.47
986	A	80.89	80.29	55	5	40	69.18	1	274.87	36.00	1.48	31.94	0.63	1.70
986	C	81.4	82.87	73	1	26	65.70	0	269.28	35.60	1.56	25.48	2.97	-2.09
986	A	85.59	84.99	40	10	50	71.81	0	264.69	41.00	1.43	28.00	0.99	0.69
986	C	87.4	88.87	72	1	27	65.43	0	256.29	40.40	1.57	31.27	0.25	2.15
986	A	90.4	89.8	85	0	15	85.38	0	254.27	28.00	1.20	31.93	0.88	0.64
986	C	90.9	92.37	41	1	58	64.69	1	248.71	24.00	1.58	28.22	-0.32	8.17
986	A	93.4	92.8	53	1	46	70.45	0	247.77	27.61	1.45	29.41	1.06	2.98
986	C	93.9	95.37	59	3	38	66.62	0	281.99	60.00	1.54	33.50	-2.39	6.68
986	C	97.14	98.61	75	2	23	73.25	0	281.33	66.00	1.40	36.84	1.11	1.13
986	A	96.4	98.84	30	5	65	71.24	47	281.29	64.77	1.44	40.75	0.20	2.83
986	A	101.14	103.58	38	5	57	75.80	0	280.33	90.39	1.35	26.76	0.15	3.21
986	C	100.5	105.51	75	0	25	71.66	0	279.94	33.00	1.43	25.97	-0.93	6.56
986	C	101.45	106.46	75	1	24	67.59	0	279.75	31.48	1.52	30.35	-2.19	7.60
986	A	102.3	106.94	60	3	37	78.59	0	279.65	41.58	1.30	28.75	1.55	1.45
986	A	103.9	108.54	89	0	11	81.59	2	279.33	60.00	1.26	29.53	-1.60	5.87
986	A	107.8	112.44	70	2	28	65.56	2	278.55	72.50	1.56	38.14	0.64	3.35
986	C	110.36	115.99	70	0	30	76.76	0	277.83	25.00	1.33	32.95	0.05	3.00
986	A	112.3	116.94	75	2	23	82.78	2	277.64	30.19	1.24	32.35	1.13	-0.08
986	C	114.76	120.39	68	0	32	70.67	0	276.94	100.68	1.45	36.67	0.45	3.70
986	A	116.3	122.3	88	1	11	72.83	0	276.56	42.48	1.41	17.61	0.93	1.47
986	A	117.7	123.7	72	2	26	70.29	1	276.28	44.17	1.46	31.48	-1.65	2.69
986	A	119.8	126.53	63	5	32	74.08	1	275.70	45.00	1.38	32.71	-0.33	2.01
986	C	122.24	127.9	60	0	40	65.86	0	275.43	59.00	1.55	37.41	-0.94	3.59
986	A	121.5	128.23	53	6	41	65.98	0	275.36	47.00	1.55	36.59	-0.26	2.89
986	C	130.13	135.79	73	0	27	74.53	0	273.84	95.00	1.37	27.29	1.51	1.86
986	A	129.57	136.57	75	0	25	66.11	0	273.68	101.00	1.55	34.60	3.42	-2.16
986	A	135.46	142.46	72	0	28	66.11	0	272.49	71.81	1.55	31.85	-1.39	3.99
986	C	143.25	147.61	73	0	27	73.94	0	271.45	49.87	1.39	34.39	0.20	2.52
986	C	153.3	157.66	65	0	35	65.39	0	269.43	96.69	1.57	31.93	-0.10	4.41
986	A	150.53	157.77	60	0	40	68.40	0	269.41	95.00	1.50	34.02	0.30	0.22
986	A	154.6	161.84	60	0	40	68.56	0	268.59	69.00	1.49	34.51	-0.99	1.65
986	A	158.39	165.63	65	1	34	64.25	0	267.82	44.40	1.59	31.16	-0.12	2.77
986	A	162.97	170.21	55	5	40	56.67	0	266.90	38.00	1.81	25.61	0.22	2.44
986	C	168.4	172.76	10	80	10	81.14	0	266.38	18.00	1.26	27.08	1.12	1.51
986	C	169.32	173.68	80	0	20	72.88	0	266.20	30.50	1.41	32.43	-0.54	4.41
986	A	168	175.24	54	2	44	66.15	0	303.75	36.00	1.55	24.35	-3.92	8.45
986	C	177.3	181.66	45	5	50	67.42	0	308.99	73.07	1.52	25.94	1.89	-1.50
986	C	178.9	183.26	76	0	24	69.67	0	305.62	70.67	1.47	30.29	-0.16	2.74
986	A	177.5	184.74	72	0	28	65.92	0	302.50	46.50	1.55	33.90	-0.93	4.33
986	C	188.4	192.76	68	2	30	70.09	0	285.59	73.55	1.46	23.40	1.47	1.27
986	A	188.85	192.88	75	0	25	73.72	0	285.34	49.00	1.39	36.93	-3.08	8.20
986	C	190.8	195.16	79	1	20	65.53	0	280.53	91.88	1.56	28.58	0.82	0.63
986	A	191.9	195.93	68	0	32	68.85	0	278.91	142.50	1.49	33.21	-0.98	3.38
986	A	197.1	201.13	80	0	20	68.72	0	267.95	29.00	1.49	30.54	-0.78	4.64
986	C	198.5	204.65	64	5	31	63.56	0	260.53	107.00	1.61	29.32	-0.15	0.98
986	A	203.1	207.13	60	0	40	66.54	0	255.30	134.00	1.54	36.02	-0.01	2.75
986	C	235.3	241.45	65	3	32	62.49	0	269.90	41.48	1.64	25.49	-0.69	3.37
986	C	245.2	251.35	55	6	49	66.75	0	270.49	32.00	1.53	25.20	-1.22	4.44
986	C	255.9	262.05	57	3	40	63.47	6	271.12	115.83	1.61	24.89	-1.79	5.61
986	C	259.71	265.86	66	1	33	65.31	0	271.35	75.50	1.57	33.72	-1.44	4.57
986	C	264.2	270.35	70	2	28	64.56	0	271.62	107.00	1.59	32.85	-0.75	3.45

Site	Hole	mbsf	med	clay	sand	silt	PW	Bio	NGR	MS	GRA	L	a	b
986	C	265.7	271.85	53	5	42	61.49	0	271.71	60.26	1.67	30.39	0.14	1.84
986	C	266.7	272.85	55	2	43	66.88	0	271.76	35.16	1.53	29.97	1.48	-1.13
986	C	276.8	282.95	75	1	24	61.74	0	272.36	33.50	1.66	28.61	-0.46	3.41
986	C	278.35	284.5	65	3	32	59.33	0	272.46	79.20	1.73	26.79	-2.60	7.52
986	C	303.1	309.25	70	2	28	65.17	0	273.92	39.00	1.57	30.69	-1.09	4.23
987	C	4.7	4.7	55	2	43	71.96	1	268.20	117.00	1.42	40.63	3.24	0.00
987	A	5.3	5.44	69	3	28	68.30	2	268.39	127.58	1.50	39.47	3.31	0.70
987	B	5.9	6.39	44	4	52	68.18	3	268.65	117.03	1.50	32.54	2.32	3.58
987	D	4.57	6.67	67	2	31	65.85	0	268.73	135.00	1.56	39.67	5.67	3.02
987	C	7.52	7.3	68	5	27	67.86	3	268.90	79.00	1.51	42.97	5.92	1.47
987	C	9.6	9.38	70	2	28	68.96	1	269.46	107.00	1.49	37.10	0.70	4.81
987	B	9.1	9.59	59	3	38	64.28	0	269.51	122.17	1.59	37.53	0.38	4.07
987	D	9.48	11.58	73	0	27	67.28	0	270.05	148.65	1.52	38.77	1.94	1.79
987	D	11.3	14.17	61	7	32	68.17	0	270.75	128.71	1.50	39.17	3.34	2.60
987	A	12.6	14.17	70	5	25	68.95	0	270.75	127.00	1.49	40.25	2.78	3.96
987	C	15.7	16.76	66	1	33	60.38	0	271.44	162.24	1.70	35.02	-0.02	3.20
987	A	15.6	17.17	65	7	28	71.21	4	271.55	246.38	1.44	36.02	0.37	2.86
987	D	14.5	17.37	66	3	31	63.80	0	271.61	127.00	1.61	31.65	2.86	-1.08
987	C	23.05	24.11	67	5	28	60.85	0	273.42	174.03	1.68	35.13	0.98	1.99
987	D	23.49	27.1	55	5	40	60.24	0	274.23	128.34	1.70	29.83	0.39	1.11
987	C	25.44	27.15	59	3	38	56.76	0	274.24	179.83	1.80	33.87	-0.02	1.52
987	C	29.36	31.07	74	0	26	60.81	0	275.30	119.00	1.68	38.18	1.52	2.75
987	A	29.3	32.65	74	1	25	59.85	0	275.72	91.83	1.71	32.97	0.59	2.43
987	C	34.7	37.05	80	0	20	61.76	0	276.91	226.14	1.66	34.92	-0.16	3.40
987	A	34.55	37.9	74	1	25	62.61	0	277.14	183.00	1.64	38.15	-0.50	6.75
987	C	37.2	39.55	63	2	35	63.52	0	277.58	141.00	1.61	30.88	-2.04	7.53
987	D	34.8	39.6	63	3	34	58.42	0	277.59	84.00	1.75	30.25	0.69	2.43
987	C	39.9	42.25	78	0	22	64.08	0	278.31	64.61	1.60	39.49	-1.72	4.33
987	A	40.4	44.89	74	1	25	59.92	0	279.02	138.80	1.71	35.93	1.24	3.15
987	D	39.86	45.51	73	1	26	64.71	0	279.18	101.17	1.58	36.97	0.59	3.78
987	A	44.6	49.09	75	1	24	59.67	0	280.15	171.06	1.72	35.70	0.46	3.85
987	A	47	52.01	68	1	31	59.64	0	280.94	73.67	1.72	31.34	0.71	1.26
987	A	51.6	56.61	75	0	25	63.67	0	282.17	128.58	1.61	35.70	0.83	3.35
987	D	50.06	56.91	72	1	27	62.48	0	282.25	89.00	1.64	35.94	1.63	1.58
987	B	52.03	57.02	60	3	37	60.81	0	282.28	116.48	1.68	34.72	0.27	4.80
987	D	54.2	61.05	70	0	30	62.70	0	283.37	109.97	1.63	38.20	1.17	1.61
987	A	58.8	64.85	67	1	32	61.10	0	284.39	238.50	1.68	35.33	2.80	0.89
987	D	59.26	67.1	61	0	39	59.41	0	285.00	218.00	1.72	36.23	-2.12	5.84
987	B	63.7	70.08	72	0	28	60.77	0	285.80	105.00	1.69	36.33	1.62	-0.23
987	D	63.2	71.04	71	2	27	61.69	0	286.06	121.00	1.66	34.32	-0.86	3.29
987	A	65.32	72.77	75	0	25	62.29	0	286.53	123.42	1.64	33.24	-1.50	4.80
987	A	66.94	74.39	65	0	35	66.41	0	286.96	91.00	1.54	38.46	2.85	0.78
987	B	69.5	75.88	69	1	30	61.91	0	287.36	199.00	1.65	12.22	-0.60	13.29
987	D	69.1	77.75	65	1	34	63.86	0	287.87	89.83	1.60	38.26	-0.18	0.40
987	A	71.7	78.76	55	0	45	59.22	2	288.14	92.00	1.73	39.31	1.72	0.85
987	D	71.3	79.95	74	0	26	60.06	0	288.46	250.00	1.70	37.23	1.74	1.64
987	B	74.4	81.37	60	5	35	60.06	0	288.84	168.00	1.71	37.01	0.11	4.74
987	A	75.9	82.96	60	0	40	62.52	0	289.27	94.04	1.64	37.06	-1.76	5.43
987	D	75.1	83.75	12	10	78	66.28	0	289.48	150.83	1.55	33.49	4.92	-0.57
987	A	77.2	84.99	65	5	30	63.09	0	289.82	125.00	1.62	29.14	-3.04	9.68
987	B	79.4	86.37	53	4	43	61.59	0	290.19	90.48	1.66	34.74	2.93	1.49
987	A	79.87	87.66	60	3	37	59.56	1	290.54	90.00	1.72	34.43	-1.26	6.49
987	D	78.4	88.28	65	3	32	61.39	0	290.70	85.13	1.67	34.02	1.62	2.32
987	B	80.95	89.87	87	0	13	64.71	0	291.13	81.97	1.58	31.42	1.55	1.45
987	B	82.83	91.75	64	1	35	61.17	0	291.64	141.50	1.67	32.24	0.17	3.52
987	A	84.4	93.15	1	6	85	69.42	0	292.01	98.97	1.48	38.16	0.71	2.30
987	D	83.4	93.28	56	3	41	61.91	0	292.05	127.38	1.65	33.19	-1.99	3.52
987	B	84.73	93.65	67	1	32	60.89	0	292.15	120.00	1.68	32.18	-2.00	6.06
987	D	84.7	94.58	54	3	43	59.12	0	292.40	97.53	1.73	38.44	2.24	0.77
987	A	87	95.75	64	1	35	66.89	0	292.71	237.16	1.53	34.48	0.31	2.47
987	D	87.4	98.5	73	1	26	62.14	0	293.45	110.50	1.65	36.42	0.72	0.53
987	A	93.75	99.14	52	4	44	61.66	0	293.63	98.00	1.66	25.80	1.02	4.77
987	A	94	99.39	66	1	32	52.51	1	293.69	75.00	1.95	28.36	-0.38	3.71

Site	Hole	mbsf	mcd	clay	sand	silt	PW	Bio	NGR	MS	GRA	L	a	b
987	A	94.69	100.08	50	4	46	55.05	0	293.88	229.00	1.86	36.16	1.65	1.93
987	D	89.8	100.9	74	0	26	57.69	0	294.10	113.72	1.78	32.30	-1.28	3.26
987	D	90.5	101.6	65	0	35	62.63	0	294.29	74.19	1.64	36.66	4.67	-2.36
987	B	90.5	103.55	67	5	28	58.69	0	294.81	158.00	1.74	32.98	-0.54	4.97
987	D	95.31	106.41	51	10	39	65.34	0	295.58	108.43	1.57	32.79	-0.21	3.97
987	B	93.5	106.55	55	2	43	62.63	0	295.62	98.00	1.64	34.15	2.19	2.89
987	D	96.47	107.57	65	1	34	65.33	0	295.90	126.00	1.57	35.70	0.04	4.08
987	D	98.9	110	83	0	17	65.32	0	296.55	75.68	1.57	38.07	1.09	2.00
987	A	103.8	111.67	70	2	28	61.21	0	297.00	140.00	1.67	33.02	-2.26	5.09
987	A	106.6	114.47	63	2	35	61.54	0	297.75	189.79	1.66	37.07	0.82	3.13
987	D	105.7	116.8	60	4	36	62.10	0	298.38	85.52	1.65	33.59	-3.46	7.23
987	A	111.1	118.97	67	1	32	60.16	0	298.97	100.00	1.70	36.51	0.05	3.67
987	D	108.65	119.75	50	8	42	65.10	2	318.00	96.00	1.57	39.51	0.31	4.48
987	D	113.85	124.95	61	1	38	61.13	0	312.67	147.00	1.68	35.51	0.40	3.12
987	D	114.48	125.58	74	0	26	64.17	0	309.92	136.94	1.60	25.70	-3.63	9.31
987	A	124.6	133.25	59	4	37	61.43	0	276.46	182.27	1.67	35.99	0.10	2.97
987	A	125.72	134.37	59	3	38	65.81	0	271.58	99.00	1.56	35.54	-1.82	4.84
987	A	129.3	137.95	52	5	43	60.88	0	261.84	84.00	1.68	34.36	-1.30	2.99
987	A	134.1	143.57	64	1	35	63.37	0	200.73	75.00	1.62	37.29	-1.75	3.11
987	D	134.5	145.6	72	2	26	64.69	0	201.00	74.00	1.58	37.51	-0.63	3.17
987	A	137.1	146.57	78	0	22	64.40	0	201.13	69.00	1.59	33.60	-0.98	2.62
987	D	138.4	149.5	56	4	40	67.06	0	201.52	52.67	1.53	33.52	-2.76	4.50
987	A	141.88	151.35	80	0	20	60.13	0	201.77	137.00	1.70	32.76	-1.69	6.10
987	A	145.1	154.57	64	1	35	64.48	0	202.19	127.00	1.59	31.49	-2.99	5.90
987	A	146.36	155.83	31	0	30	60.38	0	202.36	106.00	1.70	33.95	0.04	0.86
987	D	144.9	156	60	1	39	85.33	0	202.38	82.58	1.20	34.71	-2.00	4.35
987	D	150.25	161.35	69	1	30	62.42	0	203.10	102.50	1.64	37.14	-0.10	3.21
987	A	157.8	167.79	58	4	38	59.95	0	203.95	65.17	1.71	34.15	-3.21	5.50
987	D	158.1	169.2	68	2	30	61.41	0	204.14	104.00	1.67	33.70	-2.67	6.49
987	A	161.5	172.35	60	3	37	58.31	0	204.56	129.00	1.76	32.79	-1.43	2.51
987	D	161.9	173	67	2	31	67.32	0	204.65	69.00	1.52	26.48	-3.95	9.54
987	A	166.32	177.17	74	2	24	64.73	0	205.20	93.00	1.58	37.80	-0.29	2.95
987	D	166.8	177.9	63	2	35	66.56	0	205.30	124.71	1.54	36.42	-1.15	5.79
987	A	172.3	183.15	65	1	34	59.17	0	206.00	152.17	1.73	31.89	-2.11	5.51
987	D	173	183.53	75	0	25	63.88	0	206.05	166.03	1.60	35.05	-0.99	3.73
987	A	176.6	187.45	65	1	34	63.76	0	206.57	137.67	1.61	36.18	1.76	1.49
987	A	181	191.85	67	1	32	61.06	0	207.16	143.00	1.68	33.19	-0.87	2.96
987	A	182.4	193.25	67	1	32	62.94	0	207.34	158.17	1.63	35.32	1.66	0.26
987	A	191.12	201.97	74	1	25	74.65	0	208.51	84.81	1.37	33.34	-1.45	3.59
987	A	195.14	205.99	67	1	32	58.68	0	209.04	102.38	1.75	34.36	-0.34	1.35
987	D	200.2	210.73	73	2	25	62.71	0	209.67	99.39	1.63	33.27	-3.44	4.39
987	D	214.4	224.93	70	2	28	62.84	0	211.56	170.00	1.63	33.68	-1.82	4.84
987	D	222.06	232.59	67	2	31	65.02	0	212.58	140.76	1.58	33.75	-0.95	4.35
987	D	231.1	241.63	73	1	26	59.92	0	213.79	97.00	1.71	31.44	-1.61	3.74
987	D	234.9	245.43	63	2	35	61.59	0	214.29	150.00	1.66	34.52	0.57	2.95
987	D	240.2	250.73	68	1	31	62.67	0	215.00	253.83	1.63	35.94	-1.16	5.20
987	D	240.75	251.28	55	0	45	60.98	0	215.07	103.00	1.68	36.49	-0.40	4.62
987	D	249.7	260.23	65	5	30	64.65	0	216.26	120.16	1.58	33.17	-1.25	4.02
987	D	250.65	261.18	68	2	30	67.02	0	216.39	95.77	1.53	37.12	2.27	2.43
987	D	252.58	263.11	60	2	38	62.73	0	216.65	83.50	1.63	41.36	1.08	0.78
987	D	259.48	270.01	66	1	33	62.29	0	217.57	184.27	1.64	33.80	-0.59	3.59
987	D	264.3	274.83	60	0	40	61.50	0	218.21	127.00	1.67	40.13	-0.92	3.47
987	D	268.99	279.52	52	3	30	60.52	0	218.83	124.40	1.69	38.77	-2.19	3.23
987	D	270.49	281.02	58	3	39	60.24	0	219.03	207.80	1.70	39.66	-0.36	4.67
987	D	279.1	289.63	60	2	38	67.19	0	220.18	160.00	1.52	37.71	0.00	3.63
987	D	283.45	293.98	62	1	37	59.60	0	220.76	247.31	1.72	40.80	-1.31	6.72
987	D	297.3	307.83	62	0	38	62.02	0	222.60	115.97	1.65	40.11	0.55	2.82
987	D	298.7	309.23	63	2	35	63.66	0	222.79	123.00	1.61	42.37	1.06	2.65
987	D	325.4	335.93	51	7	42	61.50	0	226.34	595.41	1.67	35.48	-0.35	5.93
987	D	334.9	345.43	41	15	44	51.56	0	227.61	796.60	1.99	33.02	-0.85	7.10
987	D	345.8	356.33	47	12	41	49.71	0	229.06	852.00	2.06	30.21	-1.43	8.45
987	E	363.7	363.7	63	7	30	59.71	0	287.90	192.00	1.72	35.61	1.96	1.40
987	D	355.73	366.26	40	25	35	53.33	0	290.88	807.00	1.92	27.65	-1.95	9.67

VITA

Paula Ann Clark

1501 Stallings #60
College Station, TX 77840

(979) 693-5044
email: clark@iodp.tamu.edu

M.S. Texas A&M University, Department of Geophysics, College Station, TX,
May 2006

Major: Geophysics

B.S. Southwestern University, Georgetown, TX, December, 1997

Major: Physics Minor: Mathematics

Senior Research Project: *The application of seismic techniques in exploration geophysics and development of a geological model based on the analysis of seismic data as recorded by ocean bottom seismographs in the Ivory Coast Basin.*

MIS/M University of Phoenix, Graduate School of Management, Phoenix, AZ,
August 2006

Microsoft Database Administrator (MSDBA), Solutions Developer (MCSD),
Microsoft Office User Specialist (MOUS) certifications.

Integrated Ocean Drilling Program, Texas A&M University, College Station,
TX: Systems Analyst, May 2004 to Present

- Computer Systems Administrator on a scientific research ship
College of the Sequoias, Visalia, CA: Science Faculty, August 2002 to May 2004
- Geology I, three hours lecture, three hours lab, plus 2 field trips a semester
Torian Group, Inc., Visalia, CA: Software Consultant, April 2002 to May 2003
- Specializing in databases, data integrity, and programming in Visual Basic
Ocean Drilling Program, Texas A&M University, College Station, TX: Database
Analyst, May 1998 to November 2001
- Found and researched potential errors in reflectance data, initiated testing, determined correct values, had bad data eliminated from the database, the good values recalculated, the scientific equipment dismantled until repaired, and notified the scientific community.
- Found potential errors in P-wave velocity data, had bad data kept out of database, and notified scientific community of these potential errors.
- Corrected and verified 5+ years worth of physical properties data using relationships between physical properties and black & white core photographs and personal experience/knowledge (basis for Thesis).
- Migrated legacy physical properties data (6 physical properties for 70+ Legs) into Oracle providing verification during the transfer.